THE ROLE OF ACTIVATING MUTATIONS IN THE FERM DOMAIN OF JANUS KINASE 3 IN THE DEVELOPMENT OF ADULT T-CELL LEUKEMIA/LYMPHOMA

By

Natalina Elizabeth Elliott

Dissertation

Submitted to the Faculty of the

Graduate School of Vanderbilt University

in the partial fulfillment of the requirements

for the degree of

DOCTOR OF PHILOSOPHY

in

Cancer Biology

May, 2013

Nashville, Tennessee

Approved:

Professor Utpal Davé MD

Professor Stephen Brandt MD

Professor Scott Hiebert PhD

Professor William Pao MD PhD

ACKNOWLEDGEMENTS

Projects such as this are never performed alone. Much like a child, a thesis takes a village to grow. I am extremely grateful to everyone who provided support to me along the way and became a part of my personal village. Whether it be financial, educational, physical, or emotional, I could not have done it without everyone's support. Specifically I would like to thank my two best friends, Ali Wright and Janie Luther for never failing to bolster my spirits when I was down and putting up with my absence when I needed to focus. To my parents Kathy, Tony, and Gerald, despite not having any understanding of what I do, they always showed interest and unending confidence in my ability to conquer the world.

I would like to thank everyone who has ever provided helpful discussion and active interest in this project, my committee Drs. Stephen Brandt, Scott Hiebert, and William Pao for their input, support and participation as I struggled through the process of developing my thesis. Dr. Michael Engel and Sandra Zinkel for answering all of my early morning and late night emergency questions and for providing alternatives to those experimental issues that tend to crop up when least expected. In addition, I am grateful for the support of the entire Hematology/Oncology and leukemia/lymphoma group most especially the 5th floor of Vanderbilt's Preston research building for providing opportunities to discuss all options and providing a level of focus to my work. I would like to give special appreciation to my advisor Dr. Utpal Davé for taking a chance and

allowing me the great honor of being his first graduate student. I may not always show it but I am grateful for the opportunity to work for him.

I would like to thank all of the Vanderbilt core facility personnel but especially the members of Flow Cytometry Core of Vanderbilt University, Kevin Weller, Brittany Matlock, David Flaherty, and Christian Warren for all of their very helpful advice. The VMC Flow Cytometry Shared Resource is supported by the Vanderbilt Ingram Cancer Center (P30 CA68485) and the Vanderbilt Digestive Disease Research Center (DK058404).

This work would not have been possible without the financial support National Heart, Lung, and Blood Institute Award Number K08HL089403, the Doris Duke Charitable Foundation Clinical Scientist Development Award, the Leukemia & Lymphoma Society, the Vanderbilt Ingram Cancer Center (P30 CA68485), Monforton family grant, and the T.J. Martell Foundation (Dr. Utpal Davé). This work was also supported by U54 grants from the NIH CA101598, CA101388 and NIH P30CA0113696 (Dr. Victor Grann) and the Viruses, Nucleic Acids and Cancer training grant (NCI: 2T32CA009385-21) (Dr. Earl Ruley).

Now for an especially important thanks to my lab colleagues: Charnise, Shelley, Steve, Rati, Deanna, Ryan, Elizabeth, Leslie and Gabby for making going to work like coming home to family. The biggest thanks of all goes to my post-doc and coworker, Dr. Susan Cleveland, through her unlimited patience, collaboration and simple willingness to listen, she provided me with more experimental and educational support but also an unending bond of friendship.

TABLE OF CONTENTS

LIST OF TABLES

Page

LIST OF FIGURES

Page

LIST OF ABBREVIATIONS

AKT	Protein Kinase B
ATLL	Adult T-cell leukemia/lymphoma
B220	CD45R/B220 B cell antigen
BM	Bone marrow
BMTT	Bone marrow transduction transplant
c-Kit	CD117 antigen, stem cell factor receptor
CD	cluster of differentiation
CD3	T-cell co-receptor
CD4	T-cell Marker
CD8	T-cell Marker
CD25	alpha chain of the IL-2 receptor
CD34	Hematopoietic progenitor cell antigen CD34
CDK	Cyclin dependent kinase
CDKN2A	Cyclin-dependent kinase inhibitor 2A
cDNA	Complimentary DNA
DAPI	4,6- diamidino-2-phenylindole
DNA	Deoxyribonucleic acid
ERK	Extracellular-signal-regulated kinases
FACS	Fluorescence activated cell sorting
FERM	Protein regulatory domain named for band 4.1, ezrin, radixin, and moesin
GR-1	Myeloid differentiation antigen GR-1

H & E	Hematoxylin & Eosin
HAM/TSP	HTLV-I associated myelopathy/tropical spastic paraparesis
HTLV-1	Human T-lymphotropic virus Type I
IL	Interleukin
IL-2	cytokine interleukin 2 ligand of IL-2 recepetor
IL2Rα	IL-2Rα, CD25, Tac antigen Interleukin 2 receptor alpha
IL2Rβ	IL-2Rβ, CD122, Interleukin-2 receptor subunit beta
IL2Rγ	CD132, common gamma c receptor subunit
IRES	Internal ribosome entry site
JAK3	Janus kinase 3
KO	Knockout
LSK	Cells enriched for Lineage Negative/c-Kit+
Mac-1	Antigen CD11b
MIG	MSCV IRES GFP
mRNA	Messenger RNA
MSCV	Murine stem cell virus
MTT	3-(4,5-Dimethylthiazol-2-yl)-2,5-diphenyltetrazolium bromide
NK	Natural Killer cell
P14(ARF)	tumor suppressor, alternative reading frame of *CDKN2A* human
p16(INK4A)	MTS-1, *CDKN2A* tumor suppressor protein
P19(ARF)	tumor suppressor, alternative reading frame of *CDKN2A* murine
PB	Peripheral blood
PCR	Polymerase chain reaction

PI3K	phosphoinositol-3’-kinase
qRT-PCR	Quantitative real-time PCR
RNA	Ribonucleic acid
RT-PCR	Reverse transcription PCR
Sca1	Stem cell antigen 1 (Ly6a)
SCF	Stem cell factor (c-Kit ligand)
STAT	Signal transducer and activator of transcription
TYK2	Tyrosine kinase 2
WT	Wild type

CHAPTER I

INTRODUCTION

Adult T-cell leukemia/lymphoma (ATLL) is a T-cell malignancy initiated by infection with the human T-cell lymphotrophic virus type 1 (HTLV-1)[1, 2]. ATLL is a historically incurable disease where most patients succumb within the first year of diagnosis. Standard chemotherapy and monoclonal antibody treatments for ATLL tumor markers do not improve outcome[3, 4]. Development of ATLL requires HTLV-I retroviral infection, which is followed by accumulation of somatic mutations and changes in gene expression. The discovery of genes and pathways involved in the initiation of ATLL may provide novel therapeutic targets for this fatal disease. So far, no drug targets have been identified. Since the IL-2 signaling pathway plays an important role in ATLL development, mutational analysis of IL-2 signaling pathway components should yield a better understanding of disease progression and outcome. Janus kinase 3 (JAK3), a non-receptor tyrosine kinase that directly regulates the phosphorylation of signaling transducer and activator of transcription 5 (STAT5), is the most proximal kinase in the IL-2 signaling pathway. Activating somatic mutations in JAK3 were described in a few leukemias and lymphomas, including acute megakaryoblastic leukemia and natural killer/T-cell lymphoma[5-8]. Here, three mutations in the regulatory FERM domain of JAK3 were identified in four of the thirty-six ATLL patients are described. No mutations were found in twenty-three ethnically matched controls

screened. These somatic, missense mutations occurred in the amino terminal regulatory FERM domain. In cell culture assays, all three mutations induce gain of function in JAK3. Previous to this study, no activating mutations were characterized within the FERM domain of JAK3.

Here, kinase activity is inhibited by a specific kinase inhibitor, tofacitinib, for WT as well as mutant JAK3s. The major function of the JAK3 FERM domain, as previously investigated, is to bind the cytoplasmic tail of γc (common gamma chain, subunit of IL-2 receptor). JAK3 FERM domain may also play an autoregulatory role by inhibiting kinase activity in the absence of cytokine stimulation. One of the JAK3 FERM domain mutations (E183G) was characterized in vivo and found to be oncogenic in cooperation with the loss of cell cycle regulator proteins p16(INK4a) and p14(ARF), both of which are encoded by the *CDKN2A* locus.

Adult T-cell leukemia/lymphoma (ATLL)

Description of the disease

First described in Japan in 1976, Adult T-cell leukemia/lymphoma (ATLL) is an aggressive and rarely curable cancer caused by infection with the retrovirus Human T-cell Leukemia Virus type-1 (HTLV-1)[1, 9]. The virus, and the lymphoma, is endemic to islands in Japan and the Caribbean. Some sporadic cases were diagnosed elsewhere in the world including Africa, Iran, and North and South America[10-12].

ATLL is an aggressive T-cell neoplasm that is resistant to many therapeutic approaches. Onset of ATLL is most common during middle age or later. Upon diagnosis, ATLL usually runs a rapid course, with peripheral blood and bone marrow involvement, hepatomegaly, splenomegaly, peripheral lymph node enlargement, skin lesions, diffuse organ infiltration and immune suppression. Symptoms include lethargy, abdominal pain, diarrhea, cough, and ascites[1, 13]. Anemia, neutropenia, or thrombocytopenia rarely occur in ATLL patients, while pancytopenia occurs in some ATLL patients because of infiltration of leukemia cells into bone marrow. Aggressive ATLL has a poor prognosis because of resistance to chemotherapy, a high tumor burden, hypercalcemia, and profound immune deficiency[14, 15]. An elevated number of abnormal lymphocytes is common in acute and chronic ATLL. Neutrophilia is frequently observed in ATLL patients and may be caused by cytokines, such as granulocyte/macrophage colony-stimulating factor, produced by ATLL cells[16].

Because the disease is rare, mostly small case studies of 1-12 patients have been published. These studies have looked at cytotoxic chemotherapy, interferon therapy, nucleoside analogues, stem cell transplantation, and immune therapy, but no specific regimen has generated reproducible results[17, 18]. ATLL is resistant to both chemotherapy and targeted immunotherapy and these treatments do not alter the clinical course of the disease[4, 18, 19]. Historically, most patients succumb within the first year of diagnosis. Longer survival of greater than two years is rarely observed in patients presenting with chronic or smoldering forms of ATLL[20-23]. Less than 10% of the patients survive up to five

years after the initial diagnosis.

Cases of increased survival have been reported after stem cell transplantation but the treatment-related mortality is still extremely high[24]. Unfortunately, newly diagnosed patients can expect a median survival of less than 12 months. Perhaps through better understanding of the unique biology of ATLL, it may be possible to identify novel therapeutic targets.

It was observed that patients with acute ATLL benefit considerably from combined antiviral therapy with zidovudine and interferon alpha, whereas patients with ATLL of the lymphoma type may experience a better outcome with intensive chemotherapy[25]. Up to 40% of patients treated with stem-cell transplantation achieved remission for 12-18 months[26].

Very few cases of remission have been described for aggressive ATLL[27, 28]. For instance in one case study 35 patients were treated with conventional chemotherapy, followed by allogeneic hematopoietic stem cell transplantation, 29 of these patients were subsequently treated by the withdrawal of immune suppressants. Of these 29, only 2 patients were in remission at 48 and 69 months post relapse or progression at the time of publication[28]. A large scale meta-analysis of ATLL clinical case studies between 1995 and 2008 compared with patient outcomes for 100 patients with ATLL found that patients with ATLL experienced a better outcome with chemotherapy and without antiviral therapy[29].

HTLV-1 infects T cells and induces cell transformation through the expression of viral oncogenes such as *tax*[30-32]. ATLL cells are identified as activated helper T-cells with a $CD3^+$, $CD4^+$, $CD8^-$, $CD25^+$, and HLA-DR^+ surface

phenotype. In some rare cases, ATLL cells express both CD4 and CD8 on their surfaces and, very rarely, CD8 alone or lacking in both CD4 and CD8 expression[33-35]. Histological/morphological characteristics of ATLL leukemic cells include lobular nuclei and unusual surface phenotypes[1].

Human T-cell lymphotropic virus type 1 (HTLV-1)

Ten and twenty million people worldwide are estimated to be infected with the HTLV-I, but only 10%, are estimated to become chronic viral carriers of infection[11, 18, 36-39]. It should be noted that these estimates are usually based on screenings of blood donors, pregnant women and select at risk population. These methods may lead to an inaccurate estimation of the prevalence of infection[37]. The highest prevalence is reported in the Japanese islands of Okinawa and Tsushima and theoercent of the poputlaiton that is infected was estimated at between 17.1% and 36.4% in the 1980s and 1990s[40]. 3.8% of Haitians are carriers of HTLV-1 as of 1993[37]. In African studies, the prevalence is between 1.05% and 8.5%[41-43]. HTLV-1 is higher in females and increases with age[42, 44, 45]. HTLV-1 prevalence is known to vary widely over geographic and demographic populations, therefore the exact prevalence is unknown[37, 46, 47].

Viral transmission occurs by sexual contact, from mother to child via breastfeeding, and through exposure to contaminated blood, either through blood transfusion or sharing of tainted needles[48-50]. Co-infection with HTLV-I and HIV can accelerate the progression of acquired immune deficiency syndrome possibly due Tax activation of the HIV LTR[51-54]. Several receptors have been

suggested as integral to HTLV-1 infection including the glucose transporter receptor-1, neuropilin-1, and heparan sulfate proteoglycans[55-62].

Formerly referred to as Adult T-cell lymphoma virus type 1, HTLV-I was first identified in the cell line MT-2 derived from coculture of cord blood with cells isolated from an ATLL tumor[2]. HTLV-1 was the first human retrovirus to be identified and is the only known retrovirus directly linked to a human cancer. Although the majority of infected individuals remain asymptomatic throughout life, HTLV-1 infection is linked to life-threatening, incurable diseases, such as HTLV-I associated myelopathy/tropical spastic paraparesis (HAM/TSP) and ATLL in 5-10% of carriers 20-50 years after infection[2].

HTLV-I is a member of the primate T lymphotropic viruses family. Members include human T-cell leukemia/lymphotropic viruses HTLV-I, HTLV-II, HTLV-III and HTLV-IV and viruses that infect old-world primates such as Simian T-lymphotropic viruses STLV-I, STLV-II, STLV-III, and STLV-V[63-66]. HTLV-I is an enveloped, diploid single-stranded RNA virus of the Retroviridae family. Upon infection, the genome is copied into a double-stranded DNA form that integrates into the host cell genome, and at this point the virus is referred to as a provirus[67]. HTLV-1 is a complex retrovirus that specifically targets CD4 positive T cells for infection. Oligoclonal expansion of HTLV-I-infected cells *in vivo* is also observed in HAM/TSP patients and some asymptomatic HTLV-I carriers, showing that HTLV-I-infected cells have proliferative potential[68].

The HTLV-1 provirus contains multiple gene products that contribute to T-cell transformation. One of these genes is the retroviral oncogene *tax. Tax*

expression was shown to induce T-cell immortalization on its own[69]. In newly infected cells, Tax activates the expression of the cytokine Interleukin-2 (IL-2) and the alpha subunit of its receptor (IL2RA), resulting in autocrine signaling that drives cell proliferation. In patients, full transformation into ATLL involves a long latency of up to five decades. Transformation by the virus both in vitro and in patients occurs in a slow stepwise manner and progresses from a polyclonal to a monoclonal dominant clone with respect to proviral integration and decreased dependence on IL-2 for proliferation[68, 70-73]. Conversely, the level of HTLV-I antigen expression in freshly isolated peripheral ATLL cells is extremely low. Human T-cell leukemia virus type I core, envelope, polymerase and Tax proteins are recognized by HTLV-I-specific cytotoxic T-lymphocytes[74-76]. *Tax* is frequently deleted or epigenetically silenced by deletion or promoter methylation respectively, within the proviral allele; however, there is constitutive activation of proteins downstream of IL-2 induction[77, 78]. The loss of *tax* could be induced by an immune response against Tax expressing T cells[79-81].

Because the ATLL cells maintain high levels of proliferation and signaling downstream of IL-2 despite the loss of *tax* expression[82-84], this population of cells is at risk for the development of genetic and cytogenetic changes leading to lymphoma. These high levels of proliferation suggest that gain of function mutations must occur within this pathway in host cells. Activating mutations in the kinase necessary to this pathway may play a role in transformation. Somatic gain of function mutations in the IL-2 pathway would explain the long latency before disease manifestation and the extremely low penetrance of the disease.

Once the IL2Rα chain expression is up-regulated by Tax, the high affinity heterotrimer of the IL-2 receptor is formed. JAK3 is constitutively bound to the common γ chain of the IL-2 receptor where it phosphorylates its targets[85, 86]. Upon ligand binding, the non-receptor tyrosine kinases, JAK1 and JAK3 are activated; this initiates phosphorylation of important downstream substrates including signal transducer and activator of transcription 5 (STAT5). Other downstream targets such as AKT (Protein Kinase B) are important for T cell survival[87]. Although the viral oncoprotein Tax was shown to play a significant role in leukemogeneis, when most of the HTLV-I infected cells no longer express Tax*, tax* repression is important for the early carrier phase[88]. Additional cellular mutations must be acquired for the development of ATLL.

Interleukin Signaling and the JAK/STAT Pathway

Interleukin Receptor Family

Cytokines function by binding the extracellular portions of receptors, leading to the phosphorylation and activation of the receptor and proteins to the intracellular portion of the receptor. Once triggered by specific cytokines, the JAK/STAT pathway influences immune response, embryonic development, and cellular transformation. Most cytokine receptors lack intrinsic kinase activity but instead interact with the Janus kinase family of non-receptor tyrosine kinases. The activity of the JAKs directly induces downstream responses.

Interleukin 2 (IL-2) Receptor Signaling

Interleukin-2 (IL-2) was discovered in 1976 as a T-cell growth factor-exhibiting activity in the supernatants of activated T cells[89]. IL-2 is produced primarily by $CD4^+$ T cells following their activation by antigen. IL-2 is a cytokine that drives multiple aspects of T-cell growth, augments natural killer cell (NK) cytolytic activity, and induces the differentiation of regulatory T cells. The heterotrimeric IL-2 receptor is composed of α, β, and γ chains. The β and γ chains are constitutively expressed in T cells. Three different IL-2 receptor chains exist that together generate low, intermediate, and high affinity IL-2 receptors[90, 91] (Figure 1). The ligand-specific IL-2 receptor α chain (IL-2Rα,CD25, Tac antigen), which is expressed on activated but not non-activated lymphocytes, binds IL-2 with low affinity. The combination of IL2Rβ (CD122) and IL2Rγ (common cytokine receptor γ chain (γ_c) or CD132) together forms an IL-2Rβ/γ_c complex in memory T cells and NK cells that binds IL-2 with intermediate affinity. When all three receptor chains are co-expressed on activated T cells and regulatory T cells, IL-2 is bound with high affinity (Figure 1)[92]. IL-2 induces heterodimerization of IL-2Rβ and γ_c chains of its receptor and activates the Janus family tyrosine kinases, Jak1 and Jak3. Whereas Jak1 associates with IL-2Rβ, Jak3 associates primarily with γ_c but also with IL-2Rβ. Jak3-IL-2Rβ association is

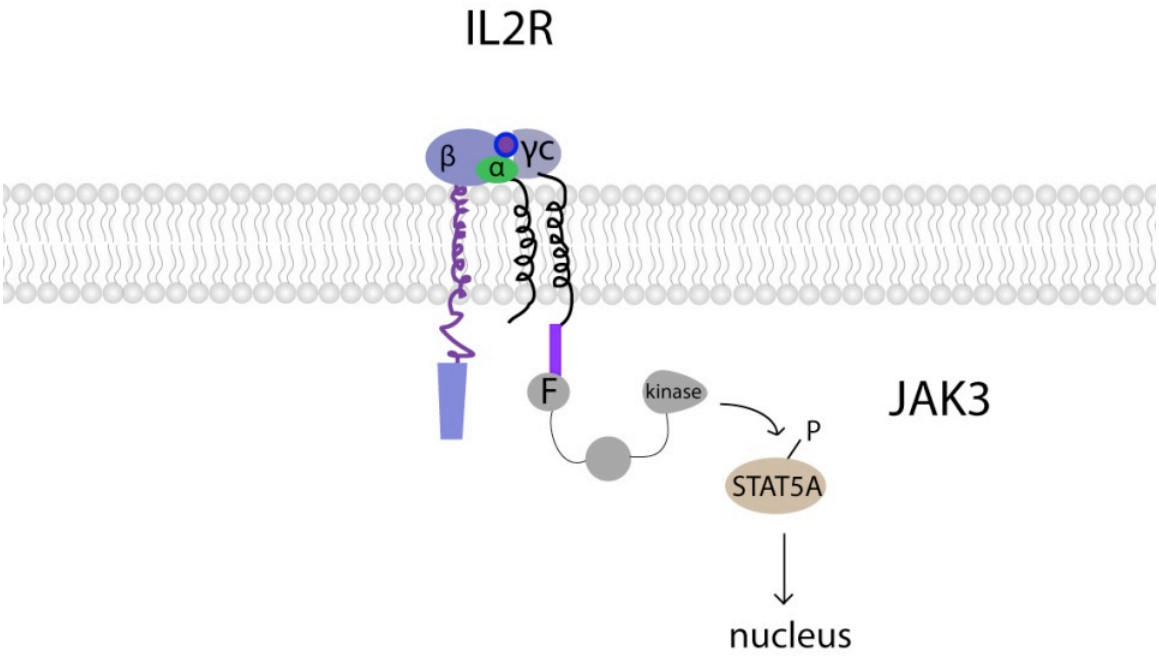

Figure 1. The heterotrimeric IL-2 receptor. IL2R is comprised of α, β, and γ subunits. JAK3 protein (grey) binds the γ subunit via the FERM domain (F). Upon stimulation with IL-2, JAK3 is activated and phosphorylates STAT5.

Jak1-independent, this association is important for IL-2-induced Stat5 activation. Jak1 and Jak3 were shown to associate only in the presence of IL-2Rβ, demonstrating that these kinases can not directly converge but instead simultaneously bind to IL-2Rβ[93, 94].

The IL-2 signal leads to the activation of three major signaling pathways: phosphoinositol-3'-kinase (PI3K)/AKT, Ras-MAP kinase, and JAK-STAT pathways, with JAK1 and JAK3, and STAT5A and STAT5B being the JAKs and STATs involved. Simultaneous loss of both Stat5a and Stat5b leads to perinatal lethality with anemia and leukopenia. Together, these three signaling pathways mediate cell growth, survival, activation-induced cell death, and differentiation[92, 95].

Janus Kinases (JAKs)

Janus Kinase Receptor Family

While JAK1, JAK2 and TYK2 are expressed ubiquitously, JAK3 is thought to be specifically expressed in hematopoietic cells including B-cells, T-cells and natural killer cells[96-98]. The moniker refers to the two-faced Roman god, Janus, because the JAKs possess two near-identical phosphate-transferring domains, the kinase and pseudokinase domains. One domain exhibits the kinase activity, while the pseudokinase domain negatively regulates the activity of the first[99-101].

The JAK proteins are comprised of FERM, SH2, pseudokinase and kinase domains[102]. The FERM domain is predominantly responsible for binding the

cytoplasmic tails of cytokine receptor chains[103, 104]. The pseudokinase domain structurally resembles a kinase domain but does not function as one and acts as a negative regulator of kinase activity[99].

Crystal structures for all four family members have been illustrated for the C-terminal kinase domains in the presence of ATP binding site occluding inhibitors including tofacitinib[105-109]. No other domains have been crystallized for any of the Janus kinases. Janus kinases are critical to the signaling induced by various interleukins. They are therefore involved in regulation of the immune system and were found to play crucial roles in the development of various diseases including cancer and autoimmune disorders that are associated with dysregulation of these signaling pathways. Since many cytokine receptor proteins lack enzymatic activity, they are dependent upon JAKs to initiate signaling upon binding of their ligands.

JAK activation results in phosphorylation of the STAT transcription factors. There are seven known members of the STAT family of transcription factors: STAT1, STAT2, STAT3, STAT4, STAT5A, STAT5B, and STAT6. Upon activation of the receptor, the relevant JAK family member is phosphorylated, allowing it to interact with and subsequently phosphorylate a specific STAT. Upon activation, STAT complexes translocate into the nucleus, bind DNA, and initiate transcription[110].

Janus Kinase 3 (JAK3)

Janus kinase 3 (JAK3) is a non-receptor tyrosine kinase vital to the regulation of B and T-cells. JAK3 has four characterized domains: the kinase domain, the pseudokinase domain, the SH2-like domain and the FERM domain. The kinase domain is the principal domain for JAK3 activity. The pseudokinase domain was shown to be involved in regulating the activity of the kinase domain[111]. JAK3 is required for signaling of the type I receptors that use the common γ_c chain. JAK3 constitutively binds the cytoplasmic tail of γ_c via the JAK3 FERM domain. Upon binding of cytokine, the receptor allosterically changes, triggering the bound JAKs to autophosphorylate and to phosphorylate the receptor itself at specific tyrosines.

Mutations that abrogate JAK3 function cause autosomal severe combined immunodeficiency disorder (SCID). JAK3 knockout mice do not possess T-cells and have a reduced number of nonfunctioning B-cells[112]. JAK3 is a mediator of interleukin-8 (IL-8) stimulation of neutrophils in addition to its well-known roles in T cells and NK cells[113].

FERM Domain

The FERM domain is named for the four proteins it was originally identified in, band 4.1, ezrin, radixin, and moesin. FERM domains are present in structural proteins such as the ezrin-radixin-moesin (ERM) family of proteins as well as in signaling proteins such as FAK and several tyrosine phosphatases[114]. Two different mechanisms for regulation of protein interactions by FERM

domains have been described. In the first mechanism, FERM domains can mediate intermolecular interactions, usually at the site of direct interaction with the cytoplasmic tails of transmembrane proteins[115]. In the second mechanism, FERM domains can function to directly regulate protein function for the core protein via intramolecular interactions. The best-characterized FERM domain-mediated interactions are those of the ERM family of proteins. The ERM proteins bind via their FERM domains to the cytoplasmic domains of transmembrane proteins such as CD44[116]. Other examples of FERM domain-mediated intermolecular interactions include binding of the FERM domains of JAKs with the γc and gp130 subunits of cytokine receptors. The FERM domains of the ERM proteins also bind intramolecularly to a site within the C terminus. This interaction obscures the CD44 binding site within the FERM domain and an actin-binding site in the C-terminal tail. The major function of the JAK3 FERM domain was described as binding the cytoplasmic tail of γ_c[117]. The FERM domain of JAK3 interacts with the C-terminal catalytic domain, and this interaction was shown to mediate catalytic activity[111]. When coexpressed, the FERM domain directly associated with and enhanced the activity of the isolated kinase domain in JAK3[111].

FERM domains are made up of three subdomains: F1 with a ubiquitin-like-grasp fold, F2 with an acyl-coenzyme A-binding protein like fold, and F3 which shares the fold of phosphotyrosine binding. F1, F2, and F3 together form a compact clover-shaped structure[118-120].

The role of Janus kinases in disease

Janus kinases are critical to the development and function of multiple hematopoietic lineages. Loss of *Jak1, Jak3, or Tyk2* results in impaired lymphopoiesis whereas *Jak2* deficiency results in embryonic lethality because of the absence of definitive erythropoiesis. These effects are attributed to lack of signaling through various cytokine induced pathways[121-129].

The JAK family kinases are central players in normal and malignant hematopoiesis and are potentially subject to oncogenic somatic mutations. These non-receptor tyrosine kinases are recruited for signal transduction by cytokine receptors that do not possess tyrosine kinase activity of their own[102]. Genetic activating or gain-of-function mutations predominantly located within the pseudokinase domains of Janus kinase family members have been associated with to the development of various hematologic malignancies. Mutations in JAK1 and JAK3 have been associated with acute myeloid leukemia, acute lymphoblastic leukemias, T cell acute lymphoblastic leukemia and natural killer/T-cell lymphoma[5, 6, 130-135 138, 146]. JAK2 mutations have been described in B lineage acute lymphoblastic leukemia, myeloid malignancies, and myeloproliferative neoplasms[133, 136-140]. One of the most studied Janus kinase mutations occurs in the pseudokinase domain of the JAK2, V617F[141]. The discovery of this mutation led to studies on drug treatments, led to advancements in understanding of the pathogenesis of disease, allowed for revisions in classification and diagnostic criteria, and provided a target for treatment of myeloproliferative neoplasms (MPNs). As valine 617 of JAK2 is conserved as valine 678 of TYK2, the effect of

a homologous mutation in TYK2 V678F also has the potential to induce disease. TYK2 V678F augments the transcriptional activity of STAT3 and STAT5 and induces BaF3 autonomous cell growth and hyper-responsive to IL-3[142]. This mutation is not derived from an existing tumor. Mutations in TYK2 have been implicated in multiple sclerosis, autoimmune disease, and systemic lupus erythematosus[143-145].

In addition to this work on ATLL, JAK3 mutations have also been implicated in the development of acute megakaryocytic leukemia and natural killer T cell lymphoma. It is important to note that the only other mutation described in the FERM domains for any members of this family is a rare non-synonymous single nucleotide polymorphism (SNP) P132T that has been implicated in acute megakaryocytic leukemia[5, 6].

IL2RG is mutated in humans with X-linked severe combined immunodeficiency (XSCID) and physically interacts with JAK3, which when mutated also causes a $T^-B^+NK^-$ form of SCID[117, 147-149]. In XSCID and JAK3-deficient SCID, the lack of signaling by IL-7 and IL-15, respectively, explains the lack of T and NK cell development[150], whereas defective signaling by IL-4 and IL-21 together explain the non-functional B cells found in this disease[151]. Some of these germline SCID mutations occur in the FERM domain of JAK3 and abolish binding to γ_c, while others create a premature stop codon, which generates a truncated kinase negative form of JAK3[149, 152]. JAK3 deficient mice express a similar phenotype with a complete loss of T and NK cell development and non-functioning B cells.

Cell Cycle Regulators ARF/INK4A

Tumor suppression and cell cycle regulation

The *CDKN2A* locus encodes two tumor suppressor genes, p16(INK4A) and p14(ARF) in human or p19(ARF) mouse, transcribed using alternative exons 1 (alpha) spliced onto the same exons 2 and 3[153]. p16(INK4A) and p14(ARF) are crucial for two cancer suppressor pathways and are both capable of inhibiting cell-cycle progression. p14(ARF) functions as an indirect stabilizer of p53, and p16(INK4A) inhibits cyclin-dependent kinase 4.

Role of CDKN2A family in leukemia

The homozygous deletion of *CDKN2A* was detected at high rates in many types of leukemias[154-159]. Alterations of *CDKN2A* expression occur in 17-68% of the acute and 5-26% of the chronic ATLL samples[160-166]. *CDKN2A* deletions were associated with the development of acute/lymphomas but not chronic/smoldering ATLL suggesting that these genetic events drive the late stage of leukemogenesis in ATLL. In chronic myelogenous leukemia, alteration of *CDKN2A* is involved in the progression to lymphoid blastic crisis from the chronic phase as well as the evolution from low grade to high grade Non-Hodgkin lymphoma[167, 168]. Similarly, there is a higher frequency of deletions of *CDKN2A* in acute lymphoblastic leukemia (ALL).

Loss of *CDKN2A* expression leads to a pathologically higher grade malignant behavior, progressive disease, and poor outcome. ATLL patients with a deleted *CDKN2A* have a significantly shorter survival rate than those with an intact gene[169]. Acute ATLL individuals with deletions of *CDKN2A* survived for less than three years, whereas ATLL patients with the gene intact survived for up to eight years[161].

Methylation of the 5' CpG island of *CDKN2A* is associated with transcriptional silencing of this gene in many neoplasms, including leukemias and lymphomas[170-172]. The *CDKN2A* is more frequently methylated in fresh tumor cells isolated from patients with acute (47%) and lymphomatous (73%) than in those with chronic (17%) and smoldering (17%) ATLL. The expression of p16 mRNA was markedly decreased in the samples with methylated *CDKN2A*, especially if the p16 promoter region was methylated. In contrast, methylation of p16 was not identified in asymptomatic HTLV-1 carrier or uninfected individuals[173]. Tax-immortalized T cell lines and normal CD4+ T cells expressed comparable levels of p16 mRNA[174].

Tax suppresses p16-mediated inhibition of U2OS cell growth and directly interacts with p16(INK4A)[175, 176]. A point mutation of p16 is present in the HTLV-I infected MT-1 cells, and these cells do not express TAX. In contrast, wild-type p16(INK4A) is abundantly expressed in MT-2 and Hut-102 cells and they do express TAX. These results suggest that inactivation of p16(INK4A) expression either by genetic alteration or possibly TAX expression is important for T cell transformation[169].

Table 1. Origins of Ethnically matched control samples.

Samples #	Specimen ID	Country of Origin
1	V280	Haiti
2	V289	Haiti
3	V290	Jamaica
4	V291	Haiti
5	V292	Haiti
6	V293	Jamaica
7	V295	Jamaica
8	V281	Jamaica
9	V296	Haiti
10	V297	Jamaica
11	V298	Haiti
12	V299	Haiti
13	V304	Haiti
14	V307	Haiti
15	V312	Jamaica
16	V314	Jamaica
17	V318	Haiti
18	V319	Jamaica
19	V321	Jamaica
20	V322	Jamaica
21	V325	Jamaica
22	V326	Jamaica
23	V327	Jamaica

CHAPTER II

MATERIALS AND METHODS

Patient samples, sequencing, and mutational analysis

Genomic DNA was isolated from 36 ATLL patients, who were treated at the NIH Clinical Center and consented under an IRB-approved protocol. Most of these patients were from Jamaica. Likewise, 23 ethnically matched control patients (Table 1) had whole blood drawn for genomic DNA preparation under an IRB-approved protocol. The entire JAK3 gene was analyzed by PCR amplification of specific exons (Table 2) and analyzed for sequence alterations by SpectruMedix's Reveal Genetic Analysis System on samples where the leukemia cells were purified from the buffy coat. Standard Sanger DNA sequencing (GeneWiz and Vanderbilt Core Sequencing facility) was subsequently used to analyze all potential mutations as determined by Reveal Genetic Analysis System. Multiple independent PCR amplicons cloned into pGEM-T Easy (Promega) were used to analyze samples that did not have pure leukemic samples or in some instances had <10% leukemic cells. Oligonucleotide primers used for PCR are available in Table 3. The proposed JAK3 FERM domain structure was determined by ClustalW alignment with the FAK FERM domain and analyzed with PyMol using FAK FERM coordinates. The crystal structure of the JAK3 kinase domain was available from the RCSB Protein Data Bank[107].

Table 2. JAK3 FERM domain mutations and SNPs identified in ATLL patients. Three DNA point mutations and 1 SNP were identified in JAK3 exon 4 in five out of the thirty-six ATLL patients sampled. One nonsynonymous SNP listed in the NCBI Entrez database P132T was identified in 1 of our 36 ATLL patients sampled. Five Single Nucleotide Polymorphysims (SNPs) are listed for JAK3 FERM domain in NCBI Entrez database.

Cluster id	Region of JAK3	# Patients	dbSNP Allele	Protein Residue
rs3212711	Intron 1	2 +HUT102	C to T	NA
rs3212712	Intron 1	2 +HUT102	G to A	NA
rs3212713	Intron 1	2 +HUT102	G to A	NA
rs3212716	Exon 3	1	C356G	Leu99 synonymous
rs3212718	Intron 3	1	A to G	NA
rs3212719	Intron 3	1	A to G	NA
rs3212723	Exon 4	1	C453A	Pro132Thr
novel mutation	Exon 4	1	T525C	Leu156Pro
novel mutation	Exon 4	2	A606G	Glu183Gly
novel mutation	Exon 4	1	G573A	Arg172Gln

Table 3 Primer list for REVEAL PCR and sequencing of 36 ATLL and 24 ethnic matched control samples

	Antisense	Sense	Product size
Exon2:	AGCTTCCAATCTTGGCCC	CAGAAGTCCAATCCCCTCTG	321
Exon3:	CAAGTGACCCACCCTCTCTG	GATCTGGACGGTTGGGTATG	356
Exon4-5:	AGCCCACGTTGCTCACTC	CCCCACCATAATGTCACTCC	592
Exon6:	TACCACTCTCCGGCCCC	TTTGTGTGTGTCCCCGC	435
Exon7-8:	TGAGGCATAGAGAAGGGGAG	ATAGGGAGTGGATGGTGTGG	537
Exon9:	ATTCAAACGTCACCTCCTCC	TACCTGAATTTGAGCCCAGG	248
Exon10:	GGCTTTAATGAGCAAGTGGC	CTGGAATGAGTTCATGGTGC	976
Exon11-12:	TTTCTCTGCATCCACGACC	TTGGGGACTTTTCACCTCTG	583
Exon13:	AGAGGTGGGAAGAACAGCC	TTGGGATTATTGGAGTGGAAG	211
Exon14:	AATTCCTCTTCCACCCAGAG	GCAGAACCTCCTCAACACAAG	261
Exon15-16:	GACTGGATGTCAGTCTGCCC	GCCAAACAGACTCTTCATTCATC	496
Exon17:	ACCACGCTCCTTCCACTG	AGATTGGGGTGGGTCTATTG	275
Exon18-19:	GCAGGAGGGTAAGAATGTGC	TCAACTCAGGAGTGGGGC	547
Exon20:	ACCCCAAACCACTCCTCAG	GCAAAACTGAGGTCGAGAGG	330
Exon21:	CTGGGGAGCAAAGCAGC	GTCACGCTTGGGGTACCTG	337
Exon22:	CAGGCGCAGACAGGTTG	CCCCTCTTCCTGTCCTTTC	253
Exon23:	TGAAAGTGCTCGACTTGCC	ATCACAGATGGCCCCTACC	382
Exon4	CAGGAAACAGCTATGACCGCCCTGGGTCATAGGAACAC	GTAAAACGACGGCCAGTGGGGTCAGCCCAGGATTG	~400
Exon16	CAGGAAACAGCTATGACCCAACCTCACCAGACACACAGG	GTAAAACGACGGCCAGTACCCCCACTTTGACAGAAGG	~400

Viruses and plasmid constructs

MSCV-ires-GFP (MIG) constructs expressing mutant JAK3 cDNAs were constructed by introducing mutations into the wild type JAK3 using Stratagene QuikChange kit (Table 4). The wild type JAK3 and A572V JAK3 mutant constructs were provided by Dr. Brian Druker and cloned into MIG. Site directed mutagenesis was verified by full sequencing of the JAK3 cDNA insert. Virus was made by transient transfections of JAK3-MIG constructs into Phoenix cells by the $CaPO_4$ method along with pCL-Eco. Viral titers were determined by flow cytometric analysis of 3T3 cellsinfected with recombinant retrovirus for GFP expression. pCMVSport6-IL2Rβ and pCMVSport6-STAT5A constructs were obtained from the Mammalian Gene Collection. IL2Rα was cloned into pcDNA 3.1(+) (Invitrogen) from pINCY-IL2Rα (Open Biosystems) construct. IL-2Rγ was amplified from HuT-102 cDNA and cloned into pcDNA 3.1(+). All inserts were fully sequenced.

Polymerase chain reactions (PCR)

Immunoglobulin Heavy chain

PCR analysis of Immunoglobulin Heavy chain (IgH) gene rearrangements and B cell differentiation was used to determine tumor clonality. Genomic DNA samples from splenic tumors were subjected to PCR with primers designed to amplify junctions between D and J regions. For nested PCR analysis of DJ recombination, genomic DNAs were subjected to PCR with primers designed to

Table 4 Primer list for site directed mutagenesis of JAK3 to introduce ATLL mutations.

	Antisense	Sense	RE Site Introduced
L156P	CCCGCGGAGGGGCACCCGGGGTCAGAGTTCCTCGTCCC	GGGCGCCTCCCCGTGGGCCCCAGTCTCAAGGAGCAGGG	ApaI
E183G	CGCTCTCGTCCGGGTCGCCGGCCCTCCCGACGACTTCTGACAGTCG	GCGAGAGCAGGCCCAGCGGCCGGGAGGGCTGCTGAAGACTGTCAGC	BglI
R172Q	CTCTCGCGCCATCTGGGCCAGGTCCAA	TTGGACCTGGCCCAGATGGCGCGAGAG	Bst51
P132T	GGTGCTCCAGGACTGTTAAGTCAAGGATAGC	GCTATCCTTGACTTAACAGTCCTGGAGCACC	MseI
K855A	GCTGCAGCTGTGCCACGGCCACC	GGTGGCCGTGGCACAGCTGCAGC	BtgI
Y100C	CGAATCCTGCACAGCAGGACTTGGG	CCCAAGTCCTGCTGTGCAGGATTCG	BsgI

amplify four possible junctions between D-Q52 and JH regions. The primers for the first round were: CACAGAGAATTCTCCATAGTTGATAGCTCAG (p1569, DH Q52-1; sense) and AGGCTCTGAGATCCCTAGACAG (p1570, JH 4-1; antisense). PCR conditions were as follows: denaturation at 95°C for 1 min, annealing at 60°C for 1 min, extension at 72°C for 2.5 min (28 cycles). Two μl from each reaction were subjected to a second round of PCR using a pair of internal primers: GCCTCAGAATTCCTGTGGTCTCTGACTGGT (p1571, DH Q52-2; sense) and GGGTCTAGACTCTCAGCCG-GCTCCCTCAGGG (p1572, JH 4-2; antisense) PCR conditions were as follows: denaturation at 95°C for 20 s, annealing at 60°C for 1 min, extension at 72°C for 2 min (35 cycles). Secondary PCR products were analyzed on a 2% agarose gel[177].

T- cell Receptor J-beta (TCRβ)

PCR analysis of gene T- cell Receptor J-beta (TCRβ) rearrangements were used to analyze tumor clonality. Genomic DNAs from splenic tumors were subjected to PCR with primers designed to specifically amplify the J-beta region of T-cell receptor gene, TGGTTTCTTCCAGCCCTCAAG (p1242) and TGGAAAGAGTGGAGATGAGGCTAAGAGAAA (p1243). PCR conditions were as follows: denaturation at 94°C for 2 min (1 cycle), 94°C for 30 sec annealing at 55°C for 1 min, extension at 72°C for 30 sec (30 cycles), final extension 72°C for 7 min (1 cycles) and 4°C hold[178].

Splinkerette (Splk)

Nested splinkerette PCR for identifying MSCV integration sites was adapted from Yang Du and Neal Copeland. One µg of genomic DNA from splenic tumors digested with NlaIII or MseI and SacI was ligated to double stranded restriction enzyme specific linker Splink-NlaIII (U250, splinkerette-LN CCTCCACTACGACTCACTGAAGGGCAAGCAGTCCTAACAACCATG and U252, Splink-NlaIII GTTGTTAGGACTGCTTGGAGGGGAAATCAATCCCCT) or Splink-MseI (U251, Splinkerette-LM CCTCCACTACGACTCACTGAAGGGCAAGCAGTCCTAACAAC and U253, Splink-MseI TAGTTGTTAGGACTGCTTGGAGGGGAAATTCAATCCCCT). Primary PCR primers were (U256, MSCV-LTR1) TCTCGCTTCTGTTCGCGCGCTTC and (U254 Splinkerette-P1) CCTCCACTACGACTCACTGAAGGGC2' and conditions were 94°C; 10 cycles 10" 94°C, 2' 70°C (-0.5° per cycle); 20 cycles 10" 94°C, 2' 65°C; final extension 7' 70°C. Secondary PCR utilized 1:50 dilution of Primary PCR product. Secondary PCR primers were (U257, MSCV-LTR3) CGTCGCCCGGGTACCCGTATTC and (U255 Splinkerette-P2) GGGCAAGCAGTCCTAACAAC. Secondary PCR conditions are 2' at 94°C; 30 cycles 15" 94°C, 30" 61°C, 1'30" 65°C; final extension 7' 68°C. Final PCR products were resolved on 2% agarose gel. Bands were cloned using pGEM-T Easy cloning vector and sequenced.

Real-time quantitative PCR

Genomic DNA for patient exhibiting L156P mutation was quantified for *tax* copies using quantitative PCR (qPCR). Tax quantification approximates the

frequency of leukemic cells in the buffy coat sample. 100 ng of total genomic DNA was used for PCR using the iQ SYBER Green Supermix (Bio-Rad) on an iCycler (Bio-Rad). PCR reactions were performed in triplicate. The expression of the gene of interest was calculated relative to the levels of STS.

Flow cytometry and protein analysis

Flow Cytometry Analysis

To obtain single cell suspensions of bone marrow, the tibias and femurs from each transplanted mouse were flushed. The spleens or thymi were pulverized to obtain single cell suspensions of transplanted mice. Peripheral blood was obtained by retro-orbital bleed under isoflurane-induced anesthesia. Red blood cells were lysed using 1ml of Erythrocyte lysis buffer for up to $2x10^7$ cells on ice for 5 minute. Following lysis $2x10^5$ to $5x10^5$ cells were aliquoted into individual tubes. The cells were stained with antibodies against: CD3, CD25, CD4, CD8, CD45.1, CD45.2, B220, CD19, Gr-1, or Mac-1.

Flow cytometry experiments were performed in the Vanderbilt Flow Cytometry Shared Resource core. Flow cytometry data acquisition was performed on an LSRII 3 laser (BD Biosciences) and analyzed with FACS Diva software (BD Biosciences). BaF3 cells transduced with various MIG-JAK3s were sorted for GFP on a FACS Aria (BD Biosciences). These cells were also stained with Vybrant Dyecycle violet (Invitrogen) and the proportion of cells in each cell cycle stage was determined by flow cytometry and analyzed using FlowJo software (Tree Star).

Western Blot Analysis

Immunoprecipitations were performed in BaF3 cells transduced with MIG-JAK3 using anti-JAK3 (Santa Cruz Biotechnology, Inc., Santa Cruz, CA) and anti-γc antibodies (R&D Biosystems, Minneapolis, MN). Detection of total and phosphorylated protein targets was performed using the LI-COR Odyssey® Infrared Imaging System. Antibodies used were anti-P-STAT5 (Y694) (BD Transduction Laboratories, BD Pharmingen, San Diego, CA), anti-P-AKT (S473), anti-ERK1/2, anti-P-ERK1/2 (T202/T204) (Cell Signaling Technology, Beverly, MA), anti-STAT5, anti-IL2Rα, anti-IL2Rβ, anti-γ_c, anti-JAK3, anti-STAT3, anti-P-STAT3 (Y705), and anti-P-JAK3 (Y980) (Santa Cruz Biotechnology, Inc., Santa Cruz, CA) and 680nm and 800nm infrared dye-conjugated secondary antibodies (LI-COR).

Immunofluorescence staining

$1x10^5$ BaF3 cells were cytospun onto glass slides at 800rpm for 5 min, fixed in 3% paraformaldehyde for 15 minutes at room temperature, washed thrice with PBS, permeabilized in 0.5% Triton X-100 for 15 minutes at 24°C, and blocked with 1% fetal bovine serum (FBS) in PBS for 30 minutes at room temperature. JAK3 was detected using a 1:50 dilution of anti-JAK3 (Santa Cruz, sc-513) in 10% FBS for 1 hour at room temperature, washed thrice with PBS and incubated with a 1:500 dilution of secondary fluorescent antibody (invitrogen 546 anti Rabbit IgG #A11010) and the nuclei were counterstained with 1μg/ml 4,6-diamidino-2-phenylindole (DAPI). Images were digitally captured using a Zeiss

LSM 510 META inverted confocal microscope.

Cell Culture

HEK 293T cells

HEK 293T and Phoenix cell lines were obtained through ATCC. Reconstitution of IL-2 receptor, JAK3/STAT5 pathway was performed by $CaPO_4$ transient transfection of 2.5 μg of pCMVSport6-STAT5a, pcDNA-3.1-IL2Rα, and pCMVSport6-IL2Rβ; 5μg of pcDNA3.1-γc and MIG-JAK3 constructs and grown in the presence of hIL-2 for 24 hours. Expression levels of all components were quantified by western blot or flow cytometry.

BaF3 cell lines and assays

BaF3 cells were obtained from Dr. Elizabeth Yang. Ba/F3 cells are IL-3-dependent mouse pro-B cells and were cultured in IMDM medium supplemented with 10% fetal bovine serum, 1% pen/strep, and 2% supernatant of the WEHI-3B cell line as a source of IL-3. BaF3 cells were serially transduced 3 times and GFP-positive cells were sorted by flow cytometry after 6 days in culture. Cytokine-independent growth assays were performed as described[179]. Once cytokine independence was established, mutant JAK3 expressing cells were maintained in the absence of mIL-3 and used in all subsequent experiments. Protein stability was determined by starving BaF3 cells of serum for 1 hour followed by the addition of 100μg/ml cycloheximide for 0, 0.5, 1, 2, and 3 hours before cells were lysed and JAK3 expression analyzed by western blot analysis.

Stably transduced BaF3 cells were incubated at 37 °C for 30 minutes, 1, 2, 3, or 4 hours with proteasome inhibitors MG132 (10μM) (Sigma) or DMSO only. Cells were then lysed in radio-immunoprecipitation assay buffer (RIPA) with protease inhibitors and analyzed by western blot with antibodies against JAK3 and tubulin. Protein expression levels were quantified and graphed[180, 181].

Stably transduced BaF3 cells were incubated at 37 °C for 1, 4, 24, or 48 hours with lysosome inhibitors chloroquine (0-200μM)(Sigma). Cells were then lysed in RIPA with protease inhibitors and analyzed by western blot with antibodies against JAK3 and tubulin[182-185].

The JAK3 inhibition assays were performed on BaF3 cells expressing mutant JAK3s using tofacitinib (Selleck Chemicals LLC, Houston, Texas) at the concentrations listed after zero, 12, and 24 hours. Cells were incubated with anti-Annexin V antibody and propidium iodide and analyzed by flow cytometry at 24 and 48 hour of incubation with tofacitinib. Protein was obtained at all time points and cells were counted at 0 and 24 hours. Inhibitors BEZ-235 (Selleck), BKM-120 (Active biochem), and CI-1040 (gift of Dr. Carlos L. Arteaga) against PI3K/mTOR, PI3K and MEK respectively were used in (3-(4,5-Dimethylthiazol-2-yl)-2,5-diphenyltetrazolium bromide) assays as described. For MTT assays, MIG-JAK3-transduced BaF3 cells were plated at 200,000 cells/well in a 96 well plate with the concentrations of 1000 cells/μl in triplicate using media without phenol red at concentrations of tofacitinib listed. At 48 hours 150μL of media was removed, 20μl of 5mg/ml 3-(4,5-Dimethylthiazol-2-yl)-2,5-diphenyltetrazolium bromide (MTT) reagent was added and cells were incubated for an additional 4.5

hours. Cells were lysed with the addition of 100µl 0.1N HCl in isopropanol. Plates were scanned on a Molecular Devices Versa Max microplate reader and data were analyzed using SoftMax Pro software.

OP9 in vitro T cell differentiation assay

OP9-DL1 and OP9-GFP cell lines were provided by Dr. Juan Carlos Zúñiga-Pflücker. The T-cell differentiation assay was performed using *JAK3*^{KO} fetal liver cell. *JAK3*^{KO} fetal liver stem cells from day E15.5 fetal livers were collected. *JAK3*^{KO} mice were acquired from Jackson Laboratory[128, 129, 186]. Mononuclear cells were isolated using lymphocyte separation medium (MediaTech). Cells were magnetically sorted to enrich for c-Kit^{+} Lin^{-} Sca-1^{+} (KLS) cells (StemCell Technologies, Inc., cat# 19756). KLS cells were enriched for using StemCell Technologies' mouse CD117 selection cocktail (cat# 18757) and the correct immunophenotype was verified by flow cytometry. Cells defined by the KLS phenotype were then transduced with MIG-JAK3, and co-cultured with irradiated OP9-DL1 or OP9-GFP cells in the presence of 6ng/ml mIL-7 and 6ng/ml mFlt3 for 28 days at a concentration of 5x10^{3} lineage-negative cells per well. KLS enriched cells were cultured in 24-well plates containing 75% confluent irradiated OP9-DL1 or OP9–GFP with 6ng/ml IL-7 and 6ng/ml Flt-3. Stem cells were collected,

Table 5 Cell lines and culture media

	Cell Culture Media
BaF3	IMDM 10% FBS, 1% Penicillin/Streptomycin, 2% WeHi conditioned media
WEHI-3B	IMDM 10% FBS, 1% Penicillin/Streptomycin
OP9-DL1	alphaMEM, 20% FBS, 1% Penicillin/Streptomycin
OP9-GFP	alphaMEM, 20% FBS, 1% Penicillin/Streptomycin
HuT-102	RPMI, 10% FBS, 1% Penicillin/Streptomycin, 100U/ml hIL-2
MT-2	RPMI, 10% FBS, 1% Penicillin/Streptomycin
HEK 293T	DMEM, 10% FBS, 1% Penicillin/Streptomycin
Phoenix	DMEM, 10% FBS, 1% Penicillin/Streptomycin

washed and plated on fresh irradiated OP9 cultures every 7 days. Lymphocytes were transferred to freshly irradiated OP9-DL1 cells and analyzed by flow cytometry for T- and B-cell differentiation markers every 7 days as described[187]. OP9-DL1 cells were maintained in culture as previously described. Cells were maintained in culture with alpha-MEM media with 20% FCS and 1% pen/strep in 100cm plates.

Additional Cell lines

Hut-102 and MT-2 cell lines were obtained through the AIDS Research and Reference Reagent Program, Division of AIDS, NIAID, NIH. All cell lines were maintained in the recommended media (Table 5).

In vitro Kinase assay

Kinase assays were performed using a LANCE®Ultra time-resolved fluorescence resonance energy transfer (TR-FRET) from Perkin Elmer. Assays use a Europium chelate donor fluorophore-conjugated antibody, PT66 (Eu), against the P-tyrosine of substrate ULight-JAK-1 (Y1023), which is a short peptide sequence from JAK1 that is phosphorylated by JAK3. The ULight substrate has a small molecular weight acceptor dye with red-shifted fluorescent emission. This assay was optimized with recombinant human JAK3 (Signal Chem, Inc, amino acids 781 to the carboxy-terminus) containing only the kinase domain. Wild type or mutant JAK3 enzymes were purified from BaF3 cells by immunoprecipitation. Enzymes were incubated in Lance JAK3 assay buffer with

10 nM ULight-JAK-1 (Y1023) and 20μM ATP. Kinase reactions were terminated after 1 hour by the addition of 2x detection mixture containing PT66 Eu (8uM final) and EDTA (6mM final). After 30 min incubation in the detection mixture, FRET was detected at 665 nm after excitation at 340 nm using Perkin Elmer's Victor V Plate Reader.

Murine *in vivo* procedures

Bone Marrow Transduction and Transplantation

For bone marrow transduction transplantation (BMTT), a single cell suspension of bone marrow cells was prepared from the tibias and femurs of 6 week old *Cdkn2a*^{KO} mice. The red blood cells were lysed with erythrocyte lysis buffer (Buffer EL, Qiagen) as explained above. Cells were then spin transduced every 2 days with MIG-JAK3 expression virus containing WT, E183G or A572V mutations with 6ug/ml polybrene. Between spin transductions, cells were cultured at 5 x10^5 cells/ml in DMEM with 15% FBS, 10μg/ml mIL-6, 100μg/ml mSCF, 6ug/ml polybrene, and 1% pen/strep for 5 days. 2x10^6 transduced bone marrow and 5 x10^5 CD45.1 supporting cells were injected retroorbitally into lethally irradiated (9Gy) recipient CD45.1 mice (Figure 18). *CDKN2A*^{KO} mice were obtained from the National Cancer Institute's mouse repository[188]. Peripheral blood of transplanted mice was obtained every 1-2 months and analyzed for expression of GFP, CD45.1 and CD45.2 by flow cytometry. Mice were sacrificed as necessary due to morbidity of disease and thymus, spleen and bone marrow were removed for further analysis.

Secondary transplantion

$2x10^6$ splenocytes isolated from primary BMTTs were retororbitally injected into sublethally irradiated (7Gy) recipient CD45.1 mice. Mice were sacrificed as necessary due to morbidity of disease and thymus, spleen and bone marrow were removed for further analysis.

Histology and peripheral blood analysis

Peripheral blood smears or sections of spleen or bone marrow were fixed in 10% formalin for 24 hours at room temperature prior to embedding in paraffin and sectioning. Sections were counterstained with hematoxylin and eosin (H&E) by the Translational Pathology Shared Resource core at Vanderbilt Medical Center.

Assessment of *JAK3*^{KO} complete blood cell counts was performed on peripheral blood obtained by retro-orbital bleed with the HEMAVET HV950FS blood analyzer (Drew Scientific, Inc) on mice 4 and 11 weeks of age[128, 129, 186].

Xenograft and engraftment

NOD.Cg-*Prkdc*^{scid} *Il2rg*^{tm1Wjl}/SzJ (NSG) mice were acquired from Jackson Laboratory. These mice are severely immunocompromised and lack mature T cells, B cells, or functional NK cells, and are deficient in cytokine signaling[189]. NSG mice were lethally irradiated at 2.5Gy and intraperitoneally injected with 5 $x10^6$ primary ATLL cells obtained from frozen buffy coat samples. Peripheral

blood of mice was obtained retroorbitally every month and tumor spread was monitored by flow cytometry with specific antibodies against human CD45 and human CD3 antigen.

NSG mice were subcutaneously injected with 10 x10^6 BaF3 cells stably expressing WT, L156P, E183G, or A572V JAK3. The injection site was monitored weekly for tumor growth and daily after palpable tumor was observed. Mice were sacrificed when palpable tumor was 1 cm in size. Peripheral blood of mice was obtained retroorbitally every week and tumor spread was monitored by flow cytometry of the peripheral blood for GFP expression.

CHAPTER III

JAK3 MUTATIONS IN ATLL

Background and significance

Chemotherapy and monoclonal antibody treatments do not alter the aggressive clinical course of ATLL. A long latency period of as much as 50 years suggests that a multistep mechanism for leukemic development is involved in the development of ATLL, although the critical events in the progression have not been fully elucidated. Targeted therapeutic treatments would be facilitated by the discovery of genes and pathways that drive or initiate ATLL. So far, these targets have not been fully determined.

The IL-2 signaling pathway is known to play a prominent role in ATLL pathogenesis; mutational analysis of IL-2 signaling pathway components should yield potentially interesting results. *Janus Kinase 3* (*JAK3*) activating mutations have been identified in other leukemias and lymphomas. Until this study, all previously characterized activating mutations were found within the pseudokinase domain[5, 6, 133, 138, 146]. Subsequent to our findings, mutations between the FERM and the SH2 domains were identified in T-ALL cell lines. These mutations were characterized and identified in, KARPAS45 and SUPT1 cells, (respective JAK3 mutations are A251T and R272H)[190]. As T cells are dependent on JAK3 for both development and function, it is unlikely that these

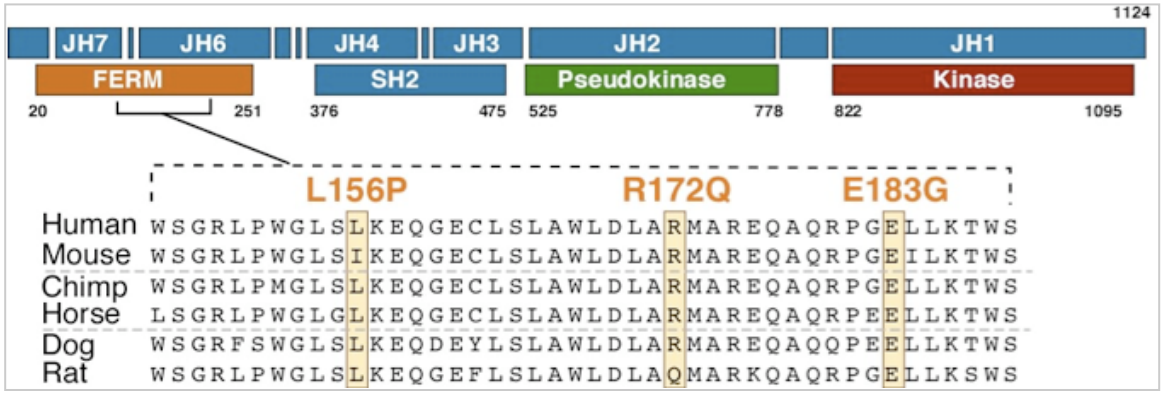

Figure 2 JAK3 FERM mutations identified in ATLL. Schematic and alignment of JAK3 proteins show 7 JAK homology (JH) domains, JH6-7 comprise the FERM domain (orange). Residue numbers and major structural domains are shown. Sequencing revealed three mutations (orange boxes) in 4 of the 36 ATLL patient samples analyzed. L156P and R172Q were identified in one patient each and E183G was found in 2 patients. The mutations occurred in residues higly conserved across mammalian species. The schematic shows JAK3 containing 7 JAK homology domains with JH6-7 comprising the FERM domain (orange). The three ATLL-derived mutations are shown in orange boxes. The mutations occurred in highly conserved residues.

mutations would induce loss of JAK3 kinase function. More likely, they will be gain of function mutations further supporting our findings. Germline SCID JAK3 point mutations occur in the FERM domain and abolish binding to γc[111]. There is also a rare SNP, P132T, which has inconsistently been shown to have a limited increased activity compared to WT and may play a role in the development of acute megakaryocytic leukemia.

Results

Identification of JAK3 mutations in ATLL patient samples

Thirty-six ATLL patients were analyzed for mutations in the *JAK3* gene by heteroduplex analysis, PCR, cloning, and sequencing[5, 191]. Sequence variants were identified in 4 patients (11%) that were not present in SNP databases or in 23 ethnically matched control individuals[192 192]. Some of our samples were purified leukemic blasts from apheresed patients and some were mixed with normal cells within buffy coat samples. These mutations occurred in the amino terminal FERM domain. L156P (leucine to proline), R172Q (arginine to glutamine), and E183G (glutamate to glycine) missense mutations occurred in residues that are highly conserved across mammalian species (Figure 2 orange boxes). All three were somatically acquired and clustered within the FERM domain of JAK3. One patient was determined to be a carrier of the P132T SNP (Table 2). Additionally, a cluster of SNP variants within introns 2-5 was identified for 3 ATLL patients (data not shown). So far, these are the only characterized activating mutations ever identified within the

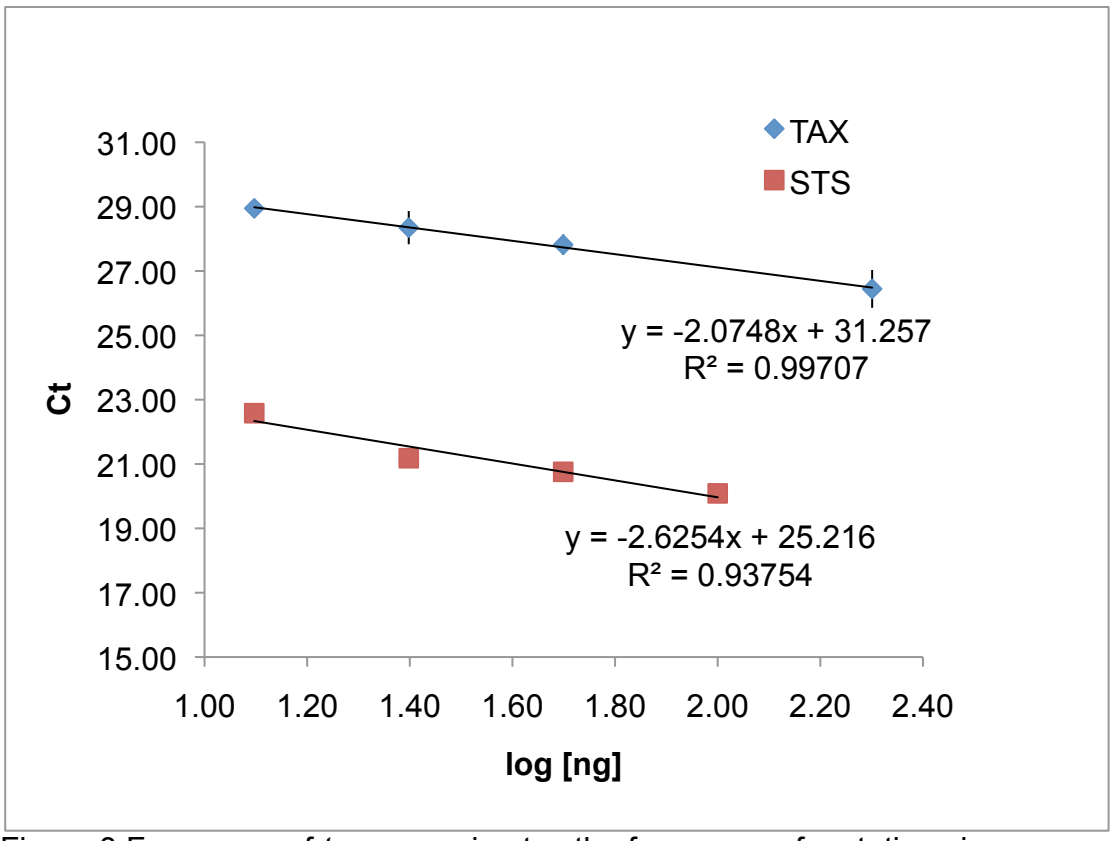

Figure 3 Frequency of *tax* approximates the frequency of mutations in one ATLL patient. One patient was identified as having a JAK3 L156P mutation at a frequency of approximately 10% as estimated by number of subclones containing the mutations. Genomic DNA for this patient was quantified for *tax* copies (blue diamonds) using quantitative PCR (qPCR). *Tax* levels are roughly 8.7% of the control Chromosome 11 short tandem sequence (STS) (red squares) levels. *Tax* frequency was calculated as the difference between mean Ct for tax (1 copy) and the mean Ct for STS (2 copies), which was 1:32. *Tax* quantification approximates the frequency of leukemic cells in the buffy coat sample. We conclude that the leukemic cell frequency is approximately the same as the frequency of L156P mutation.

FERM domain of JAK3. While more mutations were identified, this was the only cluster of mutations within the patients studied. This suggests a potential preference for the development of mutations within the FERM domain in ATLL. It could be further conjectured that these mutations may be necessary for T cell specific leukemia/lymphomas.

FERM domain mutation are clonal in primary tumor

The frequency of the allele for carrying the L156P mutation from one patient sample was roughly 10% based on the proportion of mutant positive clones sequenced during the initial analysis. This is roughly the same frequency as the genomic PCR product of the viral gene *tax* as determined by qPCR, which was 8.7% (Figure 3). This data also implies that this HTLV-1 positive tumor sample is clonal for the L156P mutation. As previous studies have shown that transformation by HTLV-1 in vitro progresses from a polyclonal to a monoclonal with respect to proviral integration, it is possible that mutations in JAK3 have the potential to induce clonal outgrowth.

JAK3 FERM domain mutations in ATLL patients do not show loss of function

$JAK3^{KO}$ fetal liver ($Lin^{-}c\text{-}Kit^{+}$) hematopoietic progenitor cells (LSKs) were isolated and co-cultured with OP9-DL1 stromal cells[187]. OP9-DL1 stromal cells with the addition of mIL-7 and mFlt3 were shown to induce wildtype LSKs from C57/B6 mice to differentiate into T cells[193].

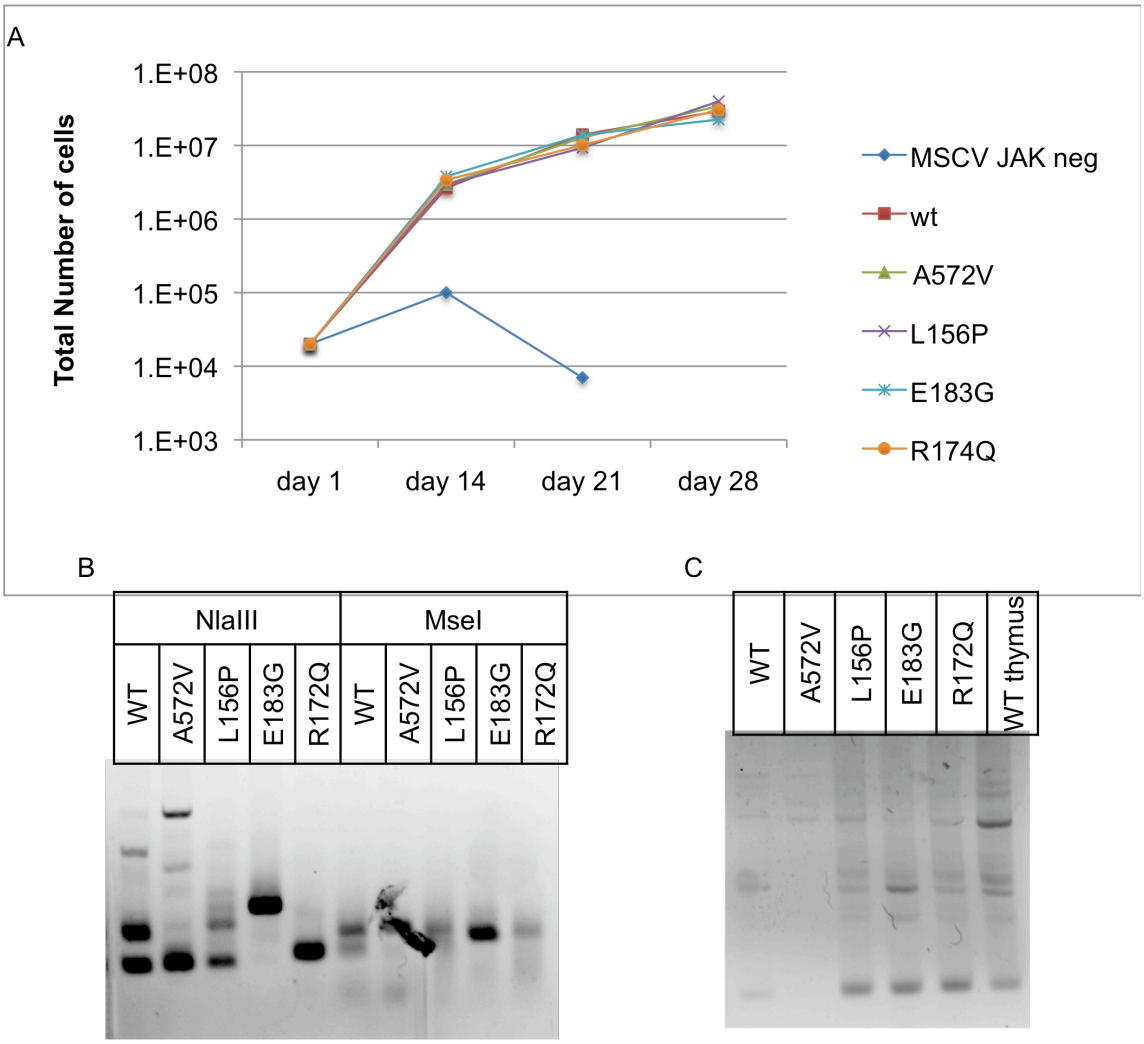

Figure 4 JAK3 expression in culture rescued T cell development. A) Graph shows cell counts over time in OP9-DL1 co-culture. JAK3^{ko} progenitor cells transduced with empty MSCV failed to proliferate and differentiate. Proliferation was rescued for those progenitors transduced with WT or mutant JAK3. This graph shows cell counts over time in OP9-DL1 co-culture. JAK3^{ko} progenitor cells transduced with empty MSCV failed to proliferate and differentiate. Proliferation was rescued for those progenitors transduced with wild type or mutant JAK3. B) Representative image of splinkerette PCR C) and TCRβ rearrangement for clonality on T cells differentiated in coculture with OP9-DL1 cells.

JAK3^{KO} cells transduced with empty MIG virus did not proliferate as expected, as JAK3^{KO} mice do not develop T cells (Figure 4A). WT JAK3 expression as well as expression of L156P, R172Q, E183G and A572V all showed consistent cell growth; thus, loss of function of JAK3 due to these newly identified mutations in ATLL was eliminated as a possibility.

Samples showed some moderate clonality by splinkerette insertion site analysis disregarding MSCV internal fragment. These were then subcloned into pGEM-T-Easy vector for sequencing analysis. After a BLAST search, none of the insertion sites was assessed to be of any relevance to the expansion of the disease. Examples of insertion sites are tubulin tyrosine ligase-like family member 11, ring finger protein 166, and hypothetical protein LOC228677. Each clone sequenced had a unique insertion site. This level of apparent clonality may be due to beginning the experiment with few cells and low transduction efficiency. Only a very small group of cells would commit to T cell differentiation and increased growth presenting with artificial clonality. This is not due to advantageous changes in gene expression because of insert site. Insertion location should not be considered paramount to the population expansion (Figure 4B). No obviously clonal TCRβ rearrangement was observed in differentiated T cells (Figure 4C).

JAK3^{KO} LSKs transduced with wild type (WT) JAK3, an activating mutant (A572V), or any of the three ATLL mutations proliferated and differentiated into CD4 and CD8 double positive cells by day 14 (Figure 5A). Differentiated LSKs showed JAK3, STAT5 and P-STAT5 expression at levels comparable to wildtype

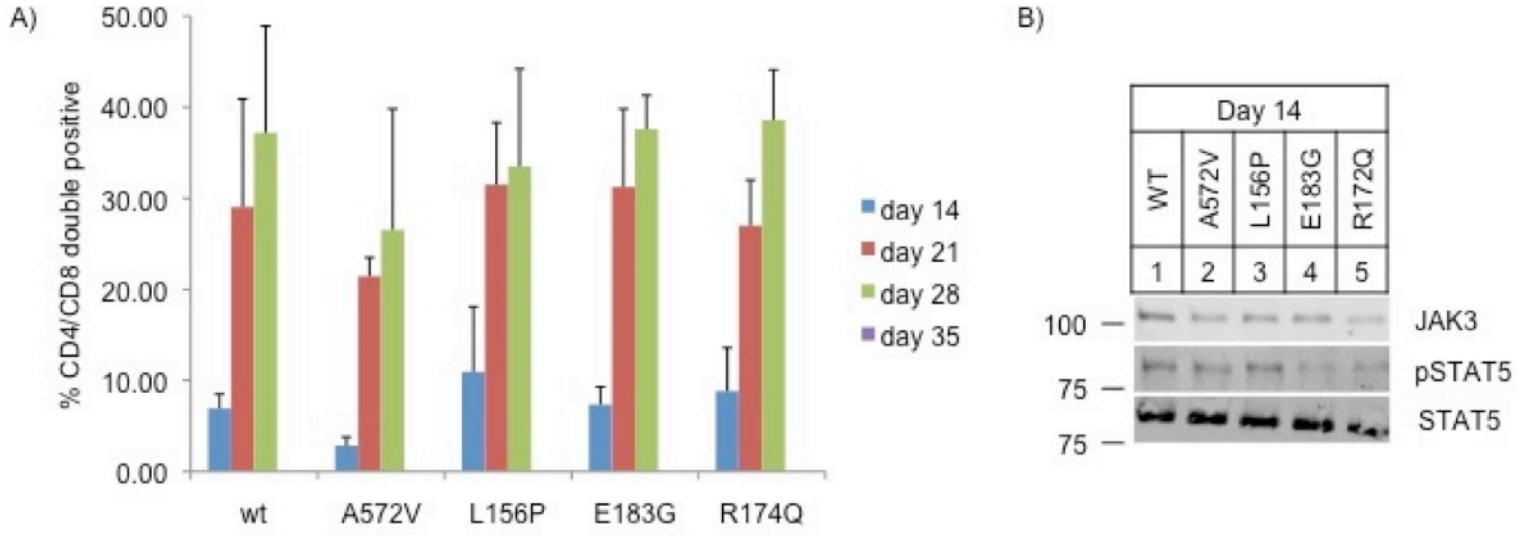

Figure 5. JAK3 rescues T cell development in JAK3^{KO} LSKs in culture. A) Graph shows the percentage of double positive, CD4^{+}CD8^{+}, cells arising in OP9-DL1 co-culture as determined by flow cytometry; bars from left to right show counts at 14, 21, and 28 days. The OP9-DL1 data is representative of two independent experiments (mean ± SEM). B) Western blot for JAK3 (106kDa), STAT5 (92kDa), and P-STAT5 (92kDa) from T-cell progenitor cell lysates harvest after 14 days on OP9-DL1 cells with cytokine. No lysates were recovered from untransduced JAK3^{KO} cells.

samples (Figure 5B). From these experiments, it was determined that the ATLL JAK3 mutations occurring in the FERM domain can rescue T cell development in $JAK3^{KO}$ LSKs and do not cause loss of JAK3 function. Interestingly, T-cell differentiation and proliferation did not occur in the transduced cells when IL-7 was omitted from culture. IL-7 is key to early T cell development. However, these mutations do not induce loss of function in this assay as indicated by the continued requirement of cytokine stimulation. This implies that these JAK3 mutants are appropriately interacting with the IL-7 receptor.

ATLL derived FERM domain mutations do not inhibit JAK3 binding to γc

The FERM domain of JAK3 binds to the cytoplasmic tail of the γc protein, which is a key component of interleukin receptors IL2R, IL4R, IL7R, IL9R, IL15R, and IL21R. Co-immunoprecipitations of JAK3 mutants with γc from transduced BaF3 cells showed that JAK3 containing L156P, R172Q, E183G, and A572V mutations bound γc to approximately the same extent as wild type JAK3. These FERM domain mutations do not appear to inhibit JAK3 binding to the γc subunit of the receptor, whereas the previously described inactive SCID mutant Y100C has been shown to abolish JAK3 receptor binding[117]. These experiments showed that the ATLL JAK3 mutations in the FERM domain did not cause loss of function but also did not alter the binding function of the FERM domain (Figure 6).

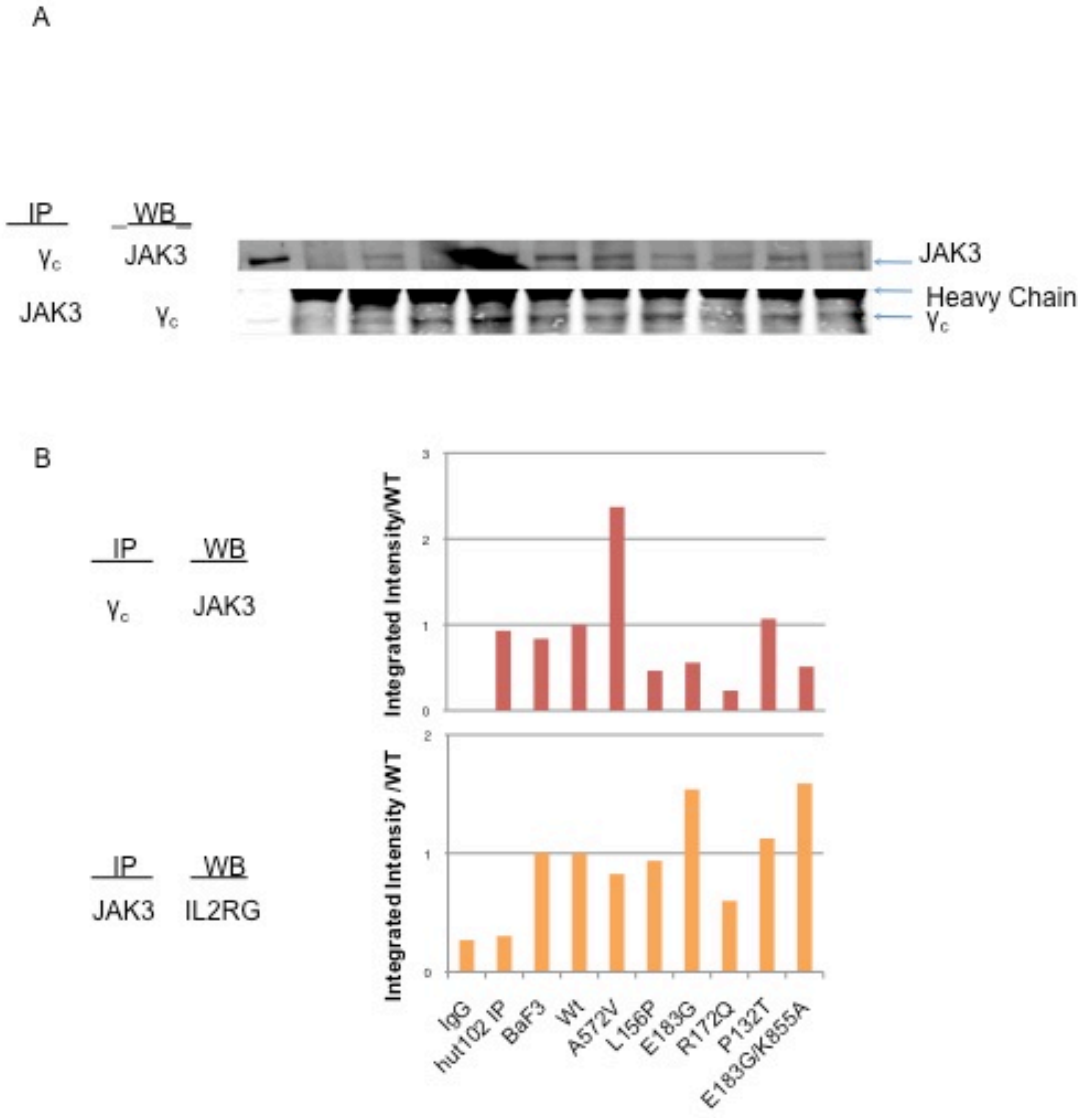

Figure 6 Mutant JAK3s show binding to γ_c comparable with that of WT JAK3. JAK3 (106 kDa) and γ_c (48 kDa) co-immunoprecipitation (IP) and Western blot (WB) analysis are shown. BaF3 cells were transduced with WT JAK3 or mutant JAK3s and then subjected to IP. Blots were performed with infrared dye labeled secondary antibodies and were quantified. The quantification is shown in bar graphs. The proteins precipitated were quantified and normalized to the comparable band seen for WT JAK3. IP data represents two independent experiments.

Discussion

The FERM domains in various proteins, such as focal adhesion kinase (FAK), play a role in autoregulation of protein function and activity[194]. The function of several structural proteins involved in a diverse group of activities including endocytosis, exocytosis, motility, and microfilament formation are also closely autoregulated by FERM domain interactions[118, 195-197]. The major function of the JAK3 FERM domain, as previously investigated, is to bind the cytoplasmic tail of γc[103]. Here, three JAK3 FERM domain mutations were identified from genomic DNA isolated from ATLL tumor samples and kinase function was verified in culture. In screening thirty-six ATLL patients and twenty-three ethnically matched controls, three activating mutations in *JAK3* were identified in highly conserved residues. Somatically acquired missense mutations L156P, R172Q, and E183G were studied. The E183G mutation was found in two different patients. One patient sample containing the L156P mutations was shown to have the same copy number of mutant JAK3 by number of mutant positive clones as presence genomic *tax* as determined by qPCR proving that the mutation is clonal for all of the tumor cells.

All mutations analyzed clustered within the FERM domain of JAK3 whose previously described function is to bind the cytoplasmic tail of γc[103, 111, 114, 117, 198]. In humans, autosomal recessive severe combined immunodeficiency (SCID) is caused by loss of function of JAK3[199]. Previously identified mutations in the FERM domain of JAK3, D169E and Y100C, are loss of function mutations found in some SCID patients[199]. Loss of function due to any of these three ATLL

mutations in JAK3 was eliminated by transducing $JAK3^{KO}$ fetal liver $Lin^{-}c\text{-}Kit^{+}$enriched hematopoietic stem cells (LSKs) with MSCV- WT or mutant JAK3 virus after which these cells were co-cultured on irradiated OP9-DL1 stromal cells. $JAK3^{KO}$ LSKs transduced with wild type (WT) JAK3 or mutant JAK3 rescued T cell proliferation and differentiation (Figure s 4 & 5). $JAK3^{KO}$ cells failed to proliferate or differentiate into CD4 and CD8 double positive T cells. A previously described activating mutant JAK3 A572V and the ATLL mutations rescued proliferative and differentiation defects in the knockouts bone marrow derived cells in culture[5, 186, 187]. Overall, these data show that these residues are not involved in the regulation of kinase receptor interactions and they do not inhibit cytokine stimulated function and T cell development.

CHAPTER IV

BIOCHEMICAL CHARACTERIZATION OF JAK3 MUTATIONS

Background and significance

The IL-2 signaling pathway plays a prominent role in ATLL pathogenesis and JAK3 is a key component of this pathway. The FERM domain of JAK3 is known to function as the site of direct interaction with the cytoplasmic tail of IL-2 receptor's γc subunit but, as we have shown, this interaction is not altered by these specific mutations. Two different mechanisms for regulation of protein interactions by FERM domains were described, intermolecular and intramolecular regulation. For example, disruption of the FERM domain of FAK increases activity and promotes FAK signaling[114]. This shows that FERMs can have autoregulatory roles in addition to regulating interactions with other proteins. If specific mutations in the FERM domain of JAK3 increase function, this could imply a similar autoregulatory role as that seen in FAK[114, 200, 201]. For an example of intermolecular interactions, the JAK3 FERM domain binds the γ subunit of the IL-2 receptor. Mutations from SCID patients abolish γc binding and thus kinase activity and an intact FERM domain is required for JAK3 binding of an ATP analog[111]. While the FERM domains mediate intermolecular interactions with cytokine receptor, they are also involved in intramolecular binding to JH1 kinase domain, thereby maintaining kinase activity[111].

Overexpression of JAK1, JAK2, and TYK2 in transient transfections gave rise to cell proliferation in BaF3 cells and considerably less so with JAK3. Only TYK2 and JAK1 provided cytokine independence after viral transduction. In the case of JAK1, this was dependent on expression of functional FERM and kinase domains. All stable expression lines showed an increase in STAT5 phosphorylation in the absence of cytokine stimulations[202].

Previously, tyrosine auto-phosphorylation at the SH2-domain of JAK3 were found to facilitate the interactions between JAK3-FERM domain and cytoskeletal proteins, demonstrating that the intramolecular interaction between FERM and SH2 domains of non-phosphorylated JAK3 prevented JAK3 from binding to structural protein villin. Tyrosine auto-phosphorylation of JAK3 at the SH2 domain decreased these intramolecular interactions and facilitated binding of the FERM domain to villin. Thus, they demonstrated the molecular mechanism of interactions between JAK3 and cytoskeletal proteins where tyrosine phosphorylation of SH2 domain acted as an intramolecular switch for the interactions between JAK3 and cytoskeletal proteins and was regulated by FERM domain interactions[203].

Localization of JAK1, JAK2 and TYK2 remain predominantly close to the membrane through an association with the cytoplasmic tail of cytokine receptors[204, 205]. In the absence of cytokine stimulation JAK3 has been described to localize to the nucleus. With low dose cytokine stimulation, JAK3 will localize to the cytosol and membrane. At high concentrations of IL-2 JAK3 localizes predominantly to the membrane in cell culture[206, 207].

The FERM domain of JAK1 has been described based on homology to non Janus kinase FERM domains that have been solved including FAK and radixin. This study noted that the FERM domains of the JAKs are only remotely similar to the core ERM proteins and more closely resembles the FERM domain of FAK. In fact there is quite a lot of divergence between the JAKs with JAK2 and JAK3 being more closely related to FAK than are JAK1 and TYK2[115].

Results

ATLL mutations increase phosphorylation of STAT5A in cell culture.

MIG constructs expressing JAK3 mutant cDNA were developed by introducing mutations into the WT JAK3 using the Stratagene QuikChange kit and verified by direct sequencing. To determine the relative activity of mutant JAK3 to WT and a known activating mutation, A572V, the IL-2 signaling pathway was recapitulated in HEK 293T cells. HEK 293T cells are deficient for all components of the IL-2 signaling pathway. Because of this, each aspect of signaling can be manipulated and controlled.

The IL-2 signaling pathway was established in HEK 293T cells by co-transfecting plasmids that express each of the three subunits of the IL-2 receptor (α,β,and γc), STAT5A, and WT or mutant JAK3. Equivalent amounts of protein were expressed in each transfection as quantified by Western blotting with infrared dye-labeled secondary antibodies against IL2Rα, IL2Rβ, γc, STAT5 and

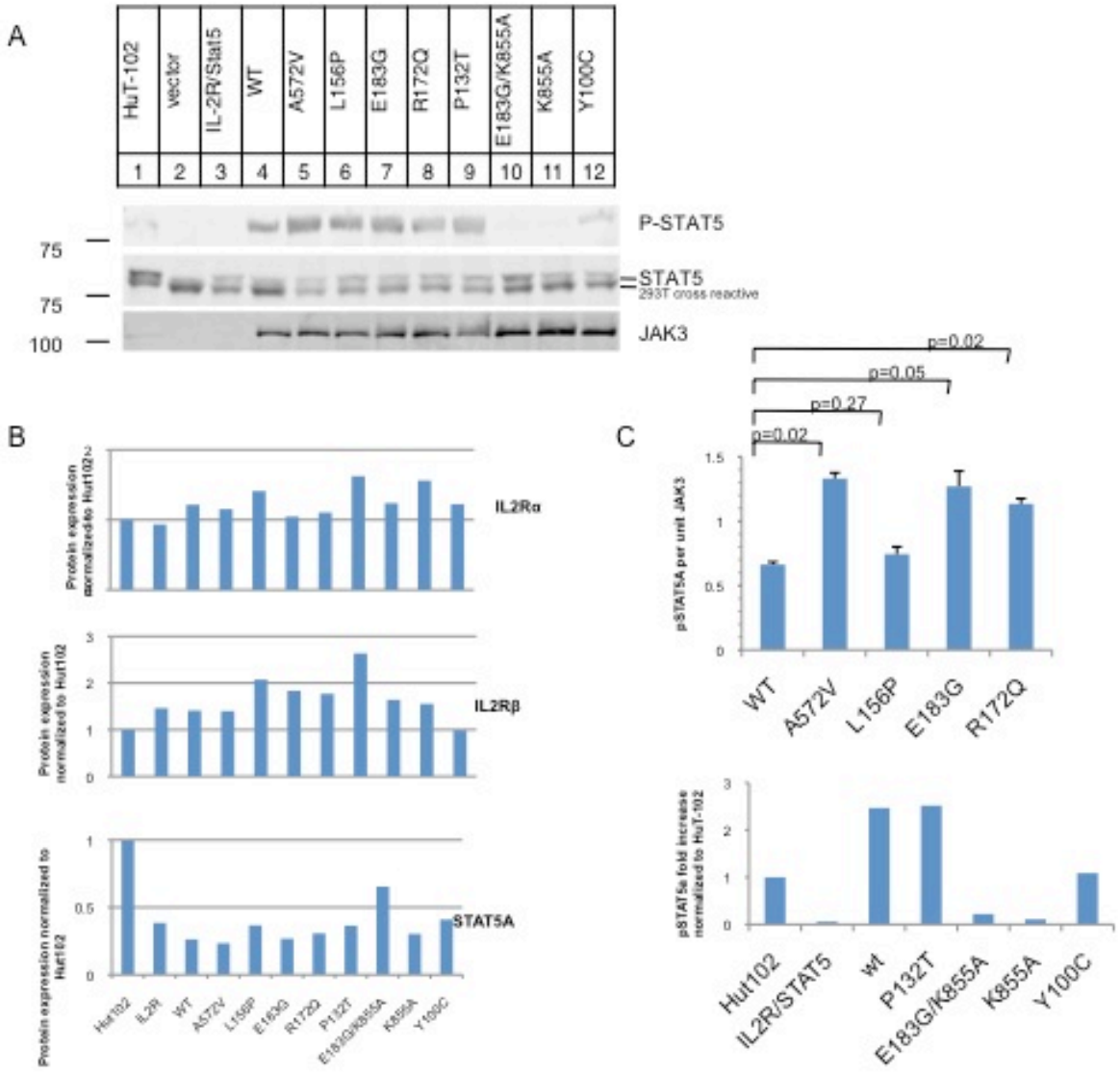

Figure 7 JAK3 FERM mutations cause increased phosphorylation of STAT5A in reconstituted IL-2 signaling in HEK 293T cells. A) Western blots show P-STAT5A (92 kDa), STAT5A and JAK3. Lane 1 shows whole cell lysate of HuT-102 cell line. STAT5A phosphorylation requires JAK3 and IL-2 (100 U/ml). B) Is a graph of protein levels of each transfected component expressed as fold over endogenous Hut-102 levels. C) Graph shows quantification of Western blots; P-STAT5A protein per unit of expressed JAK3 protein. Mutant JAK3s were compared to WT JAK3 in four independent co-transfection experiments and showed consistently higher P-STAT5A levels (mean ± SEM) (top panel). P-values were generated from Student t-test (two tailed). The bottom panel shows P-STAT5A protein levels in co-transfection experiments with various other JAK3 mutants normalized to endogenous levels in Hut-102. The K855A mutant causes loss of kinase activity in JAK3. The Y100C mutation was found in a SCID patient and P132T is a SNP.

JAK3 (Figure 7A). Protein expression was not a variable in the quantification of phosphorylation.

Phosphorylated STAT5A was quantified using a primary antibody specific to P-Y694 of STAT5A, a residue uniquely phosphorylated by JAK3[208]. Co-transfection of the IL-2R components with STAT5A showed no P-STAT5A in the absence of JAK3, demonstrating the specificity of the phosphorylation site to JAK3. Co-transfection of IL-Rα, β, γc, STAT5A, and WT JAK3 induced P-STAT5A only in the presence of exogenous IL-2 (100 U/mL). This was used to compare the relative activity of the mutant JAK3s.

P-STAT5A levels were normalized to JAK3 protein expression and loading control protein from Hut-102 cells. The L156P JAK3 mutant did not show a statistically significant increase in P-STAT5A levels in this assay as compared to WT JAK3. Increased levels of P-STAT5A were found with mutant JAK3 co-transfections in comparison to wild type JAK3 co-transfections for both E183G and R172Q (Figure 7C).

To verify that the observed P-STAT5A was caused by increased JAK3 kinase activity, a compound mutant was made, with the FERM domain mutation E183G and the catalytically inactive K855A mutation[104, 111]. This compound mutant expressed stable JAK3 protein to the same extent as WT but showed no phosphorylation of STAT5A in this assay. The K855A mutant causes loss of kinase activity in JAK3. When expressed in 293T cells K855A shows no STAT5A phosporylation. P132T, a common SNP found in 1% of the population, was also introduced into the JAK3 construct. The P132T mutations showed only slightly

increased levels of P-STAT5A as compared to WT JAK3 which were not statistically significant. STAT5A phosphorylation was diminished but not abolished with the Y100C SCID mutation. The Y100C mutant may retain some limited binding to γc when overexpressed. Reconstituted IL-2 signaling in 293T cells showed that the ATLL FERM mutations, E183G and R172Q, induced increased phosphorylation of STAT5A compared to WT JAK3.

Mutant JAK3s confer cytokine independent growth in BaF3 cells

To further establish this activating phenotype, BaF3 cells were transduced using recombinant MIG retroviruses expressing mutant or WT JAK3s and sorted for GFP^+ cells. BaF3 cells require phosphorylation of STAT5 through IL-3 signaling and become IL-3 independent when gain of function tyrosine kinases are expressed that signal through the same pathway[179]. Untransduced BaF3 cells and those with WT JAK3 did not proliferate in the absence of IL-3 and died within 3 days of initial IL-3 withdrawal. As a result, all subsequent experiments on untransduced BaF3s and those transduced with WT JAK3 always included murine IL-3. BaF3 cells transduced with mutant JAK3s grew without IL-3 and were continuously passaged as stable cell lines. Although the L156P JAK3 mutant did not show a statistically significant increase in P-STAT5A levels in the 293T assay it did show activation in BaF3 cells (Figure 8).

Retroviral integration sites were analyzed by splinkerette and showed that the stable BaF3 lines expressing mutant JAK3s were mostly polyclonal. Of those

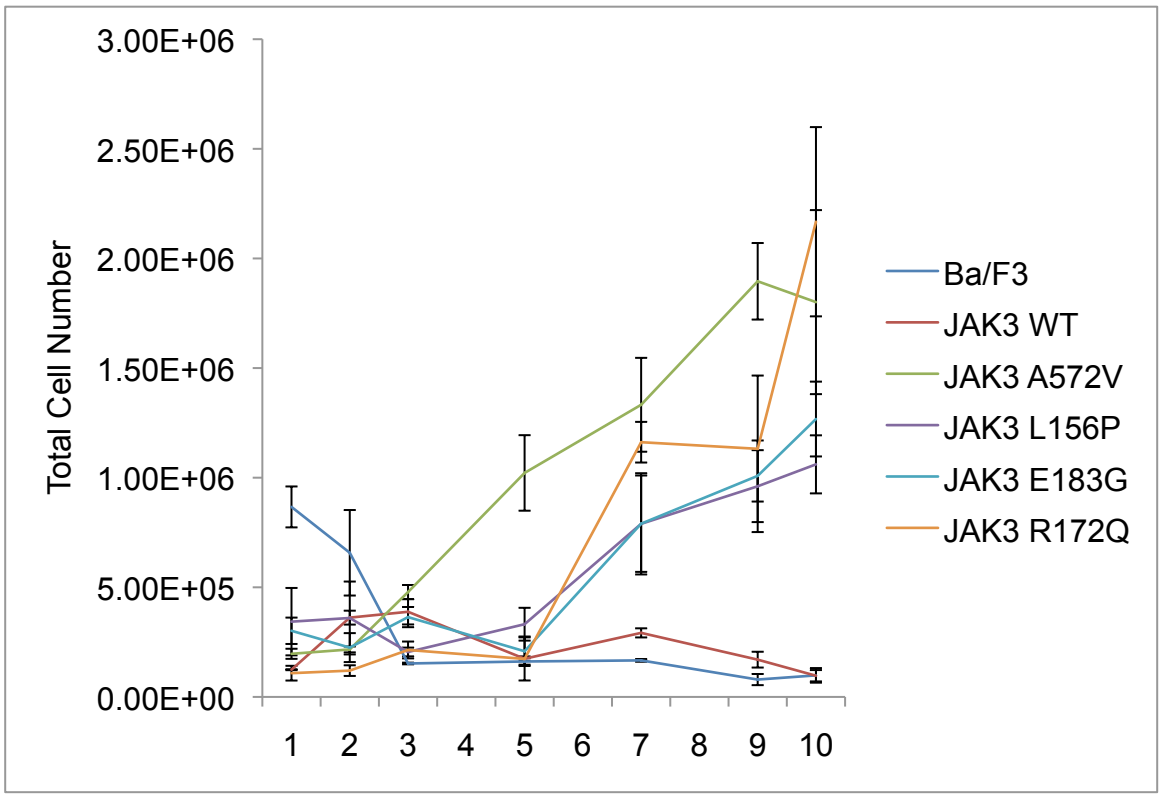

Figure 8 Mutant JAK3s confer cytokine independence in BaF3 cells. BaF3 cells transduced with JAK3s were counted daily after IL-3 withdrawal. WT JAK3 transduced and untransduced BaF3s did not survive unless supplemented with IL-3. Those transduced with mutant JAK3s became cytokine independent by 7 days.

that showed clonal integration, no integrations were found near genes that could account for cytokine independent growth (Figure 9).

Mutations in JAK3 alter protein signaling

JAK3 stimulates multiple downstream signaling pathways leading to the phosphorylation of several proteins important for the regulation of proliferation, inhibition of apoptosis and cell cycle progression. To determine which downstream targets of JAK3 activity were affected, the phosphorylation states of STAT5 (Y694), STAT3 (Y705), ERK1/2(T202 and Y204), and AKT (S473) were analyzed after acute withdrawal of IL-3 (Figure 9). The IL-3 withdrawal cultures were divided in two and IL-3 was added to one group before preparing whole cell lysates or immunoprecipitates. Phosphorylation of Y980, a residue in the activation loop of JAK3 that is autophosphorylated and positively regulates kinase activity[109, 209], was minimal in WT JAK3 but constitutive in all three mutant JAK3s. P-Y980 was not observed in BaF3 cells expressing the E183G/K855A compound mutant JAK3, confirming that Y980 is a site of autophosphorylation, and IL-3 did not consistently affect this phosphorylation. P-STAT5 was detected in all the BaF3 cells expressing mutant JAK3s but not in untransduced BaF3 cells or BaF3 cells transduced with WT JAK3 after IL-3 was withheld. P-STAT5 was increased after the addition of IL-3, which is induced in this system through JAK2. AKT phosphorylation at S473 was increased in all the mutant JAK3 expressing BaF3 cells compared to untransduced and WT JAK3 expressing BaF3s regardless of cytokines status. ERK1/2 and STAT3 phosphorylations were

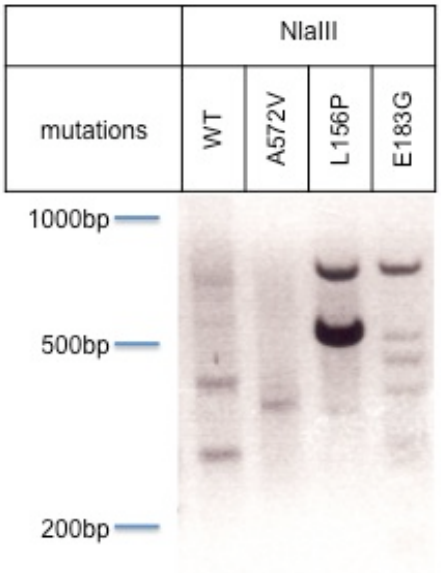

Figure 9 Viral insertion site analyses in BaF3 cells. Genomic DNA was isolated from IL-3 independent BaF3 cells and subjected to splinkerette PCR analysis to determine viral insertion sites.

present in a different pattern than JAK3, STAT5, and AKT. P-ERK1/2 was not detectable in the mutant JAK3 expressing cells without the presence of IL-3 and STAT3 was minimally phosphorylated without IL-3. This basal level of P-STAT3 was the same in untransduced BaF3 and in cells expressing WT or mutant JAK3 and could be stimulated with IL-3 addition.

In summary, the phosphorylation states of JAK3, STAT5, and AKT were correlated with cytokine independent growth of mutant JAK3-expressing cell lines, whereas ERK1/2 and STAT3 phosphorylation states were not (Figure 10). Although the L156P JAK3 mutants did not show a statistically significant increase in P-STAT5A levels in the 293T assay, it did show biologic activity in BaF3 cells.

The events that correlated with the cytokine independent growth were identified as STAT5 and AKT phosphorylation more so than that of ERK or STAT3.

The introduction of JAK3 to BaF3 cells does not change cell cycle profile

In an effort to determine if these activating mutations were hyper-proliferative, cell cycle profiles were determined by PI staining and analyzed by flow cytometry. Cell lines that expressed JAK3 mutants grown without IL-3 were not impaired in their proliferation, as they showed cell cycle profiles comparable to BaF3 cells maintained in IL-3 (Figure 11). Flow cytometry histograms show propidium iodide staining of JAK3 transduced BaF3 cells. The percentage of cells in each stage of the cell cycle is expressed as a percentage of total cells above

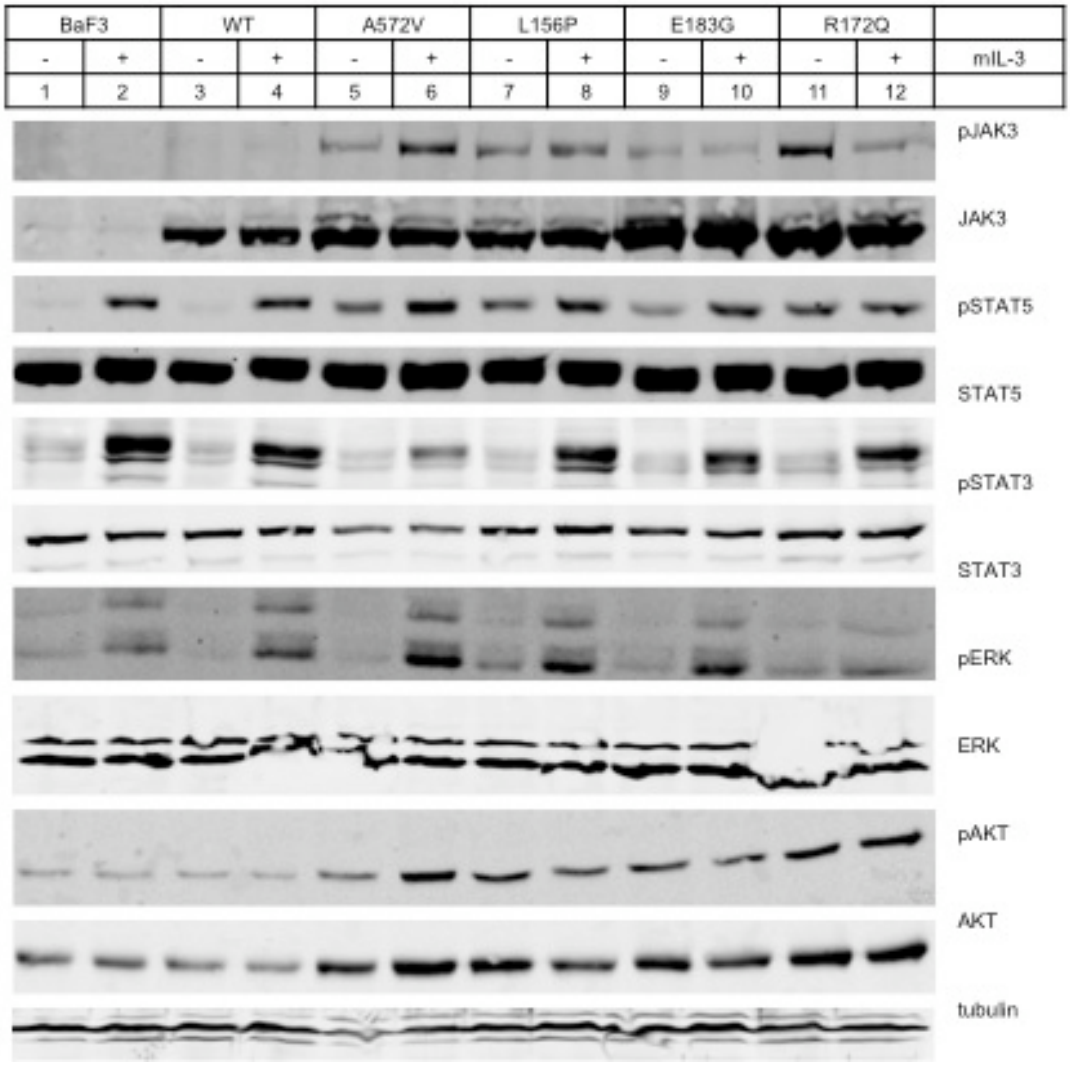

Figure 10 Protein signaling in BaF3s. BaF3 cells expressing mutant JAK3s showed constitutive autophosphorylation and phosphorylation of STAT5 (Y694) and AKT (S473) without IL-3. All western blot analyses were performed using whole cell lysates except pSTAT3 and pJAK3, which were blotted from immunoprecipitates.

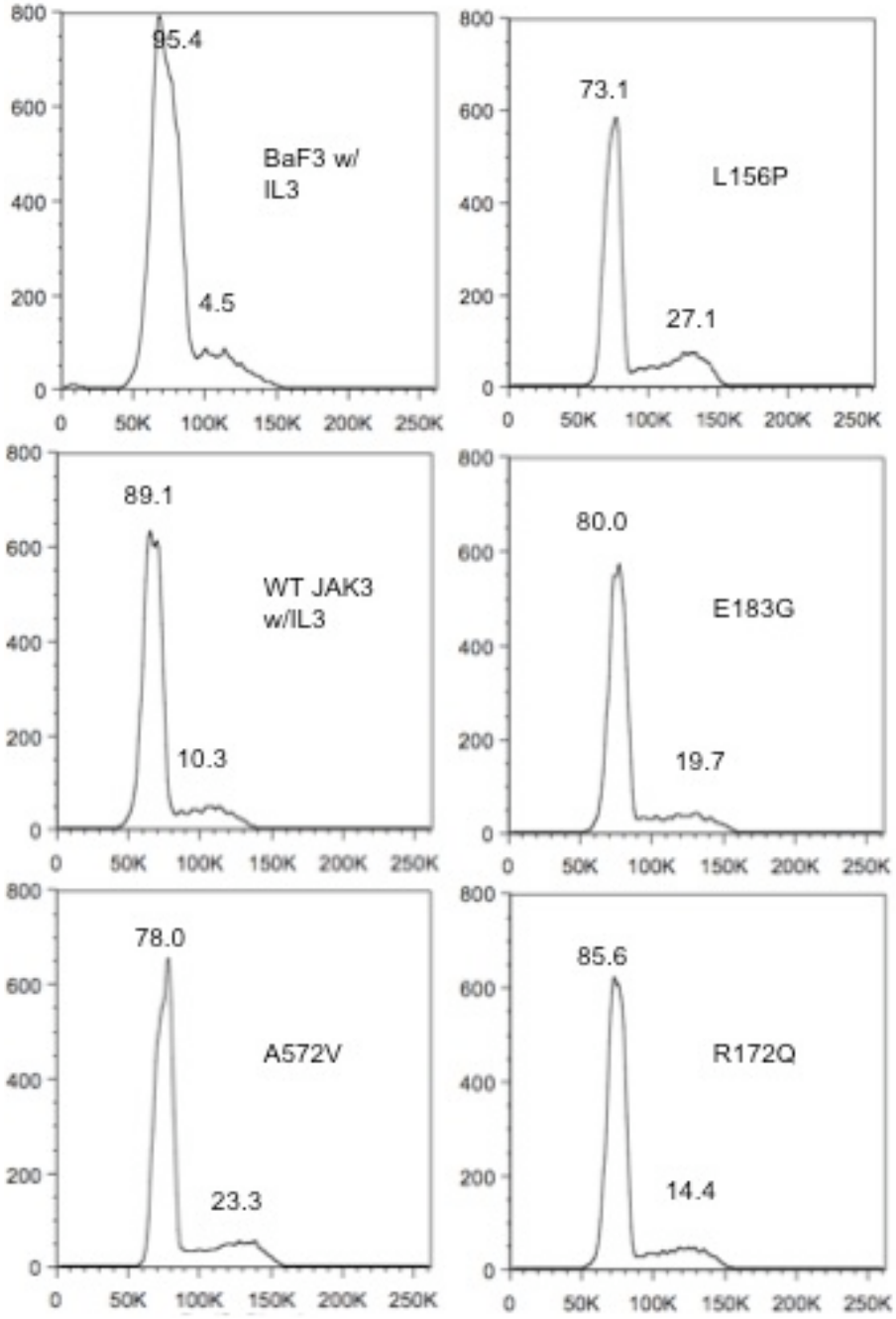

Figure 11 Cell cycle analysis of BaF3 cells. Flow cytometry histograms show Vybrant dyecycle violet staining of stable BaF3 lines. Proportion of cells in cell cycle stages G1 or S/G2 are expressed as percentage of total cells above the peaks. Mutant JAK3 transduced BaF3 cells were maintained without IL-3. A572V, L156P, and E183G mutants showed comparable proportions of cells in S/G2 phase. R172Q is more closely comparable to WT JAK3 expressing BaF3 cells. Data shown are representative of two independent experiments.

the peaks. Mutant JAK3 transduced BaF3 cells were maintained without IL-3 and showed comparable proportions of cells in S-phase as the untransduced BaF3s. R172Q mutant JAK3 transduced BaF3 cells showed increased cell numbers in S-phase.

Mutant JAK3 proteins are more stable in cultured cells

The JAK3 proteins were shown to undergo proteasome-mediated degradation after activation[210, 211]. Therefore, the stability of WT and mutant JAK3 proteins in the BaF3 cells were analyzed. Cycloheximide, an inhibitor of protein biosynthesis, was applied to BaF3 cells and quantitative western blots for JAK3 protein were performed. JAK3 protein expression was quantified using fluorescent secondary antibodies and protein signals curves were plotted verus time for the mean of five independent experiments. Linear regression analysis of the curves showed that the mutant JAK3s clustered together with similar decay times (A572V, $t_{1/2}$=4.3 h; L156P, $t_{1/2}$=3.2 h; R172Q, $t_{1/2}$=4.1 h; E183G, $t_{1/2}$=4.5 h), whereas WT JAK3 decayed more rapidly ($t_{1/2}$=1.96 h). In fact, the mutant JAK3 proteins had half-lives as much as 2-fold greater than WT JAK3 protein (Figure 12).

Degradation of activated JAK3 is not regulated by the lysosome

It was postulated that the increased stability is due to the activated phenotype of the JAK3. To determine if this activation was due to loss of regulation, BaF3 cells expressing WT or mutant JAK3 were treated with

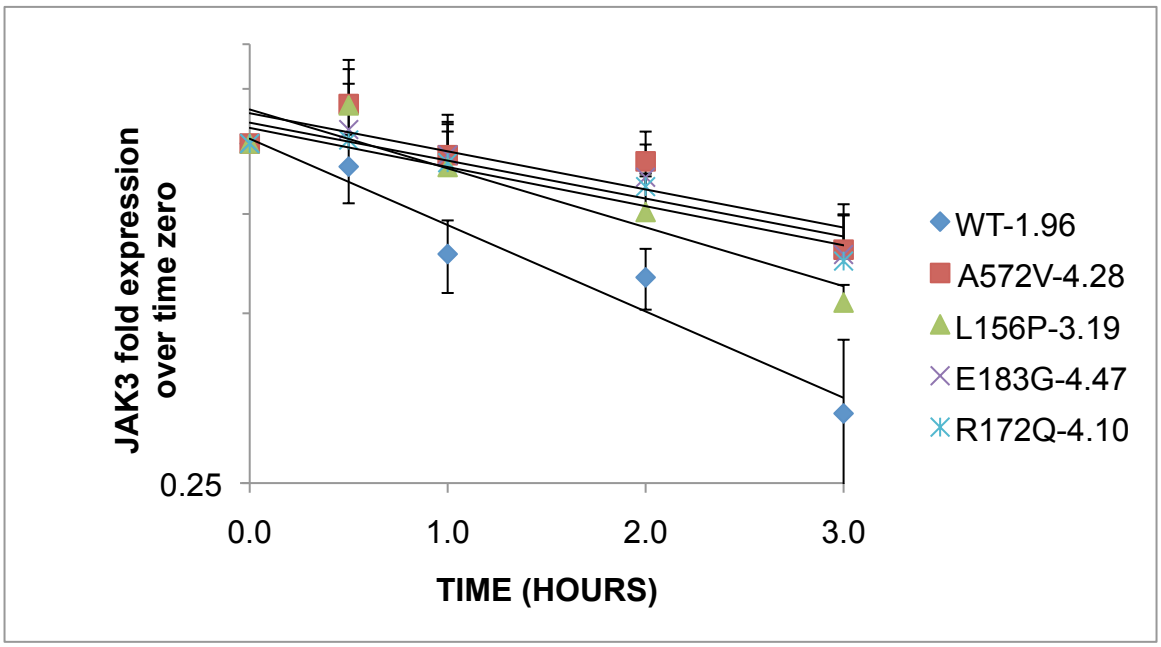

Figure 12 JAK3 stability after cycloheximide. Semi-log graph shows JAK3 protein in BaF3 cells expressing WT or mutant JAK3 after treatment with 100µg/ml cycloheximide for 0, 0.5, 1, 2, and 3 hours. The respective half-lives were calculated from linear regression of five total experiments (R^2>0.90). A572V, L156P, E183G, and R172Q are all significantly more stable than WT JAK3.

chloroquine and JAK3 expression was determined by western blot. There was no noticeable difference in JAK3 expression one hour post chloroquine treatment. By four hours, there was a slight decrease of JAK3 expression at concentrations of 100 and 200μM chloroquine for E183G and A572V. By 24 hours, all groups demonstrated an obvious decrease in JAK3 after treatment with 25μM chloroquine, which was more pronounced for the mutant JAK3s. These data imply that activated JAK3 degradation was not lysosomally regulated (Figure 13).

Degradation of activated JAK3 is regulated by the proteasome

To further characterize the mechanism of activated JAK3 degradation, BaF3 cells expressing mutant or WT JAK3 were treated with the cell-permeable proteasome inhibitor MG132. Data shown are representative of two individual experiments. In contrast to the lysosomal inhibitor, treatment with 10μM of the proteasome inhibitor MG132 did not show a decrease in the abundance of JAK3 in both A572V and E183G transduced BaF3 cell lines. These data verify that activated JAK3 is regulated by proteasomal degradation. Interestingly, both the WT and the kinase dead K855A mutant did show a slight decrease in protein expression after treatment with MG132 in as early as 30 minutes. This reduction in JAK3 expression remained consistent from 0.5 to 4 hours. The combination of these data implies that non-activated JAK3 degradation may be regulated by both the proteasome and the lysosome, whereas activated JAK3 may only be regulated by the proteasome (Figure 14).

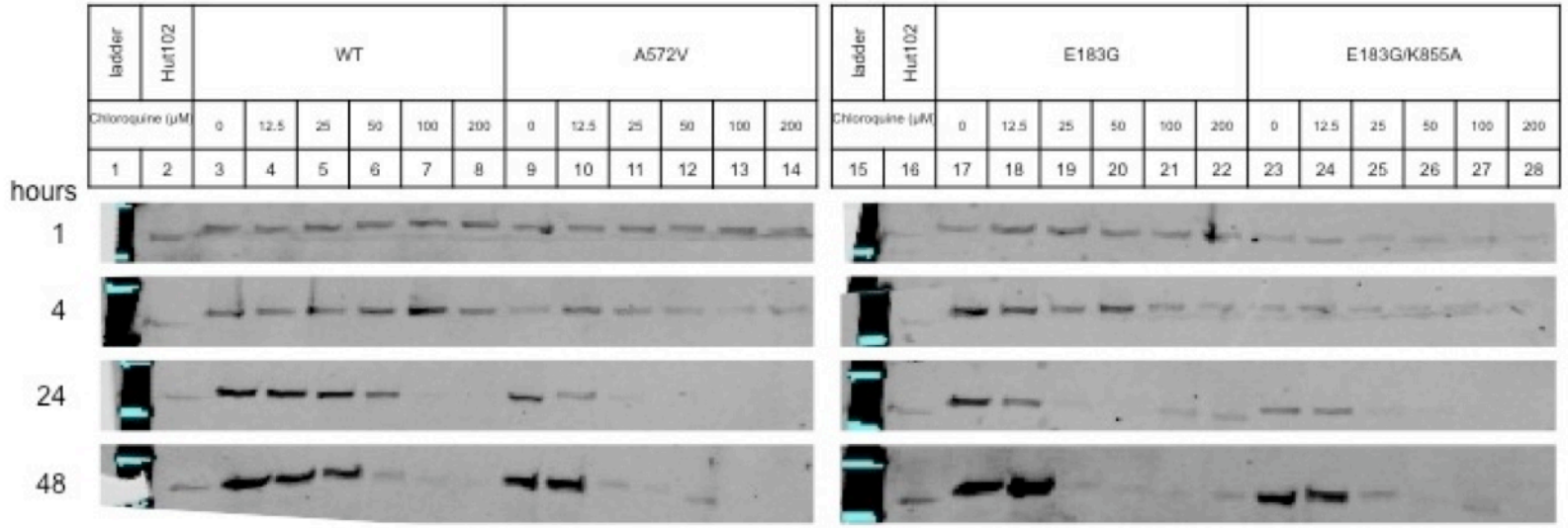

Figure 13 Lysosome inhibition does not prevent activated JAK3 degradation. Stably transduced BaF3 cells were incubated at for 1, 4, 24, or 48 hours with lysosome inhibitors chloroquine at concentrations of 0, 12.5, 25, 50, 100 or 200μM. Cells were then lysed in RIPA with protease inhibitors and analyzed by western blot with antibodies against JAK3. Little change is seen between various concentrations at 1 hour. By 4 hours there is a slight decrease in JAK3 expression at the higher concentrations of 100 and 200μM chloroquine for A572V, E183G, and E183G/K855A (lanes 13, 14, 21, 22, 27, and 28). At both 24 and 48 hours this decrease is pronounced in all JAK3 groups including WT JAK3. This experiment was only performed once.

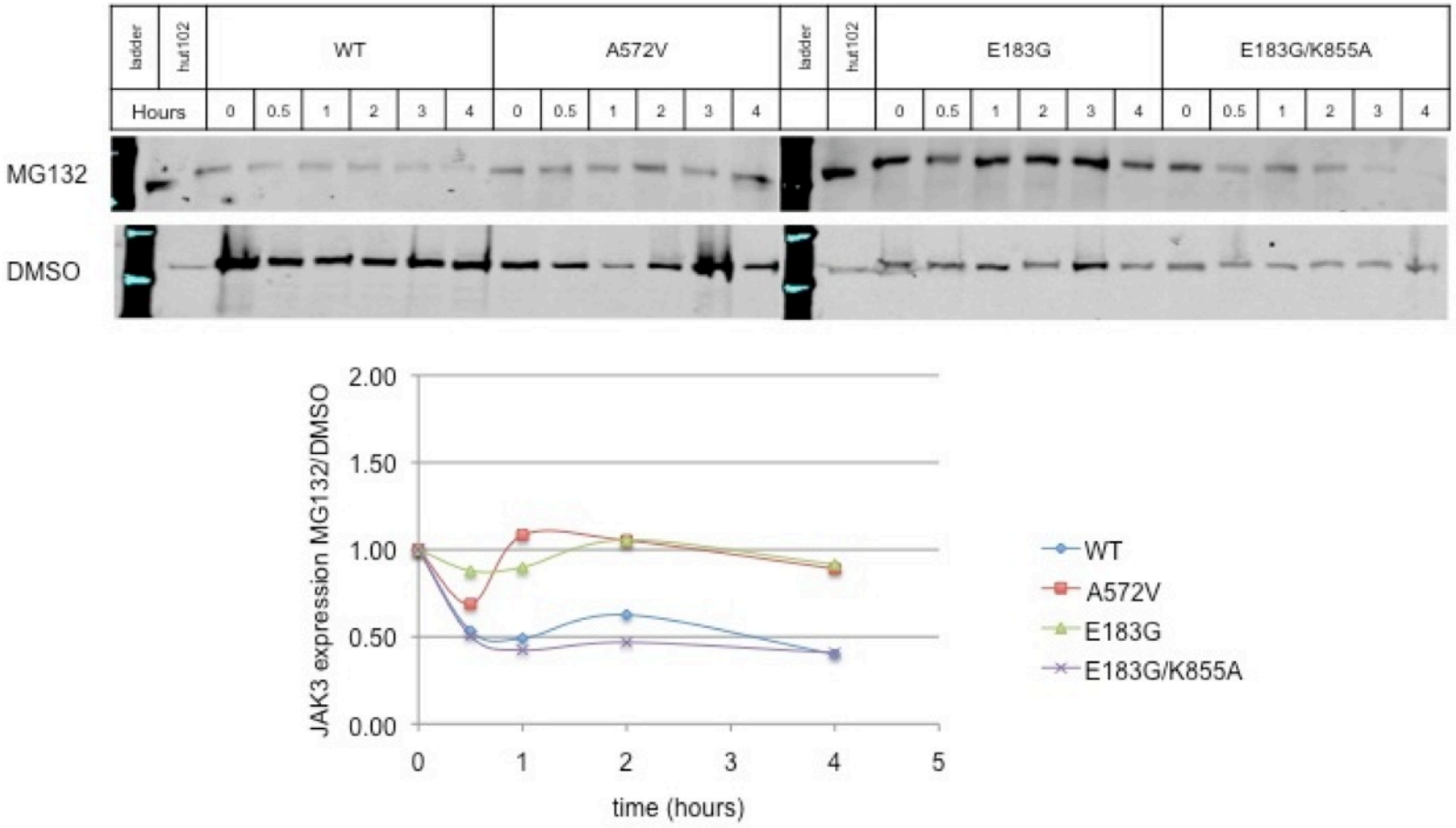

Figure 14 Proteasome inhibition decreases the rate of degradation for activated JAK3. Western blots show the expression of JAK3 after treatment with 10μM MG132 for 0, 0.5, 1, 2, 3, and 4 hours. WT and E183G/K855A both show a minimal decrease of JAK3 expression as early as 0.5 hours but JAK3 remains relatively stable from 1-4 hour and is never completely degraded. Whereas the E183G and A572V activating mutations both remain relatively stable. Blots are representative of 2 individual experiments. Graph is the average of the quantification of JAK3 expression after MG132 treatment normalized to DMSO treated samples at the same time point for two experiments.

Activated JAK3 localizes away from the nucleus

When analyzed by immunoflourescence, WT JAK3 protein in BAF3 cells was present ubiquitously throughout the cell. In contrast, the activating mutant E183G was localized strictly outside of the nucleus. Previous studies have shown that activated JAK3 is known to interact with actin binding proteins and facilitate interleukin 2-induced cytoskeletal remodeling and wound-repair[206]. It is reasonable to hypothesize that JAK3 is sequestered within cytosolic and membrane bound protein structures only when in an activated conformation. Additional forms of regulation of JAK3 may be by conformation-dependent changes in subcellular localization (Figure 15).

JAK3 mutations confer increased in vitro tyrosine kinase activity

WT or mutant JAK3s were immunoprecipitated from BaF3 cells and were incubated with a peptide substrate conjugated to fluorescent beads. Phosphorylation was detected by Förster (or fluorescence) resonance energy transfer (FRET) between the fluorophore-conjugated phospho-specific antibody to the acceptor dye on the substrate. The assay parameters were established and optimized using a recombinant kinase domain of JAK3. Incubation of immune complexes with the peptide substrate without ATP resulted in background counts. With the addition of 20μM ATP for 60 minutes at 24°C, counts were detected using recombinant purified JAK3 (a truncated protein

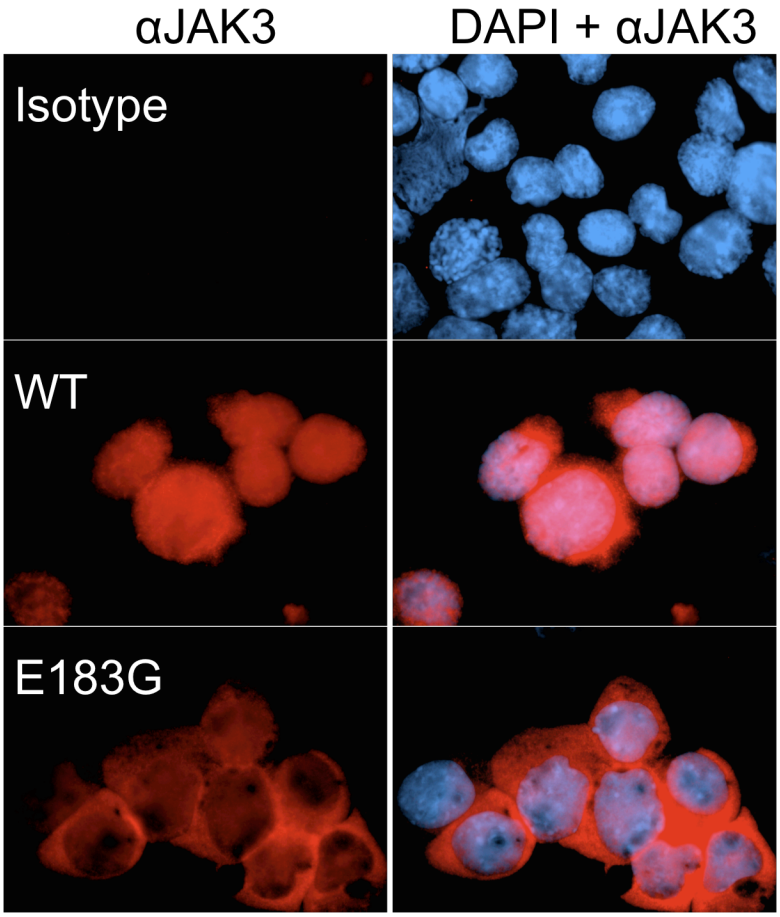

Figure 15 E183G mutant JAK3 localizes away from the nucleus in BaF3 cells. WT and E183G transduced BaF3 cells were stained for JAK3 and DAPI . These cells were then imaged with a confocal microscope. In WT-JAK3 transduced cells, JAK3 is ubiquitously expressed. E183G –JAK3 is localized away from the nucleus.

expressing the kinase domain only), WT JAK3, and each of the mutant JAK3s. No kinase activity was detected in immunoprecipitations with isotype control IgG from WT JAK3-transduced BaF3 cells, untransduced BaF3, or the compound mutant, E183G/K855A (E/K). Significantly, mutant JAK3 proteins showed increased enzyme activity compared to WT JAK3 ($P<0.001$ by Student t-test). WT JAK3 activity was less than that of the truncated JAK3 protein but was increased compared to IgG control ($P=0.008$).

A representative immunoprecipitation (IP) of JAK3 is shown in Figure 16B after the kinase assay. This was also probed using 4G10, a pan P-tyrosine antibody, and a specific antibody against P-Y980 of JAK3[209]. JAK3 showed autophosphorylation and kinase activity, as determined by phosphorylation of JAK3 tyrosine 980 in WT and mutant JAK3s, but not the compound mutant E183G/K855A. Interestingly, immune complexes that were resuspended in Laemmli buffer for SDS-PAGE immediately after the IP procedure showed P-Y980 only for mutant JAK3 proteins and not WT. In contrast, immune complexes that were equilibrated in ATP and kinase buffer followed by SDS-PAGE showed P-Y980 in both WT and mutant JAK3 proteins. Thus, the Y980 autophosphorylation assayed immediately after IP or in whole cell lysates was more predictive of enzyme activity than the SDS-PAGE after the kinase assay. This also suggested that autophosphorylation was taking place during the kinase reaction for WT JAK3 protein in vitro. Previous studies have shown that Y980 autophosphorylation can be detected in JAK3 proteins with gain of function or loss of function mutations and may not be entirely predictive of substrate

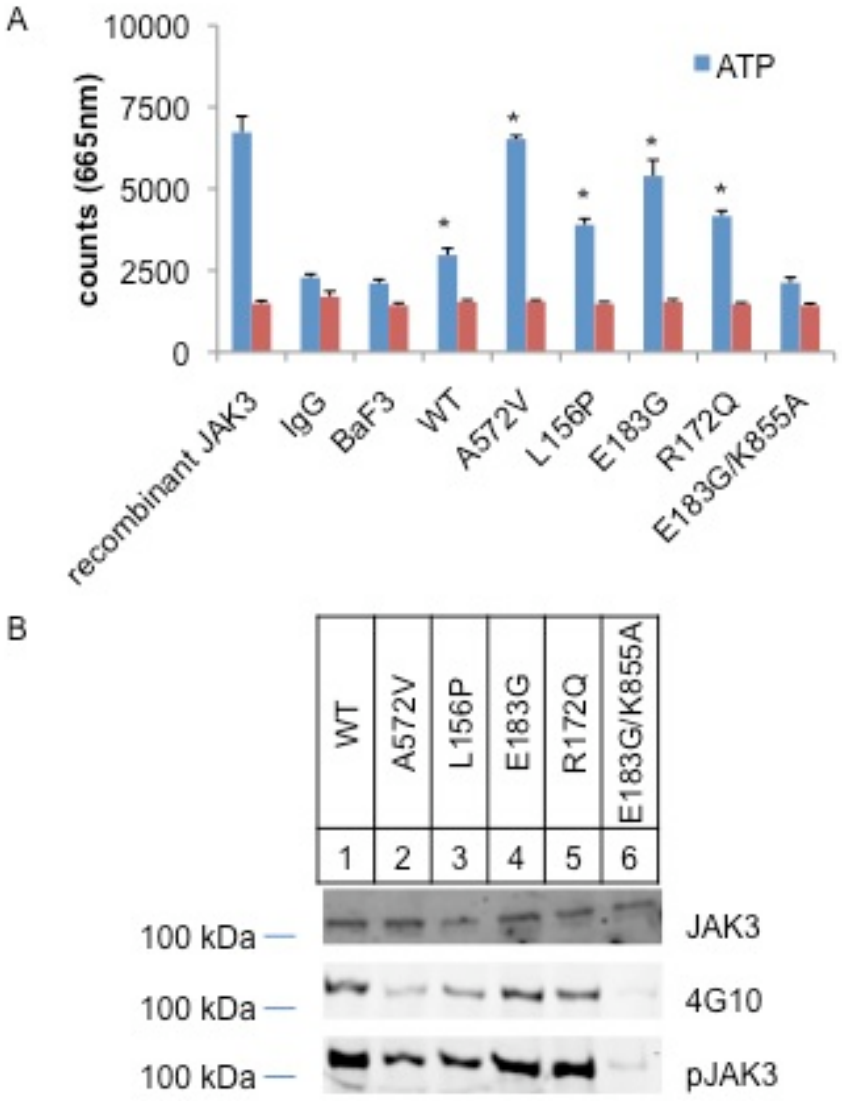

Figure 16. JAK3 FERM domain mutations show increased kinase activity in vitro. A) Direct determination of the kinase activity for FERM domain mutations using the Lance Ultra TR-FRET-based assay. Background counts were seen in assays without ATP addition (light gray bars), for BaF3 cells, and with immunoprecipitations using isotype control IgG. Recombinant human JAK3 (50 pg) was used as a positive control. Specific immune complexes of WT and mutant JAK3s showed kinase activity with ATP. The counts are shown as the average of nine independent kinase assays (mean ± SEM). Statistical comparison between mutant JAK3s and WT JAK3 showed significantly higher kinase activity in the mutants ($P<0.001$, denoted by asterisks). WT JAK3 showed statistically significant increased activity compared to IgG control ($P=0.008$). B) Shows western blots of JAK3 from a representative immunoprecipitation and the detection of autophosphorylated JAK3 after in vitro assay. 4G10 is specific for phospho-tyrosine and the third blot shows a phospho-Y980 of JAK3. Notably, a kinase dead compound mutant E183G/ K855A showed no autophosphorylation.

phosphorylation[99]. In fact, immunoprecipitated JAK3 proteins from transfected 293T cells did not show consistent Y980 phosphorylation.

Molecular modeling suggests an autoregulatory function for the JAK3 FERM domain

The frequency of mutation within the FERM domain suggests an autoregulatory role for the FERM domain, inhibiting kinase activity in the absence of cytokine stimulation and activation. The crystal structure of the JAK3 kinase domain was solved without the FERM domain[108]. Because of this, the crystal structure of the FERM domain of Focal Adhesion Kinase (FAK) was used as a model for JAK3 FERM domain structure revealing a possible structural basis for this kinase autoregulation. The FERM domain of FAK is the closest evolutionarily related FERM domain to JAK3 that has been crystallized. Amino acid side chains from the FAK FERM were shown to directly contact the intramolecular kinase domain causing occlusion of the substrate pocket[212].

When comparing the FERM domain of JAK3 to that of FAK, it was found that the mutations overlap with the subdomain of FAK that was determined to directly interact with the kinase domain of FAK regulating the activity of FAK. These data indicate that the JAK3 FERM domain may play a similar autoregulatory role, suggesting that the FERM domain may not only bind the IL-2 receptor but it may also directly interact with the kinase domain of JAK3. Upon JAK3 phosphorylation, the FERM domain may release constraints on the kinase domain allowing JAK3 activation. The three FERM domain mutations would likely

disrupt this interaction even in the absence of initial activation allowing the kinase domain to be constitutively active.

This homology based molecular model of the JAK3 FERM domain, based on the crystal structure of the FAK FERM**,** shows that all three ATLL derived mutations are within the same subdomain of the FERM. This correlates with the subdomain of the FAK FERM known to regulate FAK kinase activity, suggesting that the JAK3 FERM domain may play a similar autoregulatory role. In previous studies, FERM domain mutations from SCID patients, D169E and Y100C, found that an intact FERM domain was required for JAK3 binding of an ATP analog[111].

Therefore, the JAK3 FERM was modeled by homology to the FAK FERM domain crystal structure. The crystal structure of the JAK3 kinase domain is also shown with an alignment to FAK. The asterisks denote those residues in FAK that directly contact the intramolecular FERM domain. The residues of the FAK FERM domain that contact the FAK kinase domain (Figure 17) align in the same region as the ATLL mutations. Interestingly, this region is mainly alpha helical and the ATLL mutations are predicted to be helix disrupting.

The homologous residues in JAK3 are colored in yellow in the ribbon diagram, are at the surface available for binding, and not buried within the molecule, but only one of the six contact residues are conserved. The modeled JAK3 FERM structure suggests that the ATLL mutations could perturb the secondary structure required for autoregulation of kinase activity. Interestingly, a SCID mutation was described in this region as well, D169E, which causes decreased γc association and loss of kinase activity[213]. This SCID mutation is

```
                L156                R172        E183
JAK3        ---LSLKEQGECLSL--AVLDLARMAREQAQRPGELLKTVSYKACLPPSLRDL
FAK         DQEIALK-LG-CLEIRRSYWEMRGNALEKKSNYEVLEKDVGLKRFFPKSLLDS
                                              **  *         *  **
```

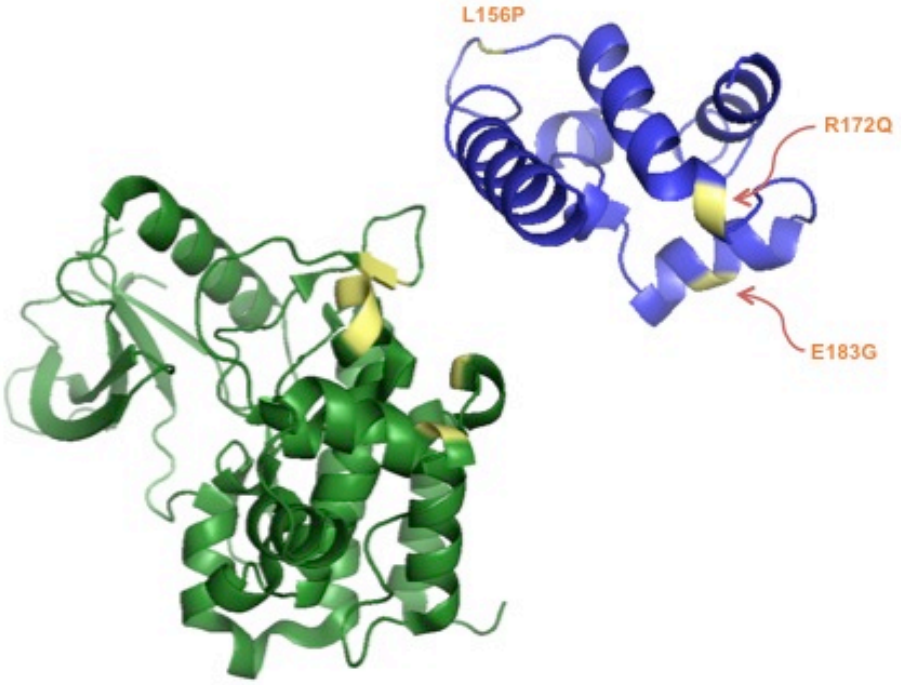


```
FAK  STRDYEIQRERIELGRCIGEGQFGDVHQGIYMSP-ENPALAVAIKTCKNCTSDSVREKFL
JAK3 ------FEERHLKYISQLGKGNFGSVELCRYDPLGDNTGALVAVKQLQHSGPDQQRD-FQ

FAK  QEALTMRQFDHPHIVKLIGVITEN---PVWIIMELCTLGELRSFLQVRKYSLDLASLILY
JAK3 REIQILKALHSDFIVKYRGVSYGPGRQSLRLVMEYLPSGCLRDFLQRHRARLDASRLLLY

FAK  AYQLSTALAYLESKRFVHRDIAARNVLVSSNDCVKLGDFGLSRYMEDSTYYKASK--GKL
JAK3 SSQICKGMEYLGSRRCVHRDLAARNILVESEAHVKIADFGLAKLLPLDKDYYVVREPGQS

FAK  PIKWMAPESINFRRFTSASDVWMFGVCMWEILMHGVKPFQGVKNNDVIG----------
JAK3 PIFWYAPESLSDNIFSRQSDVWSFGVVLYELFTYCDKSCSPSAEFLRMMGCERDVPALCR
                         ****
FAK  ---RIENGERLPMPPNCPPTLYSLMTKCWAYDPSRRPRFTELKAQLSTILEEEK------
JAK3 LLELLEEGQRLPAPPACPAEVHELMKLCWAPSPQDRPSFSALGPQLDMLWSGSRGCETHA
               *                                              *
FAK  ---------------
JAK3 FTAHPEGKHHSLSFS
```

Figure 17 ATLL FERM domain mutations align to autoregulatory region of the FAK FERM based on homology modeling. ATLL mutations (orange) align with the F2 subdomain of the FAK FERM (blue) that autoregulates the kinase domain of FAK. Asterisks denote residues of FAK FERM that contact the intramolecular FAK kinase domain. Molecular structure is based on the crystal structure of the FAK FERM domain. Those residues that are mutated in ATLL patients are highlighted (yellow). The JAK3 kinase domain (green) is shown as it would be oriented to the FERM domain. Below it, the respective kinase domains of FAK and JAK3 are aligned. The activation loop of the two proteins is in bold and the autoregulatory tyrosines, Y980 and Y981, are highlighted in orange. Asterisks show the residues of FAK that contact the intramolecular FERM. The residues of JAK3 that align with these are shown in yellow. Model of the JAK3 FERM domain based on the crystal structure of the FAK FERM. ATLL mutations identified in this study (orange) align with a subdomain of the FAK FERM that autoregulates the kinase domain of FAK. FAK FERM residues that contact the FAK kinase domain are denoted with asterisks.

only three residues away from a mutation (R172Q) that shows gain of function in our assays. These data suggest that the secondary structure of the JAK3 FERM domain is very sensitive to amino acid substitutions perhaps due to intramolecular contact with the kinase domain, analogous to FAK.

Discussion

The cell based assays and the in vitro kinase results support a gain of function activity for the mutant JAK3s. IL-2 signaling was reconstituted in HEK 293T cells, which lack IL-2R proteins. The cell line HEK 293T was utilized to transiently co-transfect all three subunits of the heterotrimeric IL-2 receptor IL-2Rα, β, and γ_c along with WT or mutant JAK3 and STAT5a. STAT5A phosphorylation (Y694) was increased with the addition of the activating mutation, A572V, and two of the FERM domain mutations, R172Q and E183G. Similar studies were done using the known SCID mutation, Y100C which was confirmed to have limited STAT5 phosphorylation. Were the Y100C mutation prevents receptor binding and R172Q and E183G most likely loose the ability to regulate kinase activity. These data demonstrate the potential dual regulatory function of the FERM domain of JAK3.

To verify that the observed P-STAT5A was caused by alterations specifically in JAK3 kinase activity, a catalytically inactive kinase mutation, K855A, was introduced into a JAK3 construct with the E183G FERM domain mutation. This compound mutant expressed stable protein to the same extent as WT JAK3 but showed no phosphorylation of STAT5A. As expected, the P132T

SNP introduced into the JAK3 construct showed the same level of P-STAT5A as WT JAK3.

Untransduced BaF3 cells and those transduced with WT JAK3 died after 3 days in culture without IL-3. All of the BaF3 cells transduced with ATLL derived mutant JAK3s continued to grow in the absence of IL-3 cytokine and became cytokine independent by day 7[139, 179]. BaF3 cells transduced with any of the JAK3 mutants continued to be passaged as stable cell lines without IL-3. Lysates prepared from cells where IL-3 was acutely withdrawn showed constitutive phosphorylation of STAT5 (Y694) and AKT (S493) and the phosphorylation of STAT5 was higher, even for mutants, in those lines when IL-3 was maintained in the media showing a distinct gain in functional activity in these JAK3 regulated pathways. BaF3 cells that expressed mutant JAK3s grew without IL-3 and were not impaired in their proliferation as they showed cell cycle profiles comparable to BaF3 cells maintained in IL-3 (Figure 8).

Based on modeling of the FAK FERM domain, it can be hypothesized that the FERM domain of JAK3 interacts with the kinase domain similar to FAK and implies a similar autoregulatory role (Figure 17).

From these observations, it can be speculated that the FERM domain of JAK3 functions in an autoinhibitory role when JAK3 activity is suppressed. Our results imply that when this suppressive function of the FERM domain is impaired, JAK3 is maintained in a near-constant activated state.

This evidence would be enhanced by a more thorough evaluation of the effects of specific mutations on JAK3 autophosphorylation as well as evaluation

of the autoregulatory properties of the JAK3 FERM domain by determining the role of each individual residue in the FERM subdomain that may interact with the kinase domain.

JAK localization has previously been described as having predominant nuclear localization of JAK1, JAK2, and TYK2[214-217]. But more recent studies have determined that JAKs are more often localized to the membrane and cytosol in the absence of stimulation[204].

Janus kinases are generally believed to be present in unstimulated cells in an inactive form. Ligand-induced receptor oligomerization, such as from cytokine interaction with its specific receptor, serves as a trigger to signal the recruitment of JAKs to close proximity of the receptors. JAK functions may not be restricted to cell surface receptors. JAK2 has been identified as the kinase that associates with p97, a member of the ATPases associated with different cellular activities, which is involved in membrane fusion and assembly of the transitional endoplasmic reticulum[218].

It is crucial not to use overexpressed proteins when subcellular localization is investigated since posttranslational protein modification processes and endogenous protein/protein interactions may become limited upon overexpression. This can lead to severe artifacts in subcellular localization. In addition, it is well known that overexpressed Janus kinases activate themselves and aggregate in the cytosol.

CHAPTER V

JAK3 FERM MUTATIONS IDENTIFIED IN ATLL ARE WEAKLY ONCOGENIC

Background and significance

Long latency between initial infection and cancer development suggests that there are most likely multiple somatic mutations after the initial requirement, HTLV-1 infection until the development of ATLL. The in vitro assays described in previous chapters show that the JAK3 proteins with FERM domain mutations are more active kinases when compared to wild type JAK3.

Previously the constitutively active A572V JAK3 mutation was shown to induce lymphoproliferative syndromes in murine bone marrow transplantation models[191]. Unfortunately, hyperproliferative lymphocytes from this transplant were not able to be serially transplanted and thus were not shown to be oncogenic. In a murine bone marrow transplant model using either WT C57/B6 of $JAK3^{KO}$, donor bone marrow was transduced with ATLL derived mutant JAK3s and lymphoproliferative disease was seen in only few individuals suggesting an extremely low penetrance of disease. Upon serial transplantation, the secondary recipients did not develop disease. It should be noted that because of the low number of primary illness, only three mice were used for secondary transplantation. It was therefore determined that JAK3 activating mutations alone cannot induce leukemia *in vivo.* The activating JAK3 mutation A572V, originally

identified in acute megakaryoblastic leukemia and later found in Natural killer/T-cell lymphoma was not able to confer disease upon serial transplantation[5, 6]. As noted by Walters et al, this observation would suggest that JAK3 activation is acting in cooperation with other mutations to confer complete transformation.

The *CDKN2A* locus encodes 2 cell cycle regulatory proteins, p14(ARF) (p19 in mice) and p16(INK4a), which share exon 2 but use different promoters and first exons and alternate reading frames. Both proteins are commonly co-deleted in a large variety of human cancers. Human genetic data suggest that both INK4a and ARF products are important tumor-suppressor proteins [221-227]. The p14(ARF) and p16(INK4a) genes have both been implicated as tumor suppressor genes by frequent mutations, deletions, or promoter hypermethylation in a variety of tumors. One of the genetic events necessary for the development of ATLL is the inactivation of tumor suppressor genes such as p14(ARF), p16(INK4a) or p53. In one study it was shown that 25% of a small cohort of ATLL patients had both p14(ARF) and p19(INK4A) suppressed through either promoter methylation or gene deletion. Two percent of these patients had loss of p14(ARF) expression only. All of the patients with loss of p14(ARF) expression had shorter survival, similar to that of patients with the p53 mutation, constant with the inactivation of p14(ARF) plays a key role in the progression of ATLL[219]. Another study found that six out of nine cell lines had lost p16(INK4a) expression and only one out of nine lost p14(ARF)[220].

Likewise, mice lacking both p16(INK4a) and p19(ARF) (*CDKN2A* ^{KO}), or p16(INK4a) only (*p16(INK4A)* ^{KO}), or p19(ARF) only (*p19(ARK)* ^{KO}) are prone to

developing tumors spontaneously and are sensitive to carcinogens, albeit with differences in latency and tumor spectra [228-230]. *Cdkn2a*^{KO} mice primarily develop B-cell lymphomas and sarcomas but can also develop a variety of tumors[231, 232].

Because cancer is a disease of accumulated mutations it was decided to look for potential cooperation between JAK3 activation and other mutations described in ATLL. The relationships between alterations in the *CDKN2A* and ATLL were previously investigated. Modifications on the *CDKN2A* were described in ATLL, including point mutations, in 18.2% of the 44 patient samples analyzed[164, 233]. Alterations in the *CDKN2A* were detected in approximately 15 to 20% of ATLL patients. Interestingly, most of the patients with *CDKN2A* alterations had the aggressive form of ATLL. p16(INK4a) is epigenetically inactivated in 5 ATLL cell lines. In one ATLL cell line exon 2 was deleted, preventing expression of both p14(ARF) and p16(INK4A)[220]. p14(ARF) mRNA expression was suppressed in 13 of 37 ATLL cases, among which 9 cases showed inactivation of both p14(ARF) and p16(INK4A)[219]. *CDKN2A* thus appears to be a major tumor suppressor gene and alterations in this gene may play an important role during late stages in the transformation process induced by HTLV-1[234]. The status of p14(ARF and p16(INK4A) is unknown for the four patient samples that contain FERM domain mutations.

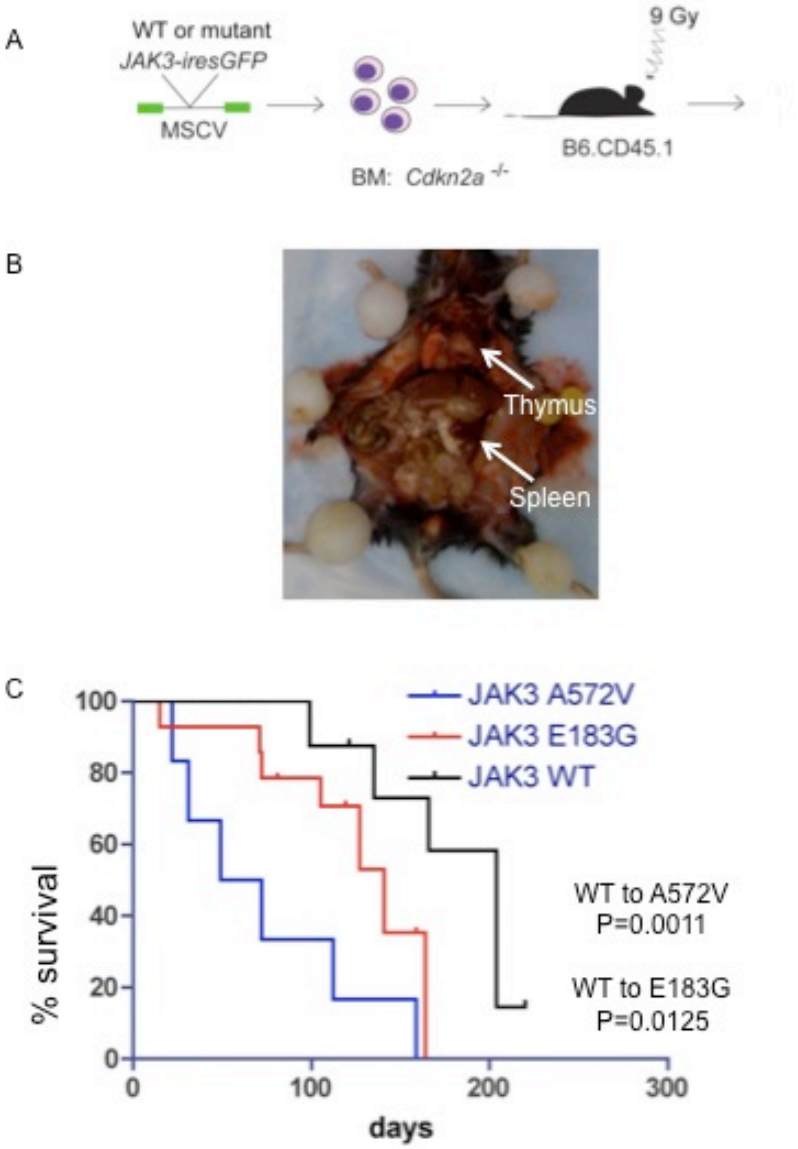

Figure 18 Activating JAK3 mutations cooperate with the loss of *CDKN2A* in vivo. A) Bone marrow was taken from the tibia and fibula for *CDKN2a*^{ko} mice and transduced with MSCV JAK3 retrovirus. Cells were maintained in culture in the presence of cytokine and virus for 5 days before retroorbital injection in to lethally irradiated B6/CD45.1 recipient mice. B) Arrows indicate enlarged spleen and thymus, C) Survival curves of BMTT recipient mice expressing WT, A572V, or E183G JAK3.

Results

The expression of activated JAK3 decreases rate of survival of *Cdkn2a*^{KO} mice

WT JAK3 and JAK3 mutants were introduced into MIG constructs which were then used to make high titer (10^6 pfu/mL) retrovirus using the Phoenix packaging cell line. These viruses were used to transduce the BaF3 cells in the preliminary studies discussed above. Hematopoietic bone marrow cells from C57B6 mice were transduced with either MIG-JAK3 WT or MIG-JAK3 mutant viruses and then transplanted into lethally irradiated C57B6-Ly5.2 recipients. Although these mice were monitored for illness, very few showed any recognizable signs of disease, even after analysis of thymi, spleen, and bone marrow by flow cytometric analysis (data not shown).

Hematopoietic bone marrow cells from *Cdkn2a*^{KO} mice were transduced with MIG-JAK3 WT or MIG-JAK3 mutant viruses and transplanted similarly into lethally irradiated C57B6-CD45.1 recipients (Figure 18A). In contrast, these mice developed palpable splenic tumors as early as 20 days post transplantation (Figure 18B). Because of the loss of both P16(INK4a) and p19(ARF) tumor suppressors, it was expected that all mice would eventually develop tumors. Remarkably, both the A572V and E183G transduction groups showed accelerated development of disease as compared to WT JAK3 transduced samples. Almost all of the mice analyzed developed large spleens (22/23 measured), with a few also showing an increase in thymus size (7/12 measured).

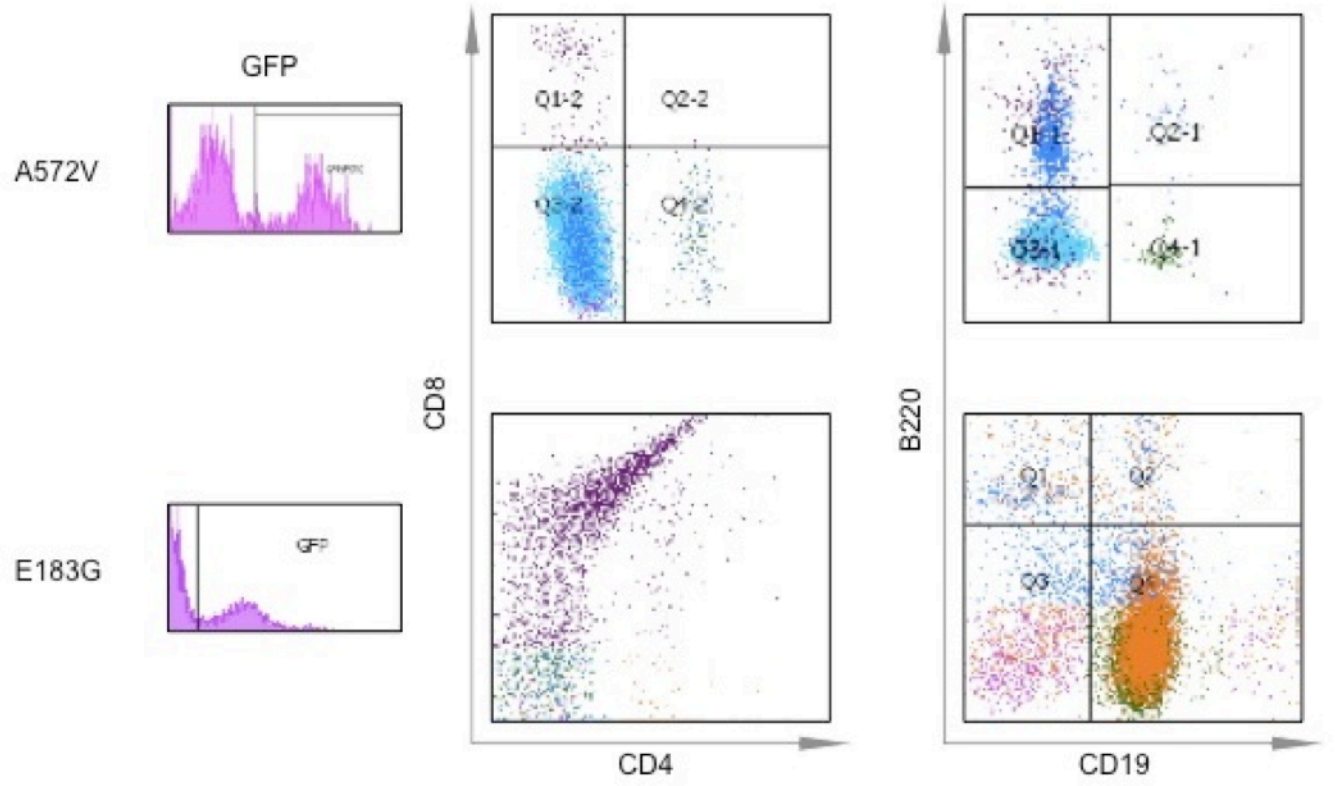

Figure 19 Activating JAK3 mutations induce mostly B-cell and some T-cell leukemias in *CDKN2A*^{KO}. Representative samples for A572V and E183G splenic tumors. Spleen, Thymus, BM and peripheral blood were stained for CD4, CD8, CD25, CD44, CD19, B220, Gr1, and Mac1 and analyzed by by flow cytometry. These results gated on GFP and CD45.2 positive cells.

All of the mice with larger thymi were from the E183G group while none were from the WT transductions (Figure 18C).

Mice expressing activated JAK3 on a *Cdkn2a*^{KO} background developed predominantly B-cell lymphomas

CD4, CD8, CD25, CD44, CD19, B220, Gr1, and Mac1 extracellular membrane-bound expression levels were analyzed by flow cytometry and results were determined for GFP/CD45.2 positive cells only from spleen, thymus and bone marrow of each mouse. For E183G mice, 9 out of 11 samples analyzed showed GFP positive splenic tumors (Figure 19). Two of these also had large thymic tumors,as compared to WT derived tumors, where only 3 out of 10 tumors were positive for JAK3 transduction as determined by GFP expression. This suggests that expression of activated JAK3 provides a growth advantage in conjunction with loss of expression of p16(INK4A) and p19(ARF) *in vivo*. Most tumors were positive for either or both of the B-cell markers CD19 and B220. As *Cdkn2a*^{KO} mice predominantly develop B-cell lymphomas, the BM from these mice may already be primed to develop in B-cell lineage.

Analysis of tumor clonality also showed a predominantly B-cell rearrangement with only some tumors having obvious clonality (Figure 20A). Rearrangement at both the Immunoglobulin heavy chain (IgH) and T-Cell receptor beta (TCRβ) gene loci was necessary to determine the clonal orgin of developed tumors. Characteristic of early lymphoid differentiation, the resulting phenotypes can be analyzed with PCR amplification. PCR was used to analyze

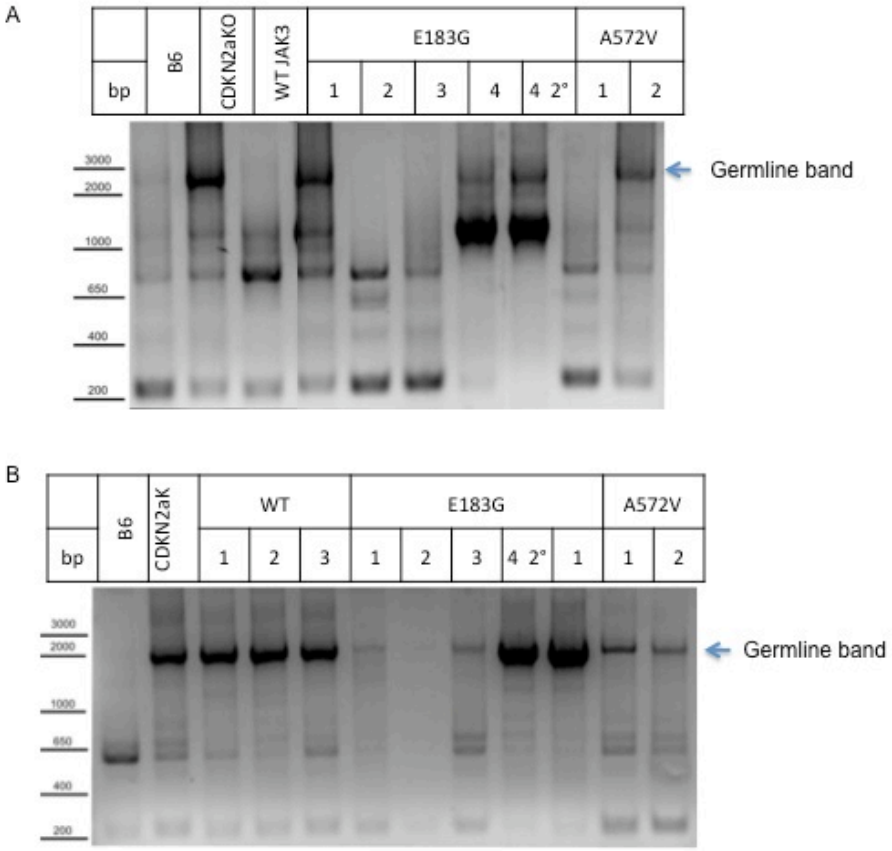

Figure 20 *CDKN2a*^{KO} BMTT PCR analysis of recombination. Genomic DNAs from splenic tumors were subjected to PCR with primers designed to amplify various junctions IgH and TCRβ . PCR products were separated in a 2% agarose gel. Genomic DNAs from B6 spleen, *CDKN2a*^{KO} were used as a negative and a positive controls, respectively. A) PCR for IgH shows some B cell tumor clonality. B) Very little TCRβ rearrangement is observed and no T-cell clonality.

the variable subunits of both IgH & TCRβ. Receptor expression during normal development is not typically clonal and a profile showing only one rearrangement suggests tumorigenesis resulting from mass proliferation in late-stage lymphocytes. There is an obvious lack of rearrangement in TCRβ. Most but not all samples showed, one or two distinct IgH rearrangements with corresponding clonality found by the insertion site analysis (Figure 20).

Oncogenic cooperation between loss of *Cdkn2a* and activated JAK3 as determined by secondary transplantation

Tumors from two GFP positive WT JAK3 and four E183G primary tumors were injected into four and eight secondary recipients, respectively. All of the serial recipient mice developed tumors but seven of eight of the E183G transplants and one out of four WT secondary recipients maintained their JAK3 expression. This suggests cooperation between the activated E183G allele that does not occur with simple overexpression of the WT JAK3 allele.

Discussion

Previously, it was described that alterations in *CDKN2A* may play an important role during late stages in the transformation process induced by HTLV-1 and that other mutations must be necessary earlier in the transformation process to induce leukemia[234]. Walters *et al* showed a pre-leukemic expansion of T-cells and megakaryocytes in transplanted bone marrow cells transduced with the A572V mutant as early as 6 weeks. They were unable to serially transplant

these cells, suggesting that this mutation is not oncogenic on its own. Thus, it can be inferred that cooperating mutations may be necessary to develop full blown leukemia.

Expression of an activated allele of JAK3, E183G, in conjunction with the loss of *Cdkn2a* leads to a decrease in the survival rate and accelerated rate of tumor formation. The resulting tumors express a range of IgH and TCRβ phenotypes but are predominantly clonal for IgH rearrangement consitant with CD19 and B220 expression by flow cytometry. The expression of activated JAK3 acts as a catalyst to accelerate tumor progression in the B-Cell leukemia/lymphoma prone *Cdkn2a* knockout cells. The addition of activated JAK3 decreases the mean survival rate in comparison to WT as would be expected if these mutations were oncogenic in nature. These BMTT samples could also be analyzed for specific protein expression to analyze signaling pathways that may be disrupted via western blot, quantitative reverse transcription PCR (qRT-PCR) or immunohistochemistry.

CHAPTER VI

JAK3 MUTANTS ARE SENSITIVE TO SPECIFIC INHIBITORS *IN VITRO*

Background and significance

The current life expectancy is roughly one year after ATLL diagnosis and >90% of patients succumb within that time. ATLL generally responds poorly to standard treatment. Chemotherapy and monoclonal antibodies directed against ATLL tumor markers were shown to have little effect. Previously we have identified three mutations that induce gain of function in JAK3 from ATLL tumors.

Because ATLL is incredibly rare, it would useful to identify potential specific drug targets, such as activated JAK3, and use existing drugs against these targets, such as tofacitinib, in conjunction with current treatments. Tofacitinib (trade name Xeljanz**,** aka tasocitinib, CP-690,550; CP-690550; CP690550), an orally active immunosuppressant, is developed by Pfizer for the treatment of rheumatoid arthritis, inflammatory bowel disease, dry eyes, ankylosing spondylitis, psoriasis, psoriatic arthritis, and for the prevention of transplant rejection. Tofacitinib specifically inhibits Janus kinase 3 (JAK3), which has a pivotal role in cytokine signal transduction[235].

Other inhibitors such as BEZ-235 (Selleck), BKM-120 (Active Biochem), and CI-1040 against PI3K/mTOR, PI3K and MEK, respectively, inhibit downstream signaling targets of JAK3 activation. The effectiveness of these various inhibitors need to be evaluated as potential treatment options for ATLL.

During clinical trials for moderate to severe rheumatoid arthritis, tofacitinib was reported to induce a higher rate of leukopenia, neutropenia, anemia, and lymphopenia in patients treated with over 30mg twice daily as compared to lower doses[236]. This phenotype is similar to that seen in JAK3 knockout mice. The thymi of $JAK3^{KO}$ are small or completely absent revealing a defect in T cell development. $JAK3^{KO}$ mice also have limited B cell development. This deficiency is likely the result of a block at the pre-B/pro-B stage of B cell development and is likely to be due to the lack of signaling through the IL-7 receptor, which is necessary for B cell development[112, 237, 238]. In addition to its well-known roles in T cells and NK cells, JAK3 mediates IL-8 stimulation in human neutrophils. This may also relate to the increased neutropenia after tofacitinib treatment[113].

Results

JAK3-specific tyrosine kinase inhibitor, tofacitinib alters phosphorylation and protein signaling

The JAK3-specific inhibitor, tofacitinib, was tested on the BaF3 cells stably expressing mutant JAK3s[239-241]. BaF3 cells were cultured expressing WT JAK3 or mutant JAK3s with 0.5, 2, or 4μM of tofacitinib or with solvent (DMSO) alone and probed for JAK3 protein, P-Y980 of JAK3, and P-STAT5A at 4 and 24 hours by quantitative Western blot analysis. The JAK3 and P-STAT5A protein levels were expressed as fold difference as compared to BaF3 cells treated with solvent alone. The BaF3 lines stably expressing mutant JAK3s showed a distinct,

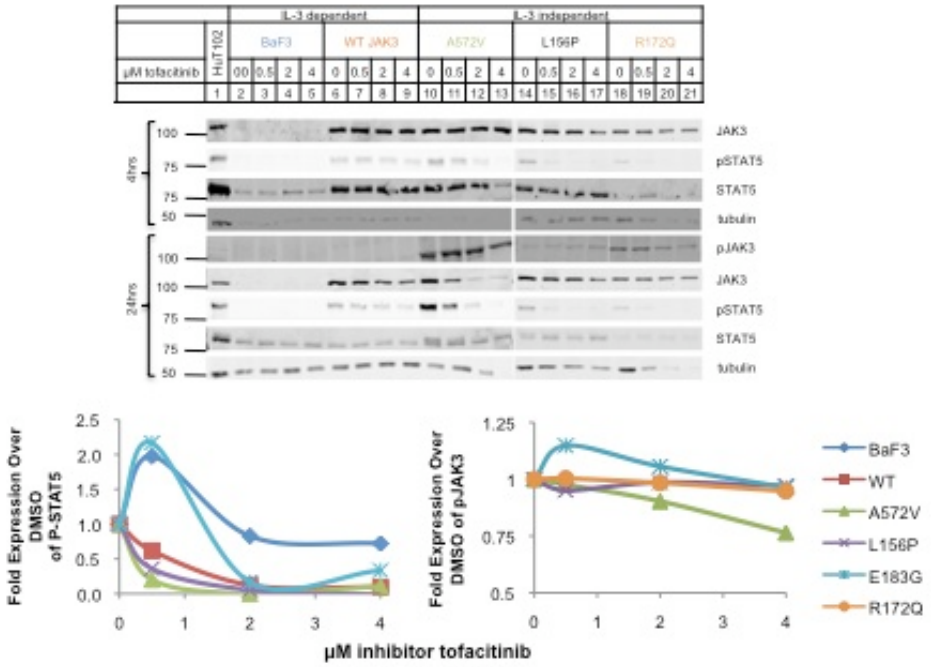

Figure 21 JAK3-specific tyrosine kinase inhibitor, tofacitinib alters phosphorylation and protein signaling. A) BaF3 cells transduced with mutant JAK3s were treated with tofacitinib at concentrations of 0, 0.5, 2.0 and 4.0 μM and analyzed by Western blot analysis at 4 and 24 hours. The Western blots and graphs that display their quantification are shown. Protein levels are expressed as fold over levels seen in cells treated with DMSO (solvent) alone. JAK3 (106 kDa) protein expression was comparable to DMSO-alone but decreased in the mutant JAK3-transduced BaF3 cells. P-STAT5 (92 kDa) levels decreased markedly with increasing concentrations of inhibitor. P-JAK3 (106kDa) levels were relatively stable. JAK3 is not phosphorylated in WT transduced cells so it could not be quantified. Tubulin (55 kDa), a loading control, remained relatively stable.

dose-dependent decrease in P-STAT5A. At 2μM, P-STAT5A levels were decreased by 80% for all BaF3 cells stably expressing mutant JAK3s. Untransduced BaF3 cells showed much lower P-STAT5A at steady state, and this quantity only decreased 30% at much higher concentrations (4μM) of tofacitinib; P-STAT5A in BaF3 cells transduced with WT JAK3 was similarly resistant to the effects of inhibitor. JAK3 and tubulin were quantified as well. BaF3 cells have STAT5 phosphorylation secondary to the IL-3/JAK2 signaling which may have variable sensitivity to tofacitinib in cell based assays even though JAK2 kinase activity is inhibited at concentrations comparable to JAK3 inhibition in cell free enzyme assays[102](Figure 21).

Tofacitinib did not inhibit Y980 phosphorylation to the same extent as STAT5A phosphorylation. P-Y980 in the A572V mutant JAK3 was most sensitive but only decreased to 75% of basal levels at the highest concentrations (4μM) (Figure 21).

Mutant JAK3s are sensitive to JAK3-specific tyrosine kinase inhibitor, tofacitinib

The inhibitor induced a decrease in P-STAT5 thath correlated with decreased growth of these BaF3 cells. The IC50 curves demonstrated a noticeable difference between BaF3 cells expressing mutant JAK3s versus those expressing WT JAK3 and in the untransduced BaF3 cells. Untransduced BaF3 cells and those expressing WT JAK3 were not as sensitive to tofacitinib and

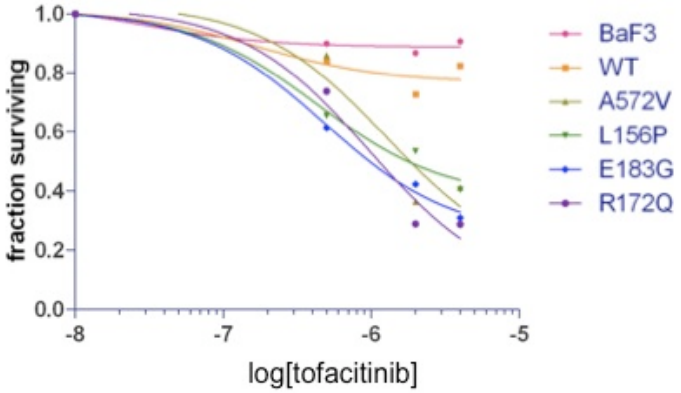

Figure 22 Mutant JAK3s are sensitive to JAK3-specific tyrosine kinase inhibitor, tofacitinib. Live cells were quantified by the MTT assay. Cell survival decreased with increasing concentrations of tofacitinib. BaF3 cells expressing mutant JAK3s were susceptible to tofacitinib (IC50: A572V, 0.22 nM; L156P, 0.27 nM, E183G, 0.087 nM, R172Q, 0.082 nM).

curve-fitting did not generate models with high correlation (R^2>0.90). Mutant JAK3 expressing BaF3s showed consistent sensitivity to tofacitinib with similar curves (Figure 22).

BaF3 cells expressing activated JAK3s are sensitive to inhibitors against JAK3 downstream targets

JAK3 specific inhibitor WHI-P131(JAK3 inhibitor 1) and pan kinase inhibitor staurosporine also inhibit phosphorylation and JAK3 signaling. HEK 293 cells transfected with IL2RA, IL2RB, IL2RG, STAT5A and JAK3 were treated with 100U/ml of hIL-2 and 0, 0.025, 0.1 and 0.25μM staurosporine. All JAK3s showed decreased phosphorylation of STAT5A in response to an increase in staurosporine concentrations and were susceptible to treatment even at concentrations as low as 0.025μM (Figure 23). To further test if the effect of tofacitinib was JAK3 specific, BaF3 cells were treated with a second cell-permeable JAK3 inhibitor, WHI-P131. WHI-P131 is an ATP-competitive inhibitor specifically against JAK3 that has no effect on JAK1, JAK2, or TYK2. Like tofacitinib, WHI-P131 inhibits cell growth to a greater extent in BaF3 cells transduced with activated JAK3 (data not shown).

To further determine the signaling pathways that were affected by JAK3 activation, transduced BaF3 cells were treated with inhibitors against downstream activation targets of the JAK3 pathway, inducing PI3K, mTOR, and ERK1/2. Cell growth was inhibited with BEZ-235. BEZ-235 binds the ATP-binding

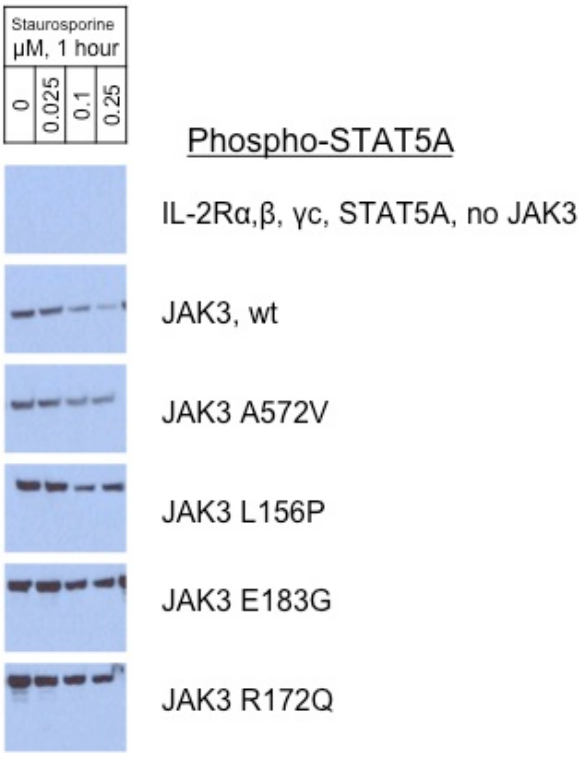

Figure 23 P-STAT5 decreases with increased concentrations of staurosporine in transfected HEK 293T cells. HEK 293T cells transiently transfected with all components of IL2R, STAT5A, and JAK3 were treated with 100U/ml hIL-2 for 24 hours then treated for 1 hour with concentrations of 0, 0.025, 0.1 and 0.25μM staurosporine.

Table 6 Mutant JAK3s are sensitive to JAK3, PI3K and mTOR inhibitors. Live BaF3 cells were quantified by the MTT assay after 24 hours on inhibitor. IC50 and goodness of fit (R^2) values for each mutant transduced into BaF3 cells were calculated based on best fit curves. ND means IC50 could not be determined due to poor curve fitting models. Goodness of fit for all MTT assays as represented by R^2 values are shown and 95% confidence intervals for IC50s are shown. Data is a compilation of two experiments done in quadruplicate.

	Tofacitinib (μM)		**BEZ-235 (nM)**		**BKM-120 (μM)**		**CI-1040 (nM)**	
	JAK3		PI3K/mTOR		PI3K		ERK 1/2	
	IC50	R^2	IC50	R^2	IC50	R^2	IC50	R^2
BaF3	ND	0.77	ND	0.60	ND	0.55	ND	0.88
WT	0.18	0.84	ND	0.44	ND	0.65	ND	0.72
A572V	0.22	0.99	12.55	0.86	3.12	0.92	ND	0.73
L156P	0.27	0.99	11.96	0.90	2.51	0.93	ND	0.64
E183G	0.09	0.99	18.14	0.96	1.99	0.91	ND	0.62
R172Q	0.08	0.90	19.21	0.84	9.12	0.96	ND	0.50

clefts of PI3K and mTOR inhibiting their activity. MTT cell proliferation experiments were performed at concentrations of 0, 0.01, 0.05, 0.1, 0.5, 1, 5, 10, 50, 100, 500, and 1000nM. Cell growth was inhibited with a pan-PI3K inhibitor PI3K, BKM-120. MTT experiments were performed at concentrations of 0, 0.025, 0.05, 0.1, 0.25, 0.5, 1, 2.5, 5, 10, 50, and 100μM. Cell growth was not inhibited by treatment with CI-1040, a non-competitive inhibitor of ERK1/2. MTT experiments were performed at concentrations of 0, 0.01, 0.05, 0.1, 0.5, 1, 5, 10, 50, 100, 500, and 1000nM. Interestingly, the BaF3 cells expressing mutant JAK3s were sensitive to PI3K and mTOR inhibitors but not to an ERK1/2 inhibitor. This finding is consistent with the STAT5A and PI3K/AKT pathways being active in the BaF3 cells expressing mutant JAK3 protein (Table 6).

Tofacitinib inhibits STAT5 phosphorylation and JAK3 expression in cultured ATLL cell lines in the absence of a JAK3 mutation.

Cell lines dependent on JAK3 for survival are susceptible to the JAK3 specific inhibitor tofacitinib[242]. BaF3 cells stably expressing JAK3 mutants and two ATLL cell lines, Hut-102 and MT-2, which do not contain JAK3 mutations were treated with tofacitinib. The BaF3 lines stably expressing JAK3 mutants showed a dose-dependent decrease in P-STAT5, whereas untransduced BaF3 cells showed lower P-STAT5 (50% of the levels observed in the control group treated with solvent alone) only at higher concentrations (4μM) of tofacitinib (Figure 21). BaF3 cells phosphorylate STAT5 by signaling through the IL-3/JAK2

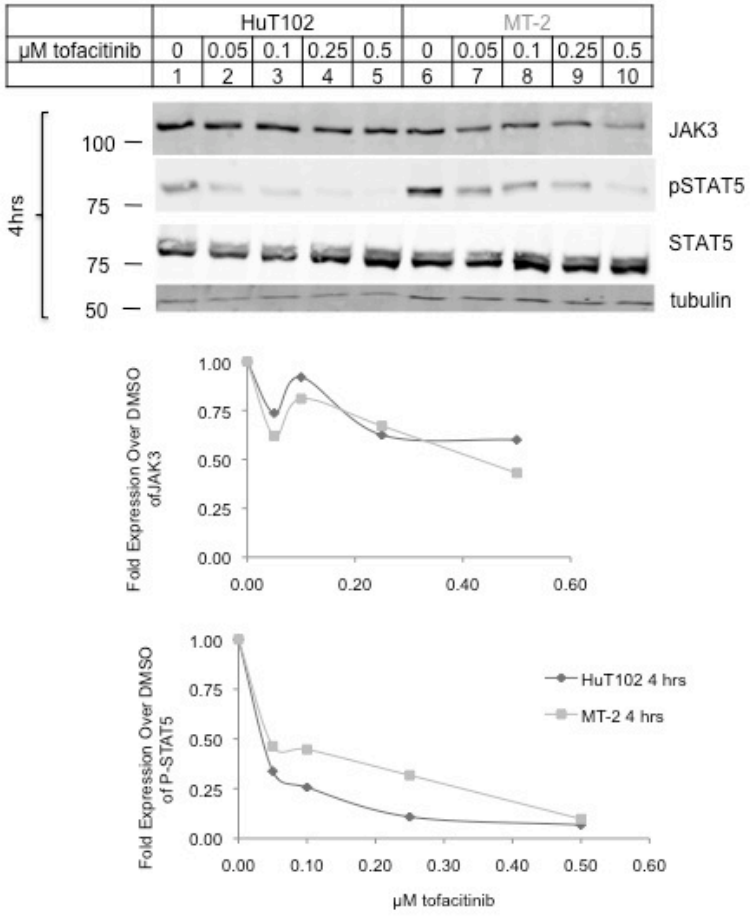

Figure 24 ATLL cell lines Hut-102 and MT-2, are sensitive to JAK3 specific tyrosine kinase inhibitor, tofacitinib. A) Human ATLL cell lines, HuT-102 and MT-2, were also treated with tofacitinib. P-STAT5A was sensitive at even lower concentrations of the inhibitor. Both cells showed decreased P-STAT5A with increasing levels of inhibitor. JAK3 (106 kDa) protein also decreased whereas tubulin (55 kDa) levels did not. B) Quantification of JAK3 and pSTAT5 for HuT-102 and MT-2 treated with tofacitinib. Protein lysates from the experiments similar to those shown in Figure 4 were blotted quantitatively for JAK3, STAT5, pSTAT5 and tubulin. JAK3 and pSTAT5 protein quantity was normalized to that seen in cells treated with DMSO (vehicle) alone.

pathway. JAK2 was shown to be sensitive to tofacitinib at high concentrations**.** The phosphorylation of STAT5 in both Hut-102 and MT-2 cells was sensitive too the tofacitinib (Figure 24). Hut-102 and MT-2 cells treated with tofacitinib greater than 1.0μM died too rapidly to be analyzed (data not shown). For this reason, Hut-102 and MT-1 cells were treated with much lower doses of tofacitinib 0, 0.05, 0.1,0.25, and 0.5μM and analyzed by western blot analysis at 4 hours. After tofacitinib treatment, JAK3 (106 kDa) protein expression was compared to DMSO only treatmentsa and was shown to be decreased in both MT-2 and Hut-102 cells. P-STAT5A (92 kDa) levels decreased with increasing concentrations of inhibitor. Tubulin (55 kDa), a loading control, remained relatively stable (Figure 24).

Discussion

All four activating JAK3 mutations characterized here were inhibited with two JAK3 inhibitors, tofacitinib and WHI-P131. Tofacitinib was one of the first JAK inhibitors to enter the clinic and was recently FDA approved for the treatment of rheumatoid arthritis. Our findings underscore the importance of this pathway in ATLL development and offer a therapeutic target for this incurable cancer.

The diminished STAT5 phosphorylation also correlated with growth inhibition at concentrations that could be achieved in culture for both BaF3 cells and ATLL cell lines dependent on JAK3. The dose response data for BaF3 cells transduced with JAK3 mutations was found to be considerably lower than the

dose responses for untransduced BaF3 cells or BaF3 cells transduced with WT JAK3. Cell proliferation decreased with an increase in tofacitinib concentration in all BaF3 cell lines expressing JAK3 mutations, as well as ATLL cell lines, Hut-102 and MT-2.

STAT5 phosphorylation in both Hut-102 and MT-2 cells, both derived from ATLL patients, was sensitive to tofacitinib. Mutations in the JAK3 gene in Hut-102 or MT-2 cells were not found, although both lines utilize JAK3 for signal transduction. Hut-102, an HTLV-1 positive ATLL derived cell line, requires exogenous IL-2 for optimal growth, and MT-2 cells contain an HTLV-1 integrant 5' of the *IL9R* gene which induces overexpression of the receptor. These high levels of IL-9R may signal through JAK3 without ligand.

It should be noted that both of our ATLL cell lines have high basal expression of phosphorylated JAK3. In a preliminary assay MT-2 cells were shown to require JAK3 expression in a knockdown assay. MT-2 cells transduced with siRNA against JAK3 were not able to maintain viability with the loss of JAK3. Upon initial JAK3 knockdown, the cells were incredibly unhealthy in culture and when those cultures were analyzed days later JAK3 expression was reaffirmed indicating that JAK3 is required for continued cell proliferation (Figure 25).

After treatment with WHI-P131, BaF3 lines stably expressing JAK3 mutants showed dose-dependent decreases in P-STAT5. Untransduced BaF3 cells showed lower P-STAT5 as compared to solvent alone and mutant transduced cells. These results were comparable to those seen with tofacitinib treatments.

BaF3 cells have STAT5 phosphorylation after treatment with IL-3 due to IL-3/JAK2 signaling, which may have variable sensitivity to tofacitinib in cell based assays. When tested *in vivo,* results may vary depending on the primary tumor sample and kinase inhibitor.

Our findings thus underscore the importance of this pathway in ATLL development and offer a potential therapeutic opportunity for this incurable cancer. Further supporting this data, proliferation was inhibited in *ex vivo* primary ATLL tumor cells by the addition of nanomolar concentrations of tofacitinib[243]. It is possible that ATLL primary tumors samples with increased P-JAK3 will be growth inhibited *in vivo* when treated with kinase inhibitors such as tofacitinib.

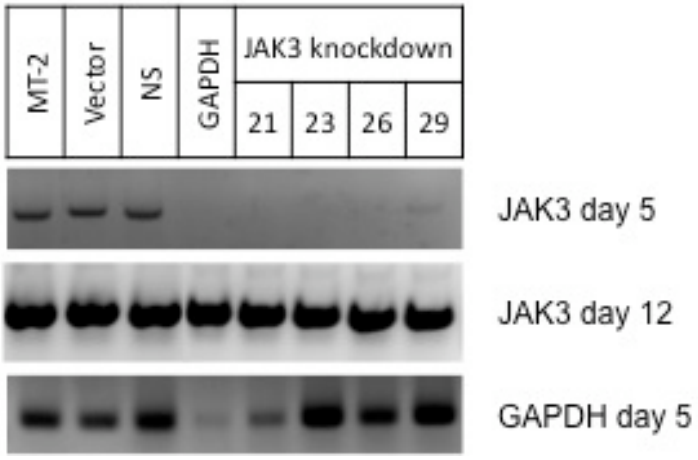

Figure 25 HTLV-1 transformed cell line, MT-2, does not maintain JAK3 knockdown. RNA was isolated from MT-2 cells 5 and 12 days post transduction with lenti-virus expressing siRNAs against JAK3. JAK3 and GAPDH expression was determined by RT-PCR and run on a 2% agarose gel.

CHAPTER VII

ACTIVATED JAK3 AS A TARGET OF DISEASE TREATMENT AND PREVENTION *IN VIVO*

Background and significance

Here, as well as in other studies, cell growth is inhibited in primary ATLL tumor cells treated ex vivo with tofacitinib at a nanomolar range[243]. BaF3 cells have increased cell proliferation in the absence of mIL-3 with the addition of JAK3 containing activating mutations L156P, R172Q, E183G, and A572V. This growth is also inhibited by treatment with tofacitinib. These in-cell studies support the efficacy of treatment with the oral JAK3 inhibitor tofacitinib.

In vivo methods that most closely duplicate disease conditions are important for further understanding of disease progression and to test novel therapeutic treatments for ATLL.

Activated JAK3 allows BaF3 cell engraftment

Transduced BaF3 cells expressing WT, L156P, E183G, and A572V JAK3 were engrafted into lethally irradiated immunocompromised NSG mice to determine the advantage of an activated JAK3 in vivo. All three activating mutations showed signs of tumor growth at the site of injection within one week (Figure 26). Engraftment was determined by flow analysis of the peripheral blood for GFP within three weeks. GFP expression at week three for WT was 1.1%, 25.0% for A572V, 1.1% for E183G, and 7.65% for L156P in the peripheral blood. Mice injected with L156P, E183G, and A572V were sacrificed by 21 days due to

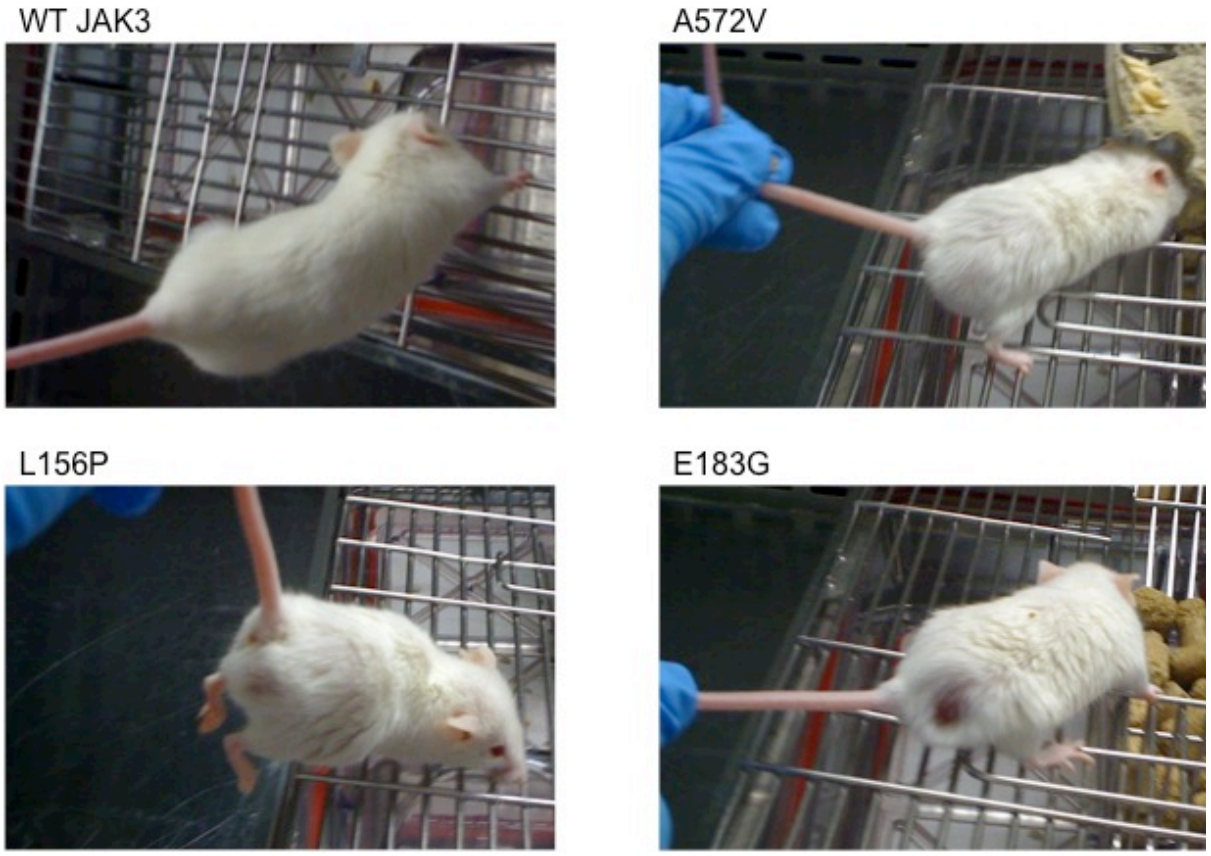

Figure 26 Activated JAK3 mutations allow engraftment into NSG mice. NSG mice were injected subcutaneously with $1x10^7$ Stably transduced BaF3 cells. WT mice did not develop tumor. A572V, E183G and L156P mice were all sacrificed after palpable tumor grew to more than 2 cm in diameter.

excessive tumor volume at the injection sight. A572V tumor volume was 1.5 cm^2, with BM infiltration of 84.1%, and spleen infiltration of 79.5% on the day of sacrifice. E183G showed signs of external ulceration at the injection site, with a tumor volume of 1 cm^2, BM infiltration of 84.6% and spleen infiltration of 80.85%. L156P tumor volume was 1cm^2, with BM infiltration of 89.0% and spleen infiltration of 85.6%. Initially WT peripheral blood was 2.2% at one week. By week 2 this was down to 1.1%. No tumor was observed at the site of injection and no engraftment was seen in the BM or spleen for WT. These data indicate that only BaF3 cells that are IL-3 independent by transduction with activated JAK3 are able to engraft NSG mice.

ATLL tumor protein signaling and generation of ATLL bearing mice

Each ATLL tumor sample has an individual phenotype specific to that tumor, certain signaling characteristics may be common to all tumors. Protein expression of and phosphorylation status were analyzed for 25 primary ATLL samples for JAK3, STAT5, AKT, and tubulin by western blot (Figure 27). STAT5 and AKT were expressed in all samples, with a lower expression level of STAT5 in 5 out of 25 samples and 3 out of 25 for AKT as compared to loading control Hut-102. JAK3 expression was less consistent, with high expression levels noted in only 10 of the 25 samples, although it was expressed in nearly all of the samples. Unfortunately, P-JAK3 is difficult to analyze in these samples due to the

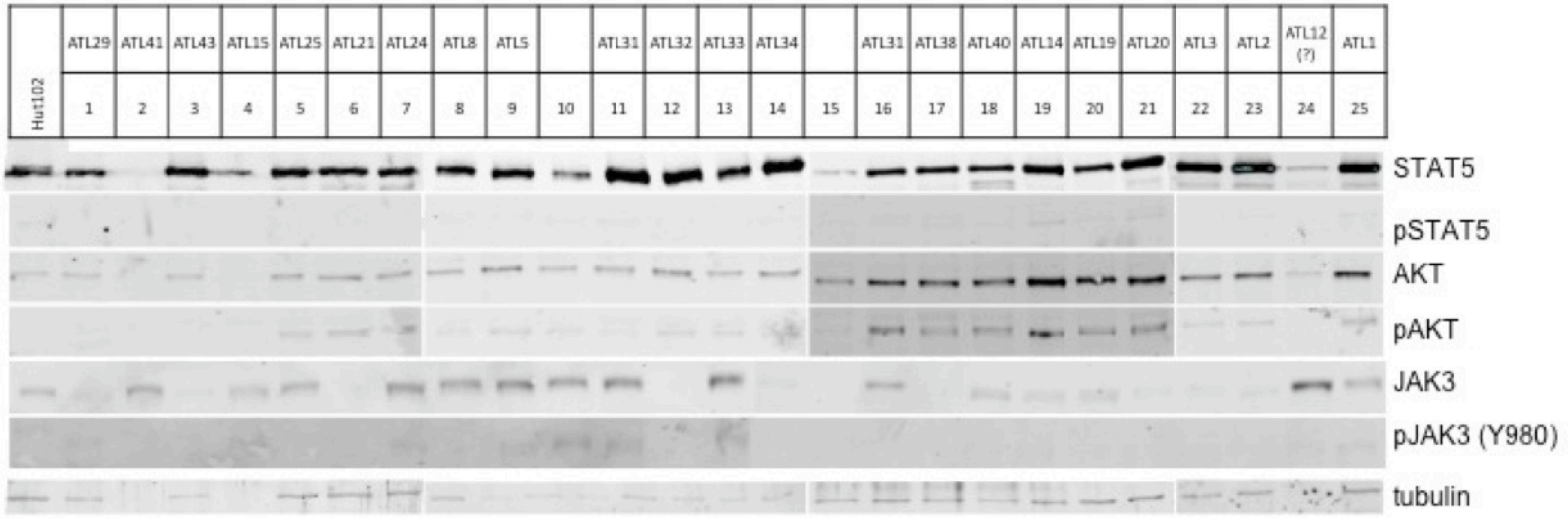

Figure 27 Primary ATLL protein expression. STAT5 and AKT is expressed in almost all ATLL tumor samples. JAK3 expression is apparent in 20 out of 25 samples.

method of protein processing used. Lanes 4, 7, 9, 10 and 11 had lightly visible P-JAK3. It is anticipated that if these samples were immunoprecipitated in appropriate buffer that the quantity of P-JAK3 positive samples would be higher. AKT is phosphorylated in most samples. STAT5 and JAK3 phosphorylation status is less obvious. Lanes 1, 10, 11, 17, 19, 20, 21, 23, and 25 showed pSTAT5.

Samples ATL31 (Figure 27, lane 11) expressing both JAK3 and STAT5 with P-JAK3 and P-STAT5 and ATL3 (Figure 27, Lane 22), which does not have P-JAK3 and had minimal STAT5 and JAK3 were injected into lethally irradiated immunocompromised NSG mice[244]. Both of these samples formed tumors in these mice as established by flow cytometry with antibodies specific to human CD45 or human CD3. With incorporation of an inducible luciferase lentivirus it will be possible to follow the specific location of tumor formation and growth *in vivo*, with the intent to treat these mice with kinase inhibitors and monitor ATLL cell survival and tumor growth. Peripheral blood was used to monitor circulating human cells with specific flow antibodies *in vivo* (Figure 28).

Discussion

In vivo models are important for validating novel therapies especially in rare diseases when clinical data is limited. In the case of ATLL, this is especially true as the non-specificity of treatment could have rapid and dire consequences. Here we show that only BaF3 cells that are cytokine independent may engraft

into immunocompromised NSG mice. These mice rapidly develop the disease, and this is an efficient assay for testing potential treatment strategies specifically against activated JAK3s.

Every tumor will express its own unique phenotype and protein signature. Recently cancer treatments have started to become more specially targeted not just to the cancer type but also to the individual case. ATLL has a known initiating factor of HTLV-1 infection and expression of viral oncogenes. What remains to be determined is the additional mutations that are necessary for diseases progression. Here, we propose that JAK3 may be commonly activated in the majority of ATLL tumors. Both AKT and STAT5 are frequently phosphorylated across tumor samples, although it is more difficult to determine whether JAK3 is also phosphorylated in multiple samples. To further support this idea, ex vivo treatment with tofacitinib experiments have been performed on ATLL primary tumor samples; these cells have considerably less cell proliferation and have increased apoptosis. Of course, there is still a need for a case by case determination of JAK3 presence and activity as some samples do not seem to express JAK3 at all. There is also the question of how effective this inhibition will be *in vivo*. NSG mice were injected with ATLL primary tumor that either had P-JAK3 or did not express JAK3 at all. Of those that developed tumor, those tumors infiltrated multiple organs including the spleen, BM, liver and kidney. These mice did not develop thymic tumors as this is most likely due to the lack of a thymus in these animals.

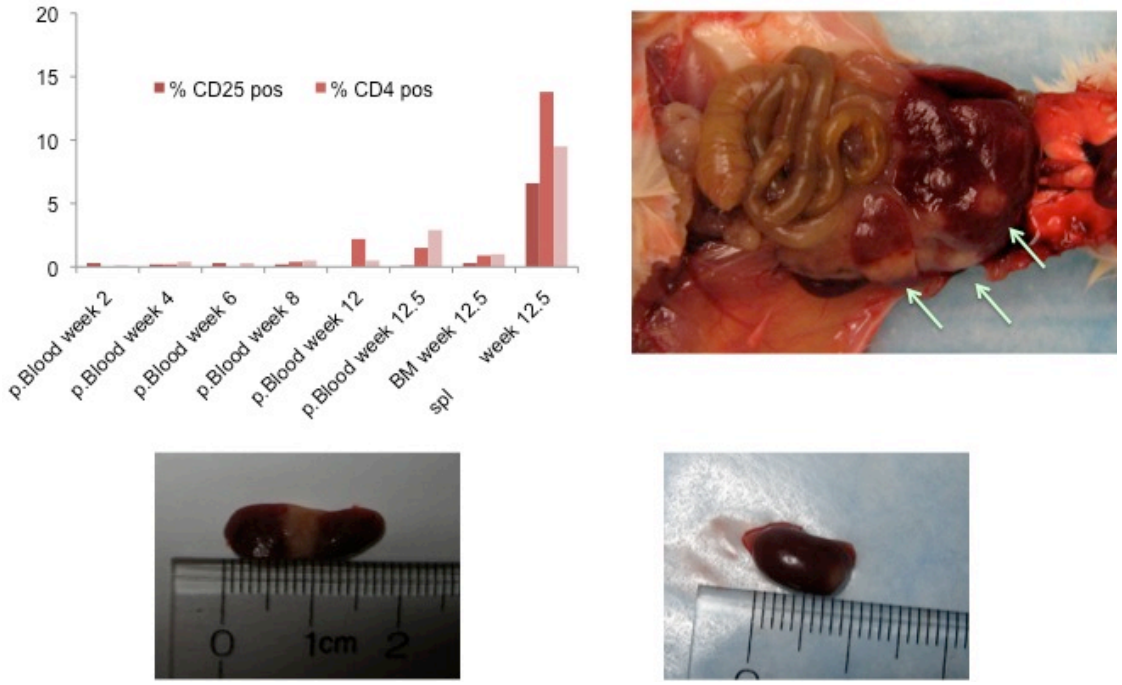

Figure 28 Xenograft mouse model displays multiple organ engraftments of ATLL tumor. NSG were subcutaneously injected with $5x10^5$ primary ATLL tumor cells. Most developed tumor within 13 weeks.

CHAPTER VIII

SUMMARY AND FUTURE DIRECTIONS

This study presents two novel findings. The first is the identification of activated JAK3 as a potential therapeutic target in the treatment of ATLL through the identification of three activating mutations. The second is a direct autoregulatory role of the FERM domain on kinase activity of JAK3.

The primary goals of this work are to acquire a better understanding of how ATLL develops and to use that knowledge to determine more specific treatment options against this vicious disease. A molecular approach was taken to identify the potential source of signaling misregulation within the IL-2 signaling pathway. Three somatic missense mutations in JAK3 were identified out of the thirty-six ATLL patients screened L156P, R172Q, and E183G. These mutations occurred in the amino terminal FERM domain and may contribute to the development of ATLL. The *in vitro* and *in vivo* effects of these mutations were characterized.

In vitro kinase assays and cell-based assays in OP9-DL1, HEK-293T, and BaF3 cells were used to determine potential alterations in JAK3 function with the incorporation of ATLL derived mutations. All three mutations were found to induce gain of function in JAK3: first in the differentiation of LSKs into T cells on OP9-DL1s, second in the increase of STAT5A phosphorylation in HEK-293T cells, and lastly in the cytokine independence and changes in phosphorylation of

JAK3, STAT5, and AKT in BaF3 cells. Gain of function from the addition of mutations to the FERM domain of JAK3 implies a novel autoregulatory role for the FERM domain on kinase activity.

One important question is whether the JAK3 mutants require receptor and ligand for signal transduction. The phosphorylation of STAT5A in the 293T cell assay required IL-2 and hematopoietic stem and progenitor cells transduced with mutant JAK3s did not differentiate or proliferate in the absence of IL-7, implying that cytokine stimulation is required. In contrast, BaF3 cells transduced with JAK3 mutants grew and cycled without cytokines, suggesting that the JAK3s did not require ligand binding to receptors. These data imply some cell type specificity in the requirement for ligand in mutant JAK3 signaling. Other proteins recruited to the receptors could play a role in this signaling. This may have pathogenic significance since these kinases are recruited by IL-2Rβ and γc. JAK1 was co-transfected in the 293T assay but produced no change in IL-2 dependence consistent with prior reports (data not shown)[245]. The observation of ligand dependent or independent growth is clinically important because if FERM domain mutations are found to require JAK3/γc utilizing ligand in T cells, then cytokines must signal either by autocrine or paracrine mechanisms. HTLV-1 infected T cells do show increased expression of IL-2 and IL-9[246]. There is also evidence for IL-9 secretion from monocytes isolated from ATLL patients and in T-cell neoplasms that resemble ATLL such as cutaneous T-cell lymphoma IL-7 secretion by keratinocytes may support tumor cell growth[247, 248].

To further understand how this activation alters JAK3 function, we looked at JAK3 stability, localization, and degradation. Previous work has described the localization as being predominantly nuclear until induced by cytokine, at which time JAK3 predominantly localizes to the membrane. Here, it was found that the activated JAK3 is localized away from the nucleus in BaF3 cells while the less active WT protein is predominantly nuclear. All activating mutations increased the stability of the protein regardless of the mutations being present in the FERM of pseudokinase domains implying that this is not due to the location of the mutations but perhaps more likely because of the activated phenotype associated with these mutations.

The ATLL mutations are also highly informative for understanding the biochemistry of JAK3 kinase activity. The homology model based on the crystal structure of FAK showed that the ATLL mutations align with the FAK FERM F2 subdomain that occludes and inhibits the activity of the FAK kinase domain and the FERM domain of JAK3 may have a similar autoregulatory role.

Interestingly, the FERM domain mutations described here also increase the overall protein stability of JAK3. The increased stability may be related to the increased activity of JAK3 since the FERM domain mutant proteins had comparable half-lives to the A572V mutant protein. It is possible that activation induces an allosteric change that makes JAK3 more stable. This allosteric change increases the ability of JAK3 to interact with structural proteins such as villin in the cytosol or γ_c at the membrane, which would explain why the activated JAK3 E183G is sequestered away from the nucleus of BaF3 cells. A detailed

crystal structure of the JAK3 FERM with its kinase domain would provide significant insight into this mechanism. Our results also raise the possibility of FERM domain mutations in other JAK kinases implicated in cancer.

JAK3 degradation has been previously described as being proteasomally regulated. Here, it was found that WT JAK3 degradation may be regulated by both the proteasome and the lysosome, whereas activated JAK3 may only be regulated by the proteasome.

The structural model of the JAK3 FERM domain shows that the three mutations will disrupt direct interaction with the kinase domain and may play a key role in tumor progression. These data suggest that these mutations increase JAK3 kinase activity *in vitro*.

These results implicate the JAK3 activation as an important therapeutic target in ATLL. JAK3 activity can be inhibited with the JAK3 specific inhibitor, tofacitinib. A mouse model could be used to probe the effects of JAK3 mutants and treatment with kinase specific inhibitors *in vivo*. Thus far, a human ATLL cell line with a gain of function JAK3 mutation has yet to be established, which would allow for testing of oncogene dependence directly. It should be noted that growth of both Hut-102 and MT-2 cell lines as well as primary ATLL cells, all of which are lacking in JAK3 mutations, had phosphorylated JAK3 and were inhibited by tofacitinib. This result suggests that there could be oncogene dependence on JAK3 even without a gain of function mutation. For example, the Hut-102 cell line requires exogenous hIL-2 for optimal growth. The MT-2 cells also have deregulation of the JAK3/γc axis in the form of HTLV-1 integration 5' of the *IL9R*

gene. This retroviral insertion induces overexpression of the receptor such that high levels of IL-9R may signal through JAK3 without ligand[249, 250]. In the 36 patient samples we analyzed, only a small percentage had activating mutations in JAK3. Another study looked at 24 patients and did not find any mutations at all. This would imply that other components of JAK3 signaling may be mutated in ATLL or othat ther mechanisms could misregulate the pathway since this pathway is upregulated in nearly all ATLL samples[251].

Further work needs to be done to identify the exact mechanism of FERM regulated kinase activity in JAK3. The most useful study would be to crystallize the entire JAK3 protein with and without mutations and directly identify how the structure is altered. Alternatively, a series of alanine substitutions in the FERM subdomain where the three mutations were identified could identify novel regulatory site(s) in both kinase regulation and interprotein interactions. These could be used in both the HEK 293T IL-2R recapitulation and the BaF3 experiments. Also, the C-terminal region of JAK3 containing the entire FERM domain was cloned into a GST fusion vector pGEX-2T for wildtype JAK3 and each of the ATLL derived JAK3 FERM domain mutations. These fusion constructs could be used in vitro kinase and GST pulldown experiments to quantifiably measure receptor interaction and the effects of mutations on kinase activity *in vitro*.

The three activating JAK3 mutations identified in ATLL are weakly oncogenic and required the loss of *Cdkn2a* gene expression to realize its potential. These mice developed tumor much more rapidly than did *Cdkn2a*^{KO}

mice with WT JAK3. That mice developed tumors characteristic of *Cdkn2a*^{KO} mice may be the result of using *Cdkn2a*^{KO} BM for the donor cell origin and results could vary in a model that is not primed for B cell tumors. Alternatively, HTLV-1 preferentially infects CD4+ T cells and though JAK3 mutations aid in the development of ATLL the T cell phenotype, this could reflect the original cell phenotype at infection. One way to test this would be in a model in which the activation of JAK3 occurs first with subsequent loss of tumor suppressors. As we were unable to show that activating mutations in JAK3 are oncogenic alone in a BMTT experiment, it may be preferable to use a transgenic mouse model to fully understand how activated JAK3 may lead to tumor development. ATLL derived JAK3 mutants were cloned from the JAK3-MIG constructs into an expression construct under the control of the *vav* proximal promoter. These constructs could be used to make T cell specific JAK3 transgenic mouse lines with activated JAK3 mutations. Alternatively, we could cotransduce WT C57/B6 BM with both Jak3 and the oncogene *tax.* These mice may preferentially develop T cell leukemias.

JAK3-specific inhibitors were clinically tested in phase I and phase II studies of rheumatoid arthritis and may be worth testing in ATLL patients[240]. The three JAK3 FERM domain mutations were shown to disrupt autoregulation of JAK3 kinase activity inducing JAK3 to be constitutively active and are oncogenic. ATLL is a remarkable example of retrovirally-induced cancer in humans.

In summary, in the research presented here, three mutations in the FERM domain of JAK3 were identified in four of the thirty-six ATLL patients and were absent in twenty-three ethnically matched controls that were screened. These

somatic, missense mutations occurred in the amino terminal regulatory FERM domain.

All three mutations were found to induce gain of function in JAK3, implying an autoregulatory role normally for the FERM domain on JAK3's kinase. One mutation E183G, was further explored in vivo and was found to be weakly oncogenic with the additional loss of tumor suppressor proteins p19(ARF) and p16(INK4A) in a BMTT model. These mutant JAK3s can be inhibited with a specific kinase inhibitor, tofacitinib, as well as inhibitors against downstream activation targets. These findings emphasize the importance of JAK3 activation in ATLL development and offer a novel therapeutic target for this otherwise incurable disease.

REFERENCES:

1. Uchiyama T, Yodoi J, Sagawa K, Takatsuki K, Uchino H. Adult T-cell leukemia: clinical and hematologic features of 16 cases. *Blood.* Sep 1977;50(3):481-492.

2. Yoshida M, Miyoshi I, Hinuma Y. Isolation and characterization of retrovirus from cell lines of human adult T-cell leukemia and its implication in the disease. *Proceedings of the National Academy of Sciences of the United States of America.* 1982;79(6):2031-2035.

3. Nasr R, El Hajj H, Kfoury Y, de The H, Hermine O, Bazarbachi A. Controversies in targeted therapy of adult T cell leukemia/lymphoma: ON target or OFF target effects? *Viruses.* Jun 2011;3(6):750-769.

4. Waldmann TA, White JD, Goldman CK, et al. The interleukin-2 receptor: a target for monoclonal antibody treatment of human T-cell lymphotrophic virus I-induced adult T-cell leukemia. *Blood.* Sep 15 1993;82(6):1701-1712.

5. Walters DK, Mercher T, Gu TL, et al. Activating alleles of JAK3 in acute megakaryoblastic leukemia. *Cancer Cell.* Jul 2006;10(1):65-75.

6. Koo GC, Tan SY, Tang T, et al. Janus Kinase 3-Activating Mutations Identified in Natural Killer/T-cell Lymphoma. *Cancer Discov.* Jul 2012;2(7):591-597.

7. Riera L, Lasorsa E, Bonello L, et al. Description of a novel Janus kinase 3 P132A mutation in acute megakaryoblastic leukemia and demonstration of previously reported Janus kinase 3 mutations in normal subjects. *Leuk Lymphoma.* Sep;52(9):1742-1750.

8. Sato T, Toki T, Kanezaki R, et al. Functional analysis of JAK3 mutations in transient myeloproliferative disorder and acute megakaryoblastic leukaemia accompanying Down syndrome. *Br J Haematol.* May 2008;141(5):681-688.

9. Takatsuki S. An etiology of anal fistula in infants. *Keio J Med.* Jan 1976;25(1):1-4.

10. Shuh M, Beilke M. The human T-cell leukemia virus type 1 (HTLV-1): new insights into the clinical aspects and molecular pathogenesis of adult T-cell leukemia/lymphoma (ATLL) and tropical spastic paraparesis/HTLV-associated myelopathy (TSP/HAM). *Microsc Res Tech.* Nov 2005;68(3-4):176-196.

11. Edlich RF, Arnette JA, Williams FM. Global epidemic of human T-cell lymphotropic virus type-I (HTLV-I). *J Emerg Med.* Jan 2000;18(1):109-119.

12. Cooper SA, van der Loeff MS, Taylor GP. The neurology of HTLV-1 infection. *Pract Neurol.* Feb 2009;9(1):16-26.

13. Matsuoka M. Human T-cell leukemia virus type I (HTLV-I) infection and the onset of adult T-cell leukemia (ATL). *Retrovirology.* 2005;2:27.

14. Takatsuki F, Yamaguchi K, Hattori T. Adult T-cell leukemia/lymphoma in Gallo RC, Wong-Staal F. *Retrovirus Biology and Human Disease.* 1990:147-159.
15. Bazarbachi A, Ghez D, Lepelletier Y, et al. New therapeutic approaches for adult T-cell leukaemia. *Lancet Oncol.* Nov 2004;5(11):664-672.
16. Yamamoto S, Hattori T, Asou N, et al. Absolute neutrophilia in adult T cell leukemia. *Jpn J Cancer Res.* Sep 1986;77(9):858-861.
17. Ratner L. Pathogenesis and treatment of human T-cell leukemia virus infection. *Immunol Res.* 2005;32(1-3):217-223.
18. Taylor GP, Matsuoka M. Natural history of adult T-cell leukemia/lymphoma and approaches to therapy. *Oncogene.* Sep 5 2005;24(39):6047-6057.
19. Waldmann TA, White JD, Carrasquillo JA, et al. Radioimmunotherapy of interleukin-2R alpha-expressing adult T-cell leukemia with Yttrium-90-labeled anti-Tac. *Blood.* Dec 1 1995;86(11):4063-4075.
20. Itoyama T, Chaganti RS, Yamada Y, et al. Cytogenetic analysis and clinical significance in adult T-cell leukemia/lymphoma: a study of 50 cases from the human T-cell leukemia virus type-1 endemic area, Nagasaki. *Blood.* Jun 1 2001;97(11):3612-3620.
21. Tsukasaki K, Krebs J, Nagai K, et al. Comparative genomic hybridization analysis in adult T-cell leukemia/lymphoma: correlation with clinical course. *Blood.* Jun 15 2001;97(12):3875-3881.
22. Tsukasaki K. Genetic instability of adult T-cell leukemia/lymphoma by comparative genomic hybridization analysis. *J Clin Immunol.* Mar 2002;22(2):57-63.
23. Tsukasaki K, Tanosaki S, DeVos S, et al. Identifying progression-associated genes in adult T-cell leukemia/lymphoma by using oligonucleotide microarrays. *Int J Cancer.* May 10 2004;109(6):875-881.
24. Kami M, Hamaki T, Miyakoshi S, et al. Allogeneic haematopoietic stem cell transplantation for the treatment of adult T-cell leukaemia/lymphoma. *Br J Haematol.* Jan 2003;120(2):304-309.
25. Dasanu CA. Newer developments in adult T-cell leukemia/lymphoma therapeutics. *Expert Opin Pharmacother.* Aug 2011;12(11):1709-1717.
26. Alduaij A, Butera JN, Treaba D, Castillo J. Complete remission in two cases of adult T-cell leukemia/lymphoma treated with hyper-CVAD: a case report and review of the literature. *Clin Lymphoma Myeloma Leuk.* Dec 2010;10(6):480-483.
27. Kamimura T, Miyamoto T, Kawano N, et al. Successful treatment by donor lymphocyte infusion of adult T-cell leukemia/lymphoma relapse following allogeneic hematopoietic stem cell transplantation. *Int J Hematol.* Jun 2012;95(6):725-730.
28. Itonaga H, Tsushima H, Taguchi J, et al. Treatment of relapsed adult T-cell leukemia/lymphoma after allogeneic hematopoietic stem cell transplantation: the Nagasaki Transplant Group experience. *Blood.* Oct 24 2012.
29. Bazarbachi A, Plumelle Y, Carlos Ramos J, et al. Meta-analysis on the use of zidovudine and interferon-alfa in adult T-cell leukemia/lymphoma

showing improved survival in the leukemic subtypes. *J Clin Oncol.* Sep 20 2010;28(27):4177-4183.

30. Green JE, Hinrichs SH, Vogel J, Jay G. Exocrinopathy resembling Sjogren's syndrome in HTLV-1 tax transgenic mice. *Nature.* Sep 7 1989;341(6237):72-74.

31. Benvenisty N, Ornitz DM, Bennett GL, et al. Brain tumours and lymphomas in transgenic mice that carry HTLV-I LTR/c-myc and Ig/tax genes. *Oncogene.* Dec 1992;7(12):2399-2405.

32. Grossman WJ, Kimata JT, Wong FH, Zutter M, Ley TJ, Ratner L. Development of leukemia in mice transgenic for the tax gene of human T-cell leukemia virus type I. *Proc Natl Acad Sci U S A.* Feb 14 1995;92(4):1057-1061.

33. Suzushima H, Asou N, Hattori T, Takatsuki K. Adult T-cell leukemia derived from S100 beta positive double-negative (CD4- CD8-) T cells. *Leuk Lymphoma.* Apr 1994;13(3-4):257-262.

34. Nicot C. Current views in HTLV-I-associated adult T-cell leukemia/lymphoma. *Am J Hematol.* Mar 2005;78(3):232-239.

35. Sibon D, Gabet AS, Zandecki M, et al. HTLV-1 propels untransformed CD4 lymphocytes into the cell cycle while protecting CD8 cells from death. *J Clin Invest.* Apr 2006;116(4):974-983.

36. Matsuoka M. Human T-cell leukemia virus type I and adult T-cell leukemia. *Oncogene.* Aug 11 2003;22(33):5131-5140.

37. Hlela C, Shepperd S, Khumalo NP, Taylor GP. The prevalence of human T-cell lymphotropic virus type 1 in the general population is unknown. *AIDS Rev.* Oct-Dec 2009;11(4):205-214.

38. Eshima N, Iwata O, Iwata S, et al. Age and gender specific prevalence of HTLV-1. *J Clin Virol.* Jun 2009;45(2):135-138.

39. de The G, Bomford R. An HTLV-I vaccine: why, how, for whom? *AIDS Res Hum Retroviruses.* May 1993;9(5):381-386.

40. Batsuuri J, Dashnyam B, Maidar J, Battulga D, Dorjsuren D, Ishida T. Absence of human T-lymphotropic retrovirus type-1 (HTLV-1) in different populations of Mongolia. *Scand J Infect Dis.* 1993;25(3):398-399.

41. Bertherat E, Makuwa M, Renaut A, Nabias R, Georges-Courbot MC. HIV-1, HTLV-I, and HTLV-II in a semiurban population in East Gabon. *J Acquir Immune Defic Syndr Hum Retrovirol.* Dec 1 1998;19(4):430-432.

42. Le Hesran JY, Delaporte E, Gaudebout C, et al. Demographic factors associated with HTLV-1 infection in a Gabonese community. *Int J Epidemiol.* Aug 1994;23(4):812-817.

43. Jeannel D, Kourouma K, Fretz C, et al. Regional differences in human retroviral infections HIV-1, HIV-2, and HTLV-I/II in rural Guinea (west Africa). *J Acquir Immune Defic Syndr Hum Retrovirol.* Mar 1 1995;8(3):315-318.

44. Grant W, Bia FJ, Chacko TM, Jean-Baptiste M, Griffith BP. Comparison of enzyme-linked immunosorbent and indirect immunofluorescence assays for the detection of human T-cell lymphotropic virus type-I antibodies in sera from rural Haiti. *Diagn Microbiol Infect Dis.* Feb 1992;15(2):121-124.

45. Morofuji-Hirata M, Kajiyama W, Nakashima K, Noguchi A, Hayashi J, Kashiwagi S. Prevalence of antibody to human T-cell lymphotropic virus type I in Okinawa, Japan, after an interval of 9 years. *Am J Epidemiol.* Jan 1 1993;137(1):43-48.
46. Maloney EM, Murphy EL, Figueroa JP, et al. Human T-lymphotropic virus type I (HTLV-I) seroprevalence in Jamaica. II. Geographic and ecologic determinants. *Am J Epidemiol.* Jun 1 1991;133(11):1125-1134.
47. Murphy EL, Figueroa JP, Gibbs WN, et al. Human T-lymphotropic virus type I (HTLV-I) seroprevalence in Jamaica. I. Demographic determinants. *Am J Epidemiol.* Jun 1 1991;133(11):1114-1124.
48. Takeuchi H, Takahashi M, Norose Y, Takeshita T, Fukunaga Y, Takahashi H. Transformation of breast milk macrophages by HTLV-I: implications for HTLV-I transmission via breastfeeding. *Biomed Res.* Feb;31(1):53-61.
49. Tajima K. Malignant lymphomas in Japan: epidemiological analysis of adult T-cell leukemia/lymphoma (ATL). *Cancer Metastasis Rev.* Nov 1988;7(3):223-241.
50. Clark J, Saxinger C, Gibbs WN, et al. Seroepidemiologic studies of human T-cell leukemia/lymphoma virus type I in Jamaica. *Int J Cancer.* Jul 15 1985;36(1):37-41.
51. Zimmermann K, Dobrovnik M, Ballaun C, Bevec D, Hauber J, Bohnlein E. trans-activation of the HIV-1 LTR by the HIV-1 Tat and HTLV-I Tax proteins is mediated by different cis-acting sequences. *Virology.* Jun 1991;182(2):874-878.
52. Ratner L, Harrington W, Feng X, et al. Human T cell leukemia virus reactivation with progression of adult T-cell leukemia-lymphoma. *PLoS One.* 2009;4(2):e4420.
53. Page JB, Lai S, Chitwood DD. HTLV increases HIV risk. *Nurs Times.* Jun 27-Jul 3 1990;86(26):10.
54. Trejo SR, Ratner L. The HTLV receptor is a widely expressed protein. *Virology.* Mar 1 2000;268(1):41-48.
55. Coskun AK, Sutton RE. Expression of glucose transporter 1 confers susceptibility to human T-cell leukemia virus envelope-mediated fusion. *J Virol.* Apr 2005;79(7):4150-4158.
56. Jones KS, Fugo K, Petrow-Sadowski C, et al. Human T-cell leukemia virus type 1 (HTLV-1) and HTLV-2 use different receptor complexes to enter T cells. *J Virol.* Sep 2006;80(17):8291-8302.
57. Kinet S, Swainson L, Lavanya M, et al. Isolated receptor binding domains of HTLV-1 and HTLV-2 envelopes bind Glut-1 on activated CD4+ and CD8+ T cells. *Retrovirology.* 2007;4:31.
58. Manel N, Kim FJ, Kinet S, Taylor N, Sitbon M, Battini JL. The ubiquitous glucose transporter GLUT-1 is a receptor for HTLV. *Cell.* Nov 14 2003;115(4):449-459.
59. Manel N, Taylor N, Kinet S, et al. HTLV envelopes and their receptor GLUT1, the ubiquitous glucose transporter: a new vision on HTLV infection? *Front Biosci.* Sep 1 2004;9:3218-3241.

60. Lambert S, Bouttier M, Vassy R, et al. HTLV-1 uses HSPG and neuropilin-1 for entry by molecular mimicry of VEGF165. *Blood.* May 21 2009;113(21):5176-5185.
61. Jin Q, Alkhatib B, Cornetta K, Alkhatib G. Alternate receptor usage of neuropilin-1 and glucose transporter protein 1 by the human T cell leukemia virus type 1. *Virology.* Jan 20;396(2):203-212.
62. Ghez D, Lepelletier Y, Lambert S, et al. Neuropilin-1 is involved in human T-cell lymphotropic virus type 1 entry. *J Virol.* Jul 2006;80(14):6844-6854.
63. Dezzutti CS, Frazier DE, Lafrado LJ, Olsen RG. Evaluation of a HTLV-1 subunit vaccine in prevention of experimental STLV-I infection in Macaca nemestrina. *J Med Primatol.* 1990;19(3-4):305-316.
64. Dezzutti CS, Frazier DE, Olsen RG. Efficacy of an HTLV-1 subunit vaccine in prevention of a STLV-1 infection in pig-tailed macaques. *Dev Biol Stand.* 1990;72:287-296.
65. Mulloy JC, Migone TS, Ross TM, et al. Human and simian T-cell leukemia viruses type 2 (HTLV-2 and STLV-2(pan-p)) transform T cells independently of Jak/STAT activation. *J Virol.* May 1998;72(5):4408-4412.
66. Slattery JP, Franchini G, Gessain A. Genomic evolution, patterns of global dissemination, and interspecies transmission of human and simian T-cell leukemia/lymphotropic viruses. *Genome Res.* Jun 1999;9(6):525-540.
67. Yoshida M. Discovery of HTLV-1, the first human retrovirus, its unique regulatory mechanisms, and insights into pathogenesis. *Oncogene.* Sep 5 2005;24(39):5931-5937.
68. Furukawa Y, Fujisawa J, Osame M, et al. Frequent clonal proliferation of human T-cell leukemia virus type 1 (HTLV-1)-infected T cells in HTLV-1-associated myelopathy (HAM-TSP). *Blood.* Aug 15 1992;80(4):1012-1016.
69. Matsumoto K, Shibata H, Fujisawa JI, et al. Human T-cell leukemia virus type 1 Tax protein transforms rat fibroblasts via two distinct pathways. *J Virol.* Jun 1997;71(6):4445-4451.
70. Kimata JT, Wong FH, Wang JJ, Ratner L. Construction and characterization of infectious human T-cell leukemia virus type 1 molecular clones. *Virology.* Nov 1 1994;204(2):656-664.
71. Hahn B, Gallo RC, Franchini G, et al. Clonal selection of human T-cell leukemia virus-infected cells in vivo and in vitro. *Mol Biol Med.* Feb 1984;2(1):29-36.
72. Kimata JT, Ratner L. Temporal regulation of viral and cellular gene expression during human T-lymphotropic virus type I-mediated lymphocyte immortalization. *J Virol.* Aug 1991;65(8):4398-4407.
73. Harrington WJ, Jr., Miller GA, Kemper RR, Byrne GE, Jr., Whitcomb CC, Rabin M. HTLV-I-associated leukemia/lymphoma in south Florida. *J Acquir Immune Defic Syndr.* 1991;4(3):284-289.
74. Jacobson S, Shida H, McFarlin DE, Fauci AS, Koenig S. Circulating CD8+ cytotoxic T lymphocytes specific for HTLV-I pX in patients with HTLV-I associated neurological disease. *Nature.* Nov 15 1990;348(6298):245-248.

75. Kannagi M, Harada S, Maruyama I, et al. Predominant recognition of human T cell leukemia virus type I (HTLV-I) pX gene products by human CD8+ cytotoxic T cells directed against HTLV-I-infected cells. *Int Immunol.* Aug 1991;3(8):761-767.
76. Elovaara I, Koenig S, Brewah AY, Woods RM, Lehky T, Jacobson S. High human T cell lymphotropic virus type 1 (HTLV-1)-specific precursor cytotoxic T lymphocyte frequencies in patients with HTLV-1-associated neurological disease. *J Exp Med.* Jun 1 1993;177(6):1567-1573.
77. Xu X, Kang SH, Heidenreich O, Okerholm M, O'Shea JJ, Nerenberg MI. Constitutive activation of different Jak tyrosine kinases in human T cell leukemia virus type 1 (HTLV-1) tax protein or virus-transformed cells. *J Clin Invest.* Sep 1995;96(3):1548-1555.
78. Migone TS, Lin JX, Cereseto A, et al. Constitutively activated Jak-STAT pathway in T cells transformed with HTLV-I. *Science.* Jul 7 1995;269(5220):79-81.
79. Kotani M, Tagawa Y, Iwakura Y. Involvement of autoimmunity against type II collagen in the development of arthritis in mice transgenic for the human T cell leukemia virus type I tax gene. *Eur J Immunol.* Jan 1999;29(1):54-64.
80. Harashima N, Kurihara K, Utsunomiya A, et al. Graft-versus-Tax response in adult T-cell leukemia patients after hematopoietic stem cell transplantation. *Cancer Res.* Jan 1 2004;64(1):391-399.
81. Kannagi M, Harashima N, Kurihara K, et al. Tumor immunity against adult T-cell leukemia. *Cancer Sci.* May 2005;96(5):249-255.
82. Nomura M, Ohashi T, Nishikawa K, et al. Repression of tax expression is associated both with resistance of human T-cell leukemia virus type 1-infected T cells to killing by tax-specific cytotoxic T lymphocytes and with impaired tumorigenicity in a rat model. *J Virol.* Apr 2004;78(8):3827-3836.
83. Taniguchi Y, Nosaka K, Yasunaga J, et al. Silencing of human T-cell leukemia virus type I gene transcription by epigenetic mechanisms. *Retrovirology.* 2005;2:64.
84. Zhao T, Matsuoka M. HBZ and its roles in HTLV-1 oncogenesis. *Front Microbiol.*3:247.
85. Miyazaki T, Kawahara A, Fujii H, et al. Functional activation of Jak1 and Jak3 by selective association with IL-2 receptor subunits. *Science.* Nov 11 1994;266(5187):1045-1047.
86. Russell SM, Johnston JA, Noguchi M, et al. Interaction of IL-2R beta and gamma c chains with Jak1 and Jak3: implications for XSCID and XCID. *Science.* Nov 11 1994;266(5187):1042-1045.
87. Robek MD, Ratner L. Immortalization of T lymphocytes by human T-cell leukemia virus type 1 is independent of the tax-CBP/p300 interaction. *J Virol.* Dec 2000;74(24):11988-11992.
88. Yip MT, Chen IS. Modes of transformation by the human T-cell leukemia viruses. *Mol Biol Med.* Feb 1990;7(1):33-44.

89. Morgan DA, Ruscetti FW, Gallo R. Selective in vitro growth of T lymphocytes from normal human bone marrows. *Science.* Sep 10 1976;193(4257):1007-1008.
90. Liao W, Lin JX, Wang L, Li P, Leonard WJ. Modulation of cytokine receptors by IL-2 broadly regulates differentiation into helper T cell lineages. *Nat Immunol.* Jun;12(6):551-559.
91. Nelson BH, Lord JD, Greenberg PD. Cytoplasmic domains of the interleukin-2 receptor beta and gamma chains mediate the signal for T-cell proliferation. *Nature.* May 26 1994;369(6478):333-336.
92. Kim HP, Imbert J, Leonard WJ. Both integrated and differential regulation of components of the IL-2/IL-2 receptor system. *Cytokine Growth Factor Rev.* Oct 2006;17(5):349-366.
93. Johnston JA, Kawamura M, Kirken RA, et al. Phosphorylation and activation of the Jak-3 Janus kinase in response to interleukin-2. *Nature.* Jul 14 1994;370(6485):151-153.
94. Zhu MH, Berry JA, Russell SM, Leonard WJ. Delineation of the regions of interleukin-2 (IL-2) receptor beta chain important for association of Jak1 and Jak3. Jak1-independent functional recruitment of Jak3 to Il-2Rbeta. *J Biol Chem.* Apr 24 1998;273(17):10719-10725.
95. Friedmann MC, Migone TS, Russell SM, Leonard WJ. Different interleukin 2 receptor beta-chain tyrosines couple to at least two signaling pathways and synergistically mediate interleukin 2-induced proliferation. *Proc Natl Acad Sci U S A.* Mar 5 1996;93(5):2077-2082.
96. Velazquez L, Fellous M, Stark GR, Pellegrini S. A protein tyrosine kinase in the interferon alpha/beta signaling pathway. *Cell.* Jul 24 1992;70(2):313-322.
97. Wilks AF, Harpur AG, Kurban RR, Ralph SJ, Zurcher G, Ziemiecki A. Two novel protein-tyrosine kinases, each with a second phosphotransferase-related catalytic domain, define a new class of protein kinase. *Mol Cell Biol.* Apr 1991;11(4):2057-2065.
98. Kawamura M, McVicar DW, Johnston JA, et al. Molecular cloning of L-JAK, a Janus family protein-tyrosine kinase expressed in natural killer cells and activated leukocytes. *Proc Natl Acad Sci U S A.* Jul 5 1994;91(14):6374-6378.
99. Chen M, Cheng A, Candotti F, et al. Complex effects of naturally occurring mutations in the JAK3 pseudokinase domain: evidence for interactions between the kinase and pseudokinase domains. *Mol Cell Biol.* Feb 2000;20(3):947-956.
100. Vihinen M, Villa A, Mella P, et al. Molecular modeling of the Jak3 kinase domains and structural basis for severe combined immunodeficiency. *Clin Immunol.* Aug 2000;96(2):108-118.
101. Saharinen P, Silvennoinen O. The pseudokinase domain is required for suppression of basal activity of Jak2 and Jak3 tyrosine kinases and for cytokine-inducible activation of signal transduction. *J Biol Chem.* Dec 6 2002;277(49):47954-47963.

102. Ghoreschi K, Laurence A, O'Shea JJ. Janus kinases in immune cell signaling. *Immunol Rev.* Mar 2009;228(1):273-287.
103. Tepass U. FERM proteins in animal morphogenesis. *Curr Opin Genet Dev.* Aug 2009;19(4):357-367.
104. Chen M, Cheng A, Chen YQ, et al. The amino terminus of JAK3 is necessary and sufficient for binding to the common gamma chain and confers the ability to transmit interleukin 2-mediated signals. *Proc Natl Acad Sci U S A.* Jun 24 1997;94(13):6910-6915.
105. Thoma G, Nuninger F, Falchetto R, et al. Identification of a potent Janus kinase 3 inhibitor with high selectivity within the Janus kinase family. *J Med Chem.* Jan 13;54(1):284-288.
106. Williams NK, Bamert RS, Patel O, et al. Dissecting specificity in the Janus kinases: the structures of JAK-specific inhibitors complexed to the JAK1 and JAK2 protein tyrosine kinase domains. *J Mol Biol.* Mar 20 2009;387(1):219-232.
107. Chrencik JE, Patny A, Leung IK, et al. Structural and thermodynamic characterization of the TYK2 and JAK3 kinase domains in complex with CP-690550 and CMP-6. *J Mol Biol.* Jul 16 2010;400(3):413-433.
108. Boggon TJ, Li Y, Manley PW, Eck MJ. Crystal structure of the Jak3 kinase domain in complex with a staurosporine analog. *Blood.* Aug 1 2005;106(3):996-1002.
109. Hall T, Emmons TL, Chrencik JE, et al. Expression, purification, characterization and crystallization of non- and phosphorylated states of JAK2 and JAK3 kinase domain. *Protein Expr Purif.* Jan 2010;69(1):54-63.
110. Hebenstreit D, Horejs-Hoeck J, Duschl A. JAK/STAT-dependent gene regulation by cytokines. *Drug News Perspect.* May 2005;18(4):243-249.
111. Zhou YJ, Chen M, Cusack NA, et al. Unexpected effects of FERM domain mutations on catalytic activity of Jak3: structural implication for Janus kinases. *Mol Cell.* Nov 2001;8(5):959-969.
112. Baird AM, Thomis DC, Berg LJ. T cell development and activation in Jak3-deficient mice. *J Leukoc Biol.* Jun 1998;63(6):669-677.
113. Henkels KM, Frondorf K, Gonzalez-Mejia ME, Doseff AL, Gomez-Cambronero J. IL-8-induced neutrophil chemotaxis is mediated by Janus kinase 3 (JAK3). *FEBS Lett.* Jan 3 2011;585(1):159-166.
114. Dunty J, Gabarra-Niecko V, King M, Ceccarelli D, Eck M, Schaller M. FERM domain interaction promotes FAK signaling. *10.1128/MCB.24.12.5353-5368.2004.* June xx 2004;24(12):5353-5368.
115. Haan S, Margue C, Engrand A, et al. Dual role of the Jak1 FERM and kinase domains in cytokine receptor binding and in stimulation-dependent Jak activation. *J Immunol.* Jan 15 2008;180(2):998-1007.
116. Louvet-Vallee S. ERM proteins: from cellular architecture to cell signaling. *Biol Cell.* Aug 2000;92(5):305-316.
117. Cacalano NA, Migone TS, Bazan F, et al. Autosomal SCID caused by a point mutation in the N-terminus of Jak3: mapping of the Jak3-receptor interaction domain. *EMBO J.* Mar 15 1999;18(6):1549-1558.

118. Pearson MA, Reczek D, Bretscher A, Karplus PA. Structure of the ERM protein moesin reveals the FERM domain fold masked by an extended actin binding tail domain. *Cell.* Apr 28 2000;101(3):259-270.
119. Hamada K, Shimizu T, Matsui T, Tsukita S, Hakoshima T. Structural basis of the membrane-targeting and unmasking mechanisms of the radixin FERM domain. *EMBO J.* Sep 1 2000;19(17):4449-4462.
120. Han BG, Nunomura W, Takakuwa Y, Mohandas N, Jap BK. Protein 4.1R core domain structure and insights into regulation of cytoskeletal organization. *Nat Struct Biol.* Oct 2000;7(10):871-875.
121. Rodig SJ, Meraz MA, White JM, et al. Disruption of the Jak1 gene demonstrates obligatory and nonredundant roles of the Jaks in cytokine-induced biologic responses. *Cell.* May 1 1998;93(3):373-383.
122. Krempler A, Qi Y, Triplett AA, Zhu J, Rui H, Wagner KU. Generation of a conditional knockout allele for the Janus kinase 2 (Jak2) gene in mice. *Genesis.* Sep 2004;40(1):52-57.
123. Ghaffari S, Kitidis C, Fleming MD, Neubauer H, Pfeffer K, Lodish HF. Erythropoiesis in the absence of Janus-kinase 2: BCR-ABL induces red cell formation in JAK2(-/-) hematopoietic progenitors. *Blood.* Nov 15 2001;98(10):2948-2957.
124. Brown MP, Nosaka T, Tripp RA, et al. Reconstitution of early lymphoid proliferation and immune function in Jak3-deficient mice by interleukin-3. *Blood.* Sep 15 1999;94(6):1906-1914.
125. Karaghiosoff M, Neubauer H, Lassnig C, et al. Partial impairment of cytokine responses in Tyk2-deficient mice. *Immunity.* Oct 2000;13(4):549-560.
126. Parganas E, Wang D, Stravopodis D, et al. Jak2 is essential for signaling through a variety of cytokine receptors. *Cell.* May 1 1998;93(3):385-395.
127. Oyamada A, Ikebe H, Itsumi M, et al. Tyrosine kinase 2 plays critical roles in the pathogenic CD4 T cell responses for the development of experimental autoimmune encephalomyelitis. *J Immunol.* Dec 1 2009;183(11):7539-7546.
128. Nosaka T, van Deursen JM, Tripp RA, et al. Defective lymphoid development in mice lacking Jak3. *Science.* Nov 3 1995;270(5237):800-802.
129. Park SY, Saijo K, Takahashi T, et al. Developmental defects of lymphoid cells in Jak3 kinase-deficient mice. *Immunity.* Dec 1995;3(6):771-782.
130. Flex E, Petrangeli V, Stella L, et al. Somatically acquired JAK1 mutations in adult acute lymphoblastic leukemia. *J Exp Med.* Apr 14 2008;205(4):751-758.
131. Jeong EG, Kim MS, Nam HK, et al. Somatic mutations of JAK1 and JAK3 in acute leukemias and solid cancers. *Clin Cancer Res.* Jun 15 2008;14(12):3716-3721.
132. Xiang Z, Zhao Y, Mitaksov V, et al. Identification of somatic JAK1 mutations in patients with acute myeloid leukemia. *Blood.* May 1 2008;111(9):4809-4812.

133. Mullighan CG, Zhang J, Harvey RC, et al. JAK mutations in high-risk childhood acute lymphoblastic leukemia. *Proc Natl Acad Sci U S A.* Jun 9 2009;106(23):9414-9418.
134. Wang Q, Qiu H, Jiang H, et al. Mutations of PHF6 are associated with mutations of NOTCH1, JAK1 and rearrangement of SET-NUP214 in T-cell acute lymphoblastic leukemia. *Haematologica.* Dec;96(12):1808-1814.
135. Hornakova T, Chiaretti S, Lemaire MM, et al. ALL-associated JAK1 mutations confer hypersensitivity to the antiproliferative effect of type I interferon. *Blood.* Apr 22 2010;115(16):3287-3295.
136. Reading NS, Lim MS, Elenitoba-Johnson KS. Detection of acquired Janus kinase 2 V617F mutation in myeloproliferative disorders by fluorescence melting curve analysis. *Mol Diagn Ther.* 2006;10(5):311-317.
137. Konoplev S, Hsieh PP, Chang CC, Medeiros LJ, Lin P. Janus kinase 2 V617F mutation is detectable in spleen of patients with chronic myeloproliferative diseases suggesting a malignant nature of splenic extramedullary hematopoiesis. *Hum Pathol.* Dec 2007;38(12):1760-1763.
138. Norton A, Fisher C, Liu H, et al. Analysis of JAK3, JAK2, and C-MPL mutations in transient myeloproliferative disorder and myeloid leukemia of Down syndrome blasts in children with Down syndrome. *Blood.* Aug 1 2007;110(3):1077-1079.
139. Malinge S, Ragu C, Della-Valle V, et al. Activating mutations in human acute megakaryoblastic leukemia. *Blood.* Nov 15 2008;112(10):4220-4226.
140. Tefferi A. JAK and MPL mutations in myeloid malignancies. *Leuk Lymphoma.* Mar 2008;49(3):388-397.
141. Bock O, Busche G, Koop C, Schroter S, Buhr T, Kreipe H. Detection of the single hotspot mutation in the JH2 pseudokinase domain of Janus kinase 2 in bone marrow trephine biopsies derived from chronic myeloproliferative disorders. *J Mol Diagn.* May 2006;8(2):170-177.
142. Shide K, Shimoda K, Kamezaki K, et al. Tyk2 mutation homologous to V617F Jak2 is not found in essential thrombocythaemia, although it induces constitutive signaling and growth factor independence. *Leuk Res.* Aug 2007;31(8):1077-1084.
143. Schuster C, Berger A, Hoelzl MA, et al. The cooperating mutation or "second hit" determines the immunologic visibility toward MYC-induced murine lymphomas. *Blood.* Oct 27;118(17):4635-4645.
144. Spach KM, Noubade R, McElvany B, Hickey WF, Blankenhorn EP, Teuscher C. A single nucleotide polymorphism in Tyk2 controls susceptibility to experimental allergic encephalomyelitis. *J Immunol.* Jun 15 2009;182(12):7776-7783.
145. Cunninghame Graham DS, Akil M, Vyse TJ. Association of polymorphisms across the tyrosine kinase gene, TYK2 in UK SLE families. *Rheumatology (Oxford).* Jun 2007;46(6):927-930.
146. Kralovics R, Passamonti F, Buser AS, et al. A gain-of-function mutation of JAK2 in myeloproliferative disorders. *N Engl J Med.* Apr 28 2005;352(17):1779-1790.

147. Noguchi M, Nakamura Y, Russell SM, et al. Interleukin-2 receptor gamma chain: a functional component of the interleukin-7 receptor. *Science.* Dec 17 1993;262(5141):1877-1880.
148. Macchi P, Villa A, Giliani S, et al. Mutations of Jak-3 gene in patients with autosomal severe combined immune deficiency (SCID). *Nature.* Sep 7 1995;377(6544):65-68.
149. Russell SM, Tayebi N, Nakajima H, et al. Mutation of Jak3 in a patient with SCID: essential role of Jak3 in lymphoid development. *Science.* Nov 3 1995;270(5237):797-800.
150. Leonard WJ. Cytokines and immunodeficiency diseases. *Nat Rev Immunol.* Dec 2001;1(3):200-208.
151. Ozaki K, Spolski R, Feng CG, et al. A critical role for IL-21 in regulating immunoglobulin production. *Science.* Nov 22 2002;298(5598):1630-1634.
152. Candotti F, Oakes SA, Johnston JA, et al. Structural and functional basis for JAK3-deficient severe combined immunodeficiency. *Blood.* Nov 15 1997;90(10):3996-4003.
153. Verdonck K, Gonzalez E, Henostroza G, et al. HTLV-1 infection is frequent among out-patients with pulmonary tuberculosis in northern Lima, Peru. *Int J Tuberc Lung Dis.* Oct 2007;11(10):1066-1072.
154. Nobori T, Miura K, Wu DJ, Lois A, Takabayashi K, Carson DA. Deletions of the cyclin-dependent kinase-4 inhibitor gene in multiple human cancers. *Nature.* Apr 21 1994;368(6473):753-756.
155. Hirama T, Koeffler HP. Role of the cyclin-dependent kinase inhibitors in the development of cancer. *Blood.* Aug 1 1995;86(3):841-854.
156. Miller CW, Aslo A, Campbell MJ, Kawamata N, Lampkin BC, Koeffler HP. Alterations of the p15, p16,and p18 genes in osteosarcoma. *Cancer Genet Cytogenet.* Feb 1996;86(2):136-142.
157. Tasaka T, Berenson J, Vescio R, et al. Analysis of the p16INK4A, p15INK4B and p18INK4C genes in multiple myeloma. *Br J Haematol.* Jan 1997;96(1):98-102.
158. de Vos S, Miller CW, Takeuchi S, Gombart AF, Cho SK, Koeffler HP. Alterations of CDKN2 (p16) in non-small cell lung cancer. *Genes Chromosomes Cancer.* Nov 1995;14(3):164-170.
159. Miller CW, Koeffler HP. Cyclin-dependent kinase inhibitors in human neoplasms. *Leukemia.* Apr 1997;11 Suppl 3:370-371.
160. Hatta Y, Hirama T, Miller CW, Yamada Y, Tomonaga M, Koeffler HP. Homozygous deletions of the p15 (MTS2) and p16 (CDKN2/MTS1) genes in adult T-cell leukemia. *Blood.* May 15 1995;85(10):2699-2704.
161. Yamada Y, Hatta Y, Murata K, et al. Deletions of p15 and/or p16 genes as a poor-prognosis factor in adult T-cell leukemia. *J Clin Oncol.* May 1997;15(5):1778-1785.
162. Fujiwara H, Arima N, Hashimoto-Tamaoki T, et al. Alteration of p16 (CDKN2) gene is associated with interleukin-2-induced tumor cell growth in adult T-cell leukemia. *Exp Hematol.* Jun 1999;27(6):1004-1009.
163. Hangaishi A, Ogawa S, Imamura N, et al. Inactivation of multiple tumor-suppressor genes involved in negative regulation of the cell cycle,

MTS1/p16INK4A/CDKN2, MTS2/p15INK4B, p53, and Rb genes in primary lymphoid malignancies. *Blood.* Jun 15 1996;87(12):4949-4958.

164. Uchida T, Kinoshita T, Watanabe T, et al. The CDKN2 gene alterations in various types of adult T-cell leukaemia. *Br J Haematol.* Sep 1996;94(4):665-670.

165. Hennet T, Hagen FK, Tabak LA, Marth JD. T-cell-specific deletion of a polypeptide N-acetylgalactosaminyl-transferase gene by site-directed recombination. *Proceedings of the National Academy of Sciences of the United States of America.* 1995;92(26):12070-12074.

166. Cayuela JM, Hebert J, Sigaux F. Homozygous MTS1 (p16INK4A) deletion in primary tumor cells of 163 leukemic patients. *Blood.* Feb 1 1995;85(3):854.

167. Serra A, Gottardi E, Della Ragione F, Saglio G, Iolascon A. Involvement of the cyclin-dependent kinase-4 inhibitor (CDKN2) gene in the pathogenesis of lymphoid blast crisis of chronic myelogenous leukaemia. *Br J Haematol.* Nov 1995;91(3):625-629.

168. Gombart AF, Morosetti R, Miller CW, Said JW, Koeffler HP. Deletions of the cyclin-dependent kinase inhibitor genes p16INK4A and p15INK4B in non-Hodgkin's lymphomas. *Blood.* Aug 15 1995;86(4):1534-1539.

169. Hatta Y, Koeffler HP. Role of tumor suppressor genes in the development of adult T cell leukemia/lymphoma (ATLL). *Leukemia.* Jun 2002;16(6):1069-1085.

170. Herman JG, Jen J, Merlo A, Baylin SB. Hypermethylation-associated inactivation indicates a tumor suppressor role for p15INK4B. *Cancer Res.* Feb 15 1996;56(4):722-727.

171. Herman JG, Merlo A, Mao L, et al. Inactivation of the CDKN2/p16/MTS1 gene is frequently associated with aberrant DNA methylation in all common human cancers. *Cancer Res.* Oct 15 1995;55(20):4525-4530.

172. Merlo A, Herman JG, Mao L, et al. 5' CpG island methylation is associated with transcriptional silencing of the tumour suppressor p16/CDKN2/MTS1 in human cancers. *Nat Med.* Jul 1995;1(7):686-692.

173. Nosaka K, Maeda M, Tamiya S, Sakai T, Mitsuya H, Matsuoka M. Increasing methylation of the CDKN2A gene is associated with the progression of adult T-cell leukemia. *Cancer Res.* Feb 15 2000;60(4):1043-1048.

174. Akagi T, Ono H, Shimotohno K. Expression of cell-cycle regulatory genes in HTLV-I infected T-cell lines: possible involvement of Tax1 in the altered expression of cyclin D2, p18Ink4 and p21Waf1/Cip1/Sdi1. *Oncogene.* Apr 18 1996;12(8):1645-1652.

175. Suzuki T, Kitao S, Matsushime H, Yoshida M. HTLV-1 Tax protein interacts with cyclin-dependent kinase inhibitor p16INK4A and counteracts its inhibitory activity towards CDK4. *EMBO J.* Apr 1 1996;15(7):1607-1614.

176. Suzuki T, Narita T, Uchida-Toita M, Yoshida M. Down-regulation of the INK4 family of cyclin-dependent kinase inhibitors by tax protein of HTLV-1 through two distinct mechanisms. *Virology.* Jul 5 1999;259(2):384-391.

177. Yu D, Thomas-Tikhonenko A. A non-transgenic mouse model for B-cell lymphoma: in vivo infection of p53-null bone marrow progenitors by a Myc retrovirus is sufficient for tumorigenesis. *Oncogene.* Mar 14 2002;21(12):1922-1927.
178. Agata Y, Tamaki N, Sakamoto S, et al. Regulation of T cell receptor beta gene rearrangements and allelic exclusion by the helix-loop-helix protein, E47. *Immunity.* Dec 2007;27(6):871-884.
179. Klucher KM, Lopez DV, Daley GQ. Secondary mutation maintains the transformed state in BaF3 cells with inducible BCR/ABL expression. *Blood.* May 15 1998;91(10):3927-3934.
180. Janas JA, Van Aelst L. Oncogenic tyrosine kinases target Dok-1 for ubiquitin-mediated proteasomal degradation to promote cell transformation. *Mol Cell Biol.* Jul;31(13):2552-2565.
181. Sattler M, Verma S, Byrne CH, et al. BCR/ABL directly inhibits expression of SHIP, an SH2-containing polyinositol-5-phosphatase involved in the regulation of hematopoiesis. *Mol Cell Biol.* Nov 1999;19(11):7473-7480.
182. Mishima Y, Terui Y, Taniyama A, et al. Autophagy and autophagic cell death are next targets for elimination of the resistance to tyrosine kinase inhibitors. *Cancer Sci.* Nov 2008;99(11):2200-2208.
183. Carew JS, Nawrocki ST, Kahue CN, et al. Targeting autophagy augments the anticancer activity of the histone deacetylase inhibitor SAHA to overcome Bcr-Abl-mediated drug resistance. *Blood.* Jul 1 2007;110(1):313-322.
184. Saitoh S. Chaperones and transport proteins regulate TLR4 trafficking and activation. *Immunobiology.* Jul 2009;214(7):594-600.
185. Royer Y, Staerk J, Costuleanu M, Courtoy PJ, Constantinescu SN. Janus kinases affect thrombopoietin receptor cell surface localization and stability. *J Biol Chem.* Jul 22 2005;280(29):27251-27261.
186. Thomis DC, Gurniak CB, Tivol E, Sharpe AH, Berg LJ. Defects in B lymphocyte maturation and T lymphocyte activation in mice lacking Jak3. *Science.* Nov 3 1995;270(5237):794-797.
187. Schmitt TM, Zuniga-Pflucker JC. Induction of T cell development from hematopoietic progenitor cells by delta-like-1 in vitro. *Immunity.* Dec 2002;17(6):749-756.
188. Sharpless NE, Bardeesy N, Lee KH, et al. Loss of p16Ink4a with retention of p19Arf predisposes mice to tumorigenesis. *Nature.* Sep 6 2001;413(6851):86-91.
189. Shultz LD, Schweitzer PA, Christianson SW, et al. Multiple defects in innate and adaptive immunologic function in NOD/LtSz-scid mice. *J Immunol.* Jan 1 1995;154(1):180-191.
190. Kalender Atak Z, De Keersmaecker K, Gianfelici V, et al. High accuracy mutation detection in leukemia on a selected panel of cancer genes. *PLoS One.* 2012;7(6):e38463.
191. Cornejo MG, Kharas MG, Werneck MB, et al. Constitutive JAK3 activation induces lymphoproliferative syndromes in murine bone marrow transplantation models. *Blood.* Mar 19 2009;113(12):2746-2754.

192. Grann VR, Ziv E, Joseph CK, et al. Duffy (Fy), DARC, and neutropenia among women from the United States, Europe and the Caribbean. *Br J Haematol.* Oct 2008;143(2):288-293.
193. Schmitt TM, de Pooter RF, Gronski MA, Cho SK, Ohashi PS, Zuniga-Pflucker JC. Induction of T cell development and establishment of T cell competence from embryonic stem cells differentiated in vitro. *Nat Immunol.* Apr 2004;5(4):410-417.
194. Cooper LA, Shen TL, Guan JL. Regulation of focal adhesion kinase by its amino-terminal domain through an autoinhibitory interaction. *Mol Cell Biol.* Nov 2003;23(22):8030-8041.
195. Campbell ID, Ginsberg MH. The talin-tail interaction places integrin activation on FERM ground. *Trends Biochem Sci.* Aug 2004;29(8):429-435.
196. Lipinski CA, Tran NL, Dooley A, et al. Critical role of the FERM domain in Pyk2 stimulated glioma cell migration. *Biochem Biophys Res Commun.* Oct 27 2006;349(3):939-947.
197. Li Q, Nance MR, Kulikauskas R, et al. Self-masking in an intact ERM-merlin protein: an active role for the central alpha-helical domain. *J Mol Biol.* Feb 2 2007;365(5):1446-1459.
198. Girault JA, Labesse G, Mornon JP, Callebaut I. The N-termini of FAK and JAKs contain divergent band 4.1 domains. *Trends Biochem Sci.* Feb 1999;24(2):54-57.
199. O'Shea JJ, Husa M, Li D, et al. Jak3 and the pathogenesis of severe combined immunodeficiency. *Mol Immunol.* Jul 2004;41(6-7):727-737.
200. Ceccarelli DF, Song HK, Poy F, Schaller MD, Eck MJ. Crystal structure of the FERM domain of focal adhesion kinase. *J Biol Chem.* Jan 6 2006;281(1):252-259.
201. Cohen LA, Guan JL. Residues within the first subdomain of the FERM-like domain in focal adhesion kinase are important in its regulation. *J Biol Chem.* Mar 4 2005;280(9):8197-8207.
202. Knoops L, Hornakova T, Royer Y, Constantinescu SN, Renauld JC. JAK kinases overexpression promotes in vitro cell transformation. *Oncogene.* Mar 6 2008;27(11):1511-1519.
203. Mishra J, Karanki SS, Kumar N. Identification of molecular switch regulating interactions of Janus kinase 3 with cytoskeletal proteins. *J Biol Chem.* Sep 25 2012.
204. Behrmann I, Smyczek T, Heinrich PC, et al. Janus kinase (Jak) subcellular localization revisited: the exclusive membrane localization of endogenous Janus kinase 1 by cytokine receptor interaction uncovers the Jak.receptor complex to be equivalent to a receptor tyrosine kinase. *J Biol Chem.* Aug 20 2004;279(34):35486-35493.
205. Ihle JN, Witthuhn BA, Quelle FW, Yamamoto K, Silvennoinen O. Signaling through the hematopoietic cytokine receptors. *Annu Rev Immunol.* 1995;13:369-398.

206. Kumar N, Mishra J, Narang VS, Waters CM. Janus kinase 3 regulates interleukin 2-induced mucosal wound repair through tyrosine phosphorylation of villin. *J Biol Chem.* Oct 19 2007;282(42):30341-30345.
207. Mishra J, Waters CM, Kumar N. Molecular mechanism of interleukin-2-induced mucosal homeostasis. *Am J Physiol Cell Physiol.* Mar;302(5):C735-747.
208. Lin JX, Mietz J, Modi WS, John S, Leonard WJ. Cloning of human Stat5B. Reconstitution of interleukin-2-induced Stat5A and Stat5B DNA binding activity in COS-7 cells. *J Biol Chem.* May 3 1996;271(18):10738-10744.
209. Zhou YJ, Hanson EP, Chen YQ, et al. Distinct tyrosine phosphorylation sites in JAK3 kinase domain positively and negatively regulate its enzymatic activity. *Proc Natl Acad Sci U S A.* Dec 9 1997;94(25):13850-13855.
210. Murray PJ. The JAK-STAT signaling pathway: input and output integration. *J Immunol.* Mar 1 2007;178(5):2623-2629.
211. Ungureanu D, Saharinen P, Junttila I, Hilton DJ, Silvennoinen O. Regulation of Jak2 through the ubiquitin-proteasome pathway involves phosphorylation of Jak2 on Y1007 and interaction with SOCS-1. *Mol Cell Biol.* May 2002;22(10):3316-3326.
212. Lietha D, Cai X, Ceccarelli DF, Li Y, Schaller MD, Eck MJ. Structural basis for the autoinhibition of focal adhesion kinase. *Cell.* Jun 15 2007;129(6):1177-1187.
213. Roberts JL, Lengi A, Brown SM, et al. Janus kinase 3 (JAK3) deficiency: clinical, immunologic, and molecular analyses of 10 patients and outcomes of stem cell transplantation. *Blood.* Mar 15 2004;103(6):2009-2018.
214. Sorenson RL, Stout LE. Prolactin receptors and JAK2 in islets of Langerhans: an immunohistochemical analysis. *Endocrinology.* Sep 1995;136(9):4092-4098.
215. Ragimbeau J, Dondi E, Vasserot A, Romero P, Uze G, Pellegrini S. The receptor interaction region of Tyk2 contains a motif required for its nuclear localization. *J Biol Chem.* Aug 17 2001;276(33):30812-30818.
216. Ram PA, Waxman DJ. Interaction of growth hormone-activated STATs with SH2-containing phosphotyrosine phosphatase SHP-1 and nuclear JAK2 tyrosine kinase. *J Biol Chem.* Jul 11 1997;272(28):17694-17702.
217. Lobie PE, Ronsin B, Silvennoinen O, Haldosen LA, Norstedt G, Morel G. Constitutive nuclear localization of Janus kinases 1 and 2. *Endocrinology.* Sep 1996;137(9):4037-4045.
218. Lavoie C, Chevet E, Roy L, et al. Tyrosine phosphorylation of p97 regulates transitional endoplasmic reticulum assembly in vitro. *Proc Natl Acad Sci U S A.* Dec 5 2000;97(25):13637-13642.
219. Kohno T, Yamada Y, Tawara M, et al. Inactivation of p14ARF as a key event for the progression of adult T cell leukemia/lymphoma. *Leuk Res.* Dec 2007;31(12):1625-1632.

220. Uenogawa K, Hatta Y, Arima N, et al. Azacitidine induces demethylation of p16INK4a and inhibits growth in adult T-cell leukemia/lymphoma. *Int J Mol Med.* Nov;28(5):835-839.
221. Hussussian CJ, Struewing JP, Goldstein AM, et al. Germline p16 mutations in familial melanoma. *Nat Genet.* Sep 1994;8(1):15-21.
222. Kamb A, Gruis NA, Weaver-Feldhaus J, et al. A cell cycle regulator potentially involved in genesis of many tumor types. *Science.* Apr 15 1994;264(5157):436-440.
223. FitzGerald MG, Harkin DP, Silva-Arrieta S, et al. Prevalence of germ-line mutations in p16, p19ARF, and CDK4 in familial melanoma: analysis of a clinic-based population. *Proc Natl Acad Sci U S A.* Aug 6 1996;93(16):8541-8545.
224. Randerson-Moor JA, Harland M, Williams S, et al. A germline deletion of p14(ARF) but not CDKN2A in a melanoma-neural system tumour syndrome family. *Hum Mol Genet.* Jan 1 2001;10(1):55-62.
225. Rizos H, Puig S, Badenas C, et al. A melanoma-associated germline mutation in exon 1beta inactivates p14ARF. *Oncogene.* Sep 6 2001;20(39):5543-5547.
226. Becker TM, Rizos H, Kefford RF, Mann GJ. Functional impairment of melanoma-associated p16(INK4a) mutants in melanoma cells despite retention of cyclin-dependent kinase 4 binding. *Clin Cancer Res.* Oct 2001;7(10):3282-3288.
227. Hewitt C, Lee Wu C, Evans G, et al. Germline mutation of ARF in a melanoma kindred. *Hum Mol Genet.* May 15 2002;11(11):1273-1279.
228. Serrano M. Cancer regression by senescence. *N Engl J Med.* May 10 2007;356(19):1996-1997.
229. Kamijo T, Zindy F, Roussel MF, et al. Tumor suppression at the mouse INK4a locus mediated by the alternative reading frame product p19ARF. *Cell.* Nov 28 1997;91(5):649-659.
230. Krimpenfort P, Quon KC, Mooi WJ, Loonstra A, Berns A. Loss of p16Ink4a confers susceptibility to metastatic melanoma in mice. *Nature.* Sep 6 2001;413(6851):83-86.
231. Altomare DA, Menges CW, Xu J, et al. Losses of both products of the Cdkn2a/Arf locus contribute to asbestos-induced mesothelioma development and cooperate to accelerate tumorigenesis. *PLoS One.*6(4):e18828.
232. Zhang S, Ramsay ES, Mock BA. Cdkn2a, the cyclin-dependent kinase inhibitor encoding p16INK4a and p19ARF, is a candidate for the plasmacytoma susceptibility locus, Pctr1. *Proc Natl Acad Sci U S A.* Mar 3 1998;95(5):2429-2434.
233. Uchida T, Kinoshita T, Murate T, Saito H, Hotta T. CDKN2 (MTS1/p16INK4A) gene alterations in adult T-cell leukemia/lymphoma. *Leuk Lymphoma.* Mar 1998;29(1-2):27-35.
234. Uchida T, Kinoshita T, Saito H, Hotta T. CDKN2 (MTS1/p16INK4A) gene alterations in hematological malignancies. *Leuk Lymphoma.* Feb 1997;24(5-6):449-461.

235. Tofacitinib. *Drugs R D.* 2010;10(4):271-284.
236. Zerbini CA, Lomonte AB. Tofacitinib for the treatment of rheumatoid arthritis. *Expert Rev Clin Immunol.* May;8(4):319-331.
237. Aringer M, Cheng A, Nelson JW, et al. Janus kinases and their role in growth and disease. *Life Sci.* 1999;64(24):2173-2186.
238. Corcoran AE, Smart FM, Cowling RJ, Crompton T, Owen MJ, Venkitaraman AR. The interleukin-7 receptor alpha chain transmits distinct signals for proliferation and differentiation during B lymphopoiesis. *EMBO J.* Apr 15 1996;15(8):1924-1932.
239. Changelian PS, Moshinsky D, Kuhn CF, et al. The specificity of JAK3 kinase inhibitors. *Blood.* Feb 15 2008;111(4):2155-2157.
240. West K. CP-690550, a JAK3 inhibitor as an immunosuppressant for the treatment of rheumatoid arthritis, transplant rejection, psoriasis and other immune-mediated disorders. *Curr Opin Investig Drugs.* May 2009;10(5):491-504.
241. Ghoreschi K, Laurence A, O'Shea JJ. Selectivity and therapeutic inhibition of kinases: to be or not to be? *Nat Immunol.* Apr 2009;10(4):356-360.
242. Kudlacz E, Perry B, Sawyer P, et al. The novel JAK-3 inhibitor CP-690550 is a potent immunosuppressive agent in various murine models. *Am J Transplant.* Jan 2004;4(1):51-57.
243. Ju W, Zhang M, Jiang JK, et al. CP-690,550, a therapeutic agent, inhibits cytokine-mediated Jak3 activation and proliferation of T cells from patients with ATL and HAM/TSP. *Blood.* Feb 10 2011;117(6):1938-1946.
244. Banerjee P, Tripp A, Lairmore MD, et al. Adult T-cell leukemia/lymphoma development in HTLV-1-infected humanized SCID mice. *Blood.* Apr 1;115(13):2640-2648.
245. Kirken RA, Rui H, Malabarba MG, et al. Activation of JAK3, but not JAK1, is critical for IL-2-induced proliferation and STAT5 recruitment by a COOH-terminal region of the IL-2 receptor beta-chain. *Cytokine.* Oct 1995;7(7):689-700.
246. Fung M, Chu Y-L, Fink JL, Wallace A, McGuire K. IL-2- and STAT5-regulated cytokine gene expression in cells expressing the Tax protein of HTLV-1. *Oncogene.* 2005;24(29):4624-4633.
247. Chen J, Petrus M, Bryant BR, et al. Induction of the IL-9 gene by HTLV-I Tax stimulates the spontaneous proliferation of primary adult T-cell leukemia cells by a paracrine mechanism. *Blood.* May 15 2008;111(10):5163-5172.
248. Yamanaka K, Clark R, Rich B, et al. Skin-derived interleukin-7 contributes to the proliferation of lymphocytes in cutaneous T-cell lymphoma. *Blood.* Mar 15 2006;107(6):2440-2445.
249. Kubota S, Siomi H, Hatanaka M, Pomerantz RJ. Cis/trans-activation of the interleukin-9 receptor gene in an HTLV-I-transformed human lymphocytic cell. *Oncogene.* Apr 4 1996;12(7):1441-1447.
250. Malka Y, Hornakova T, Royer Y, et al. Ligand-independent homomeric and heteromeric complexes between interleukin-2 or -9 receptor subunits and the gamma chain. *J Biol Chem.* Nov 28 2008;283(48):33569-33577.

251. Nicot C, Mulloy JC, Ferrari MG, et al. HTLV-1 p12(I) protein enhances STAT5 activation and decreases the interleukin-2 requirement for proliferation of primary human peripheral blood mononuclear cells. *Blood.* Aug 1 2001;98(3):823-829.